

Experimental and Theoretical Challenges in the Search for the Quark Gluon Plasma:

The STAR Collaboration's Critical Assessment of the Evidence from RHIC Collisions

J. Adams^c M.M. Aggarwal^{ac} Z. Ahammed^{aq} J. Amonett^t
 B.D. Anderson^t D. Arkhipkin^m G.S. Averichev^l S.K. Badyal^s
 Y. Bai^{aa} J. Balewski^q O. Barannikova^{af} L.S. Barnby^c
 J. Baudot^r S. Bekele^{ab} V.V. Belaga^l
 A. Bellingeri-Laurikainen^{al} R. Bellwied^{at} J. Bergerⁿ
 B.I. Bezverkhny^{av} S. Bharadwaj^{ag} A. Bhasin^s A.K. Bhati^{ac}
 V.S. Bhatia^{ac} H. Bichsel^{as} J. Bielcik^{av} J. Bielcikova^{av}
 A. Billmeier^{at} L.C. Bland^d C.O. Blyth^c B.E. Bonner^{ah}
 M. Botje^{aa} A. Boucham^{al} J. Bouchet^{al} A.V. Brandin^y
 A. Bravar^d M. Bystersky^k R.V. Cadman^a X.Z. Cai^{ak}
 H. Caines^{av} M. Calderón de la Barca Sánchez^q J. Castillo^u
 O. Catu^{av} D. Cebra^g Z. Chajecki^{ab} P. Chaloupka^k
 S. Chattopadhyay^{aq} H.F. Chen^{aj} Y. Chen^h J. Cheng^{ao}
 M. Cherney^j A. Chikanian^{av} W. Christie^d J.P. Coffin^r
 T.M. Cormier^{at} J.G. Cramer^{as} H.J. Crawford^f D. Das^{aq}
 S. Das^{aq} M.M. de Moura^{ai} T.G. Dedovich^l
 A.A. Derevschikov^{ae} L. Didenko^d T. Dietelⁿ S.M. Dogra^s
 W.J. Dong^h X. Dong^{aj} J.E. Draper^g F. Du^{av} A.K. Dubey^o
 V.B. Dunin^l J.C. Dunlop^d M.R. Dutta Mazumdar^{aq}
 V. Eckardt^w W.R. Edwards^u L.G. Efimov^l V. Emelianov^y
 J. Engelage^f G. Eppley^{ah} B. Erasmus^{al} M. Estienne^{al}
 P. Fachini^d J. Faivre^r R. Fatemi^q J. Fedorisin^l K. Filimonov^u
 P. Filip^k E. Finch^{av} V. Fine^d Y. Fisyak^d J. Fu^{ao}
 C.A. Gagliardi^{am} L. Gaillard^c J. Gans^{av} M.S. Ganti^{aq}

F. Geurts^{ah} V. Ghazikhanian^h P. Ghosh^{aq} J.E. Gonzalez^h
 H. Gos^{ar} O. Grachov^{at} O. Grebenyuk^{aa} D. Grosnick^{ap}
 S.M. Guertin^h Y. Guo^{at} A. Gupta^s T.D. Gutierrez^g
 T.J. Hallman^d A. Hamed^{at} D. Hardtke^u J.W. Harris^{av}
 M. Heinz^b T.W. Henry^{am} S. Hepplemann^{ad} B. Hippolyte^r
 A. Hirsch^{af} E. Hjort^u G.W. Hoffmann^{an} H.Z. Huang^h
 S.L. Huang^{aj} E.W. Hughes^e T.J. Humanic^{ab} G. Igo^h
 A. Ishihara^{an} P. Jacobs^u W.W. Jacobs^q M. Jedynak^{ar}
 H. Jiang^h P.G. Jones^c E.G. Judd^f S. Kabana^b K. Kang^{ao}
 M. Kaplanⁱ D. Keane^t A. Kechechyan^l V.Yu. Khodyrev^{ae}
 J. Kiryluk^v A. Kisiel^{ar} E.M. Kislov^l J. Klay^u S.R. Klein^u
 D.D. Koetke^{ap} T. Kolleggerⁿ M. Kopytine^t L. Kotchenda^y
 M. Kramer^z P. Kravtsov^y V.I. Kravtsov^{ae} K. Krueger^a
 C. Kuhn^r A.I. Kulikov^l A. Kumar^{ac} R.Kh. Kutuev^m
 A.A. Kuznetsov^l M.A.C. Lamont^{av} J.M. Landgraf^d S. Langeⁿ
 F. Laue^d J. Lauret^d A. Lebedev^d R. Lednicky^l S. Lehocka^l
 M.J. LeVine^d C. Li^{aj} Q. Li^{at} Y. Li^{ao} G. Lin^{av}
 S.J. Lindenbaum^z M.A. Lisa^{ab} F. Liu^{au} H. Liu^{aj} L. Liu^{au}
 Q.J. Liu^{as} Z. Liu^{au} T. Ljubicic^d W.J. Llope^{ah} H. Long^h
 R.S. Longacre^d M. Lopez-Noriega^{ab} W.A. Love^d Y. Lu^{au}
 T. Ludlam^d D. Lynn^d G.L. Ma^{ak} J.G. Ma^h Y.G. Ma^{ak}
 D. Magestro^{ab} S. Mahajan^s D.P. Mahapatra^o R. Majka^{av}
 L.K. Mangotra^s R. Manweiler^{ap} S. Margetis^t C. Markert^t
 L. Martin^{al} J.N. Marx^u H.S. Matis^u Yu.A. Matulenko^{ae}
 C.J. McClain^a T.S. McShane^j F. Meissner^u Yu. Melnick^{ae}
 A. Meschanin^{ae} M.L. Miller^v N.G. Minaev^{ae} C. Mironov^t
 A. Mischke^{aa} D.K. Mishra^o J. Mitchell^{ah} B. Mohanty^{aq}
 L. Molnar^{af} C.F. Moore^{an} D.A. Morozov^{ae} M.G. Munhoz^{ai}
 B.K. Nandi^{aq} S.K. Nayak^s T.K. Nayak^{aq} J.M. Nelson^c
 P.K. Netrakanti^{aq} V.A. Nikitin^m L.V. Nogach^{ae}
 S.B. Nurushev^{ae} G. Odyniec^u A. Ogawa^d V. Okorokov^y
 M. Oldenburg^u D. Olson^u S.K. Pal^{aq} Y. Panebratsev^l
 S.Y. Panitkin^d A.I. Pavlinov^{at} T. Pawlak^{ar} T. Peitzmann^{aa}
 V. Perevoztchikov^d C. Perkins^f W. Peryt^{ar} V.A. Petrov^{at}
 S.C. Phatak^o R. Picha^g M. Planinic^{aw} J. Pluta^{ar} N. Porile^{af}

J. Porter^{as} A.M. Poskanzer^u M. Potekhin^d E. Potrebenikova^ℓ
 B.V.K.S. Potukuchi^s D. Prindle^{as} C. Pruneau^{at} J. Putschke^w
 G. Rakness^{ad} R. Raniwala^{ag} S. Raniwala^{ag} O. Ravel^{al}
 R.L. Ray^{an} S.V. Razin^ℓ D. Reichhold^{af} J.G. Reid^{as}
 J. Reinnarth^{al} G. Renault^{al} F. Retiere^u A. Ridiger^y
 H.G. Ritter^u J.B. Roberts^{ah} O.V. Rogachevskiy^ℓ J.L. Romero^g
 A. Rose^u C. Roy^{al} L. Ruan^{aj} M. Russcher^{aa} R. Sahoo^o
 I. Sakrejda^u S. Salur^{av} J. Sandweiss^{av} M. Sarsour^q I. Savin^m
 P.S. Sazhin^ℓ J. Schambach^{an} R.P. Scharenberg^{af} N. Schmitz^w
 J. Seger^j P. Seyboth^w E. Shahaliev^ℓ M. Shao^{aj} W. Shao^e
 M. Sharma^{ac} W.Q. Shen^{ak} K.E. Shestermanov^{ae}
 S.S. Shimanskiy^ℓ E. Sichtermann^u F. Simon^w R.N. Singaraju^{aq}
 N. Smirnov^{av} R. Snellings^{aa} G. Sood^{ap} P. Sorensen^u
 J. Sowinski^q J. Speltz^r H.M. Spinka^a B. Srivastava^{af}
 A. Stadnik^ℓ T.D.S. Stanislaus^{ap} R. Stockⁿ A. Stolpovsky^{at}
 M. Strikhanov^y B. Stringfellow^{af} A.A.P. Suaide^{ai}
 E. Sugarbaker^{ab} C. Suire^d M. Sumbera^k B. Surrow^v
 M. Swanger^j T.J.M. Symons^u A. Szanto de Toledo^{ai} A. Tai^h
 J. Takahashi^{ai} A.H. Tang^{aa} T. Tarnowsky^{af} D. Thein^h
 J.H. Thomas^u S. Timoshenko^y M. Tokarev^ℓ S. Trentalange^h
 R.E. Tribble^{am} O.D. Tsai^h J. Ulery^{af} T. Ullrich^d
 D.G. Underwood^a G. Van Buren^d M. van Leeuwen^u
 A.M. Vander Molen^x R. Varma^p I.M. Vasilevski^m
 A.N. Vasiliev^{ae} R. Vernet^r S.E. Vigdor^q Y.P. Viyogi^{aq}
 S. Vokal^ℓ S.A. Voloshin^{at} W.T. Waggoner^j F. Wang^{af}
 G. Wang^t G. Wang^e X.L. Wang^{aj} Y. Wang^{an} Y. Wang^{ao}
 Z.M. Wang^{aj} H. Ward^{an} J.W. Watson^t J.C. Webb^q
 G.D. Westfall^x A. Wetzler^u C. Whitten Jr.^h H. Wieman^u
 S.W. Wissink^q R. Witt^b J. Wood^h J. Wu^{aj} N. Xu^u Z. Xu^d
 Z.Z. Xu^{aj} E. Yamamoto^u P. Yepes^{ah} V.I. Yurevich^ℓ
 I. Zborovsky^k H. Zhang^d W.M. Zhang^t Y. Zhang^{aj}
 Z.P. Zhang^{aj} R. Zoukarneev^m Y. Zoukarneeva^m
 A.N. Zubarev^ℓ

STAR Collaboration

- ^aArgonne National Laboratory, Argonne, Illinois 60439, USA
- ^bUniversity of Bern, 3012 Bern, Switzerland
- ^cUniversity of Birmingham, Birmingham, United Kingdom
- ^dBrookhaven National Laboratory, Upton, New York 11973, USA
- ^eCalifornia Institute of Technology, Pasadena, California 91125, USA
- ^fUniversity of California, Berkeley, California 94720, USA
- ^gUniversity of California, Davis, California 95616, USA
- ^hUniversity of California, Los Angeles, California 90095, USA
- ⁱCarnegie Mellon University, Pittsburgh, Pennsylvania 15213, USA
- ^jCreighton University, Omaha, Nebraska 68178, USA
- ^kNuclear Physics Institute AS CR, 250 68 Řež/Prague, Czech Republic
- ^lLaboratory for High Energy (JINR), Dubna, Russia
- ^mParticle Physics Laboratory (JINR), Dubna, Russia
- ⁿUniversity of Frankfurt, Frankfurt, Germany
- ^oInstitute of Physics, Bhubaneswar 751005, India
- ^pIndian Institute of Technology, Mumbai, India
- ^qIndiana University, Bloomington, Indiana 47408, USA
- ^rInstitut de Recherches Subatomiques, Strasbourg, France
- ^sUniversity of Jammu, Jammu 180001, India
- ^tKent State University, Kent, Ohio 44242, USA
- ^uLawrence Berkeley National Laboratory, Berkeley, California 94720, USA
- ^vMassachusetts Institute of Technology, Cambridge, MA 02139-4307
- ^wMax-Planck-Institut für Physik, Munich, Germany
- ^xMichigan State University, East Lansing, Michigan 48824, USA
- ^yMoscow Engineering Physics Institute, Moscow Russia
- ^zCity College of New York, New York City, New York 10031, USA
- ^{aa}NIKHEF and Utrecht University, Amsterdam, The Netherlands
- ^{ab}Ohio State University, Columbus, Ohio 43210, USA
- ^{ac}Panjab University, Chandigarh 160014, India
- ^{ad}Pennsylvania State University, University Park, Pennsylvania 16802, USA
- ^{ae}Institute of High Energy Physics, Protvino, Russia
- ^{af}Purdue University, West Lafayette, Indiana 47907, USA
- ^{ag}University of Rajasthan, Jaipur 302004, India
- ^{ah}Rice University, Houston, Texas 77251, USA
- ^{ai}Universidade de Sao Paulo, Sao Paulo, Brazil
- ^{aj}University of Science & Technology of China, Anhui 230027, China

^{ak}*Shanghai Institute of Applied Physics, Shanghai 201800, China*
^{al}*SUBATECH, Nantes, France*
^{am}*Texas A&M University, College Station, Texas 77843, USA*
^{an}*University of Texas, Austin, Texas 78712, USA*
^{ao}*Tsinghua University, Beijing 100084, China*
^{ap}*Valparaiso University, Valparaiso, Indiana 46383, USA*
^{aq}*Variable Energy Cyclotron Centre, Kolkata 700064, India*
^{ar}*Warsaw University of Technology, Warsaw, Poland*
^{as}*University of Washington, Seattle, Washington 98195, USA*
^{at}*Wayne State University, Detroit, Michigan 48201, USA*
^{au}*Institute of Particle Physics, CCNU (HZNU), Wuhan 430079, China*
^{av}*Yale University, New Haven, Connecticut 06520, USA*
^{aw}*University of Zagreb, Zagreb, HR-10002, Croatia*

Abstract

We review the most important experimental results from the first three years of nucleus-nucleus collision studies at RHIC, with emphasis on results from the STAR experiment, and we assess their interpretation and comparison to theory. The theory-experiment comparison suggests that central Au+Au collisions at RHIC produce dense, rapidly thermalizing matter characterized by: (1) initial energy densities above the critical values predicted by lattice QCD for establishment of a Quark-Gluon Plasma (QGP); (2) nearly ideal fluid flow, marked by constituent interactions of very short mean free path, established most probably at a stage preceding hadron formation; and (3) opacity to jets. Many of the observations are consistent with models incorporating QGP formation in the early collision stages, and have not found ready explanation in a hadronic framework. However, the measurements themselves do not yet establish unequivocal evidence for a transition to this new form of matter. The theoretical treatment of the collision evolution, despite impressive successes, invokes a suite of distinct models, degrees of freedom and assumptions of as yet unknown quantitative consequence. We pose a set of important open questions, and suggest additional measurements, at least some of which should be addressed in order to establish a compelling basis to conclude definitively that thermalized, deconfined quark-gluon matter has been produced at RHIC.

Key words:

PACS: 25.75.-q

Contents

1	Introduction	8
2	Predicted Signatures of the QGP	12
2.1	Features of the Phase Transition in Lattice QCD	12
2.2	Hydrodynamic Signatures	15
2.3	Statistical Models	21
2.4	Jet Quenching and Parton Energy Loss	22
2.5	Saturation of Gluon Densities	25
2.6	Manifestations of Quark Recombination	27
3	Bulk properties	30
3.1	Rapidity Densities	31
3.2	Hadron Yields and Spectra	34
3.3	Hadron yields versus the reaction plane	37
3.4	Quantum Correlation Analyses	45
3.5	Correlations and fluctuations	46
3.6	Summary	52
4	Hard Probes	54
4.1	Inclusive hadron yields at high p_T	54
4.2	Dihadron azimuthal correlations	56
4.3	Theoretical interpretation of hadron suppression	59
4.4	Rapidity-dependence of high p_T hadron yields in d+Au collisions	61
4.5	Outlook	64
5	Some Open Issues	66
5.1	What experimental crosschecks can be performed on apparent QGP signatures at RHIC?	67

5.2	Do the observed consistencies with QGP formation demand a QGP-based explanation?	72
6	Overview and Outlook	75
6.1	What have we learned from the first three years of RHIC measurements?	75
6.2	Are we there yet?	82
6.3	What are the critical needs from future experiments?	84
6.4	Outlook	88
7	Appendix A: Charge	89
8	Appendix B: Definitions of the Quark-Gluon Plasma in Nuclear Physics Planning Documents	90
	References	94

1 Introduction

The Relativistic Heavy Ion Collider was built to create and investigate strongly interacting matter at energy densities unprecedented in a laboratory setting – matter so hot that neutrons, protons and other hadrons are expected to “melt”. Results from the four RHIC experiments already demonstrate that the facility has fulfilled its promise to reach such extreme conditions during the early stages of nucleus-nucleus collisions, forming matter that exhibits heretofore unobserved behavior. These results are summarized in this work and in a number of excellent recent reviews [1–5]. They afford RHIC the exciting scientific opportunity to discover the properties of matter under conditions believed to pertain during a critical, though fleeting, stage of the universe’s earliest development following the Big Bang. The properties of such matter test fundamental predictions of Quantum ChromoDynamics (QCD) in the non-perturbative regime.

In this document we review the results to date from RHIC experiments, with emphasis on those from STAR, in the context of a narrower, more pointed question. The specific prediction of QCD most often highlighted in discussions of RHIC since its conception is that of a transition from hadronic matter to a Quark-Gluon Plasma (QGP) phase, defined below. Recent theoretical claims [6–8] that a type of QGP has indeed been revealed by RHIC experiments and interest in this subject by the popular press [9,10] make it especially timely to evaluate where we are with respect to this particular goal. The present paper has been written in response to a charge (see Appendix A) from the STAR Collaboration to itself, to assess whether RHIC results yet support a compelling discovery claim for the QGP, applying the high standards of scientific proof merited by the importance of this issue. We began this assessment before the end of the fourth successful RHIC running period, and we have based our evaluation on results from the first three RHIC runs, which are often dramatic, sometimes unexpected, and generally in excellent agreement among the four RHIC experiments (and we utilize results from all of the experiments here). Since we began, some analyses of data from run 4 have progressed to yield publicly presented results that amplify or quantify some of our conclusions in this work, but do not contradict any of them.

In addressing our charge, it is critical to begin by defining clearly what we mean by the QGP, since theoretical expectations of its properties have evolved significantly over the 20 years since the case for RHIC was first made. For our purposes here, we take the QGP to be a **(locally) thermally equilibrated state of matter in which quarks and gluons are deconfined from hadrons, so that color degrees of freedom become manifest over nuclear, rather than merely nucleonic, volumes**. In concentrating on thermalization and deconfinement, we believe our definition to be consistent

with what has been understood by the physics community at large since RHIC was first proposed, as summarized by planning documents quoted in Appendix B. In particular, thermalization is viewed as a necessary condition to be dealing with a state of matter, whose properties can be meaningfully compared to QCD predictions or applied to the evolution of the early universe. Observation of a deconfinement transition has always been a primary goal for RHIC, in the hope of illuminating the detailed mechanism of the normal color confinement in QCD. For reasons presented below, we do significantly omit from our list of necessary conditions some other features discussed as potentially relevant over the years since RHIC’s conception.

- We do not demand that the quarks and gluons in the produced matter be non-interacting, as has been considered in some conceptions of the QGP. Lattice QCD calculations suggest that such an ideal state may be approached in static bulk QGP matter only at temperatures very much higher than that required for the deconfinement transition. Furthermore, attainment of thermalization on the ultra-short timescale of a RHIC collision must rely on frequent interactions among the constituents during the earliest stages of the collision – a requirement that is not easily reconcilable with production of an ideal gas. While the absence of interaction would allow considerable simplifications in the calculation of thermodynamic properties of the matter, we do not regard this as an essential feature of color-deconfined matter. In this light, some have suggested [6–8] that we label the matter we seek as the sQGP, for strongly-interacting Quark-Gluon Plasma. Since we regard this as the form of QGP that should be normally anticipated, we consider the ‘s’ qualifier to be superfluous.
- We do not require evidence of a first- or second-order phase transition, even though early theoretical conjecture [11] often focused on possible QGP signatures involving sharp changes in experimental observables with collision energy density. In fact, the nature of the predicted transition from hadron gas to QGP has only been significantly constrained by quite recent theory. Our definition allows for a QGP discovery in a thermodynamic regime beyond a possible critical point. Most modern lattice QCD calculations indeed suggest the existence of such a critical point at baryon densities well above those where RHIC collisions appear to first form the matter. Nonetheless, such calculations still predict a rapid (but unaccompanied by discontinuities in thermodynamic observables) crossover transition in the bulk properties of strongly interacting matter at zero baryon density.
- We consider that evidence for chiral symmetry restoration would be sufficient to demonstrate a new form of matter, but is not *necessary* for a compelling QGP discovery. Most lattice QCD calculations do predict that this transition will accompany deconfinement, but the question is certainly not definitively decided theoretically. If clear evidence for deconfinement can be provided by the experiments, then the search for manifestations of chiral symmetry restoration will be one of the most profound goals of

further investigation of the matter's properties, as they would provide the clearest evidence for fundamental modifications to the QCD vacuum, with potentially far-reaching consequences.

The above “relaxation” of demands, in comparison to initial expectations before initiation of the RHIC program, makes a daunting task even more challenging. The possible absence of a first- or second-order phase transition reduces hopes to observe some well-marked changes in behavior that might serve as an experimental “smoking gun” for a transition to a new form of matter. Indeed, even if there were a sharp transition as a function of bulk matter temperature, it would be unlikely to observe non-smooth behavior in heavy-ion collisions, which form finite-size systems spanning some range of local temperatures even at fixed collision energy or centrality. We thus have to rely more heavily for evidence of QGP formation on the comparison of experimental results with theory. But theoretical calculation of the properties of this matter become subject to all the complexities of strong QCD interactions, and hence to the technical limitations of lattice gauge calculations. Even more significantly, these QCD calculations must be supplemented by other models to describe the complex dynamical passage of heavy-ion collision matter into and out of the QGP state. Heavy ion collisions represent our best opportunity to make this unique matter in the laboratory, but we place exceptional demands on these collisions: they must not only produce the matter, but then must serve “pump and probe” functions somewhat analogous to the modern generation of condensed matter instruments – and they must do it all on distance scales of femtometers and a time scale of 10^{-23} seconds!

There are two basic classes of probes at our disposal in heavy ion collisions. In studying electroweak collision products, we exploit the *absence* of final-state interactions (FSI) with the evolving strongly interacting matter, hoping to isolate those produced during the early collision stages and bearing the imprints of the bulk properties characterizing those stages. But we have to deal with the relative scarcity of such products, and competing origins from hadron decay and interactions during later collision stages. Most of the RHIC results to date utilize instead the far more abundant produced hadrons, where one exploits (but then must understand) the FSI. It becomes critical to distinguish *partonic* FSI from *hadronic* FSI, and to distinguish both from initial-state interactions and the effects of (so far) poorly understood parton densities at very low momentum fraction in the entrance-channel nuclei. Furthermore, the formation of hadrons from a QGP involves soft processes (parton fragmentation and recombination) that cannot be calculated from perturbative QCD and are *a priori* not well characterized (nor even cleanly separable) inside hot strongly interacting matter.

In light of all these complicating features, it is remarkable that the RHIC experiments have already produced results that appear to confirm some of the

more striking, and at least semi-quantitative, predictions made on the basis of QGP formation! Other, unexpected, RHIC results have stimulated new models that explain them within a QGP-based framework. The most exciting results reveal phenomena not previously observed or explored at lower center-of-mass energies, and indeed are distinct from the observations on which a circumstantial case for QGP formation was previously argued at CERN [12]. In order to assess whether a discovery claim is now justified, we must judge the robustness of both the new experimental results and the theoretical predictions they seem to bear out. Do the RHIC data *demand* a QGP explanation? Can they alternatively be accounted for in a hadronic framework? Are the theories and models used for the predictions mutually compatible? Are those other experimental results that currently appear to deviate from theoretical expectations indicative of details yet to be worked out, or rather of fundamental problems with the QGP explanation?

We organize our discussion as follows. In Chapter 2 we briefly summarize the most relevant theoretical calculations and models, their underlying assumptions, limitations and most robust predictions. We thereby identify the *crucial* QGP features we feel must be demonstrated experimentally to justify a compelling discovery claim. We divide the experimental evidence into two broad areas in Chapters 3-4, focusing first on what we have learned about the bulk thermodynamic properties of the early stage collision matter from such measures as hadron spectra, collective flow and correlations among the soft hadrons that constitute the vast majority of outgoing particles. We discuss the consistency of these results with thermalization and the exposure of new (color) degrees of freedom. Next we provide an overview of the observations of hadron production yields and angular correlations at high transverse momentum ($p_T \gtrsim 4$ GeV/c), and what they have taught us about the nature of FSI in the collision matter and their bearing on deconfinement.

In Chapter 5 we focus on open questions for experiment and theory, on important crosschecks and quantifications, on predictions not yet borne out by experiment and experimental results not yet accommodated by theory. Finally, we provide in Chapter 6 an extended summary, conclusions and outlook, with emphasis on additional measurements and theoretical improvements that we feel are needed to strengthen the case for QGP formation. The summary of results in Chap. 6 is extended so that readers already familiar with most of the theoretical and experimental background material covered in Chaps. 2-5 can skip to the concluding section without missing the arguments central to our assessment of the evidence.

The STAR detector and its capabilities have been described in detail elsewhere [13], and will not be discussed.

2 Predicted Signatures of the QGP

The promise, and then the delivery, of experimental results from the AGS, SPS and RHIC have stimulated impressive and important advances over the past decade in the theoretical treatment of the thermodynamic and hydrodynamic properties of hot strongly interacting matter and of the propagation of partons through such matter. However, the complexities of heavy-ion collisions and of hadron formation still lead to a patchwork of theories and models to treat the entire collision evolution, and the difficulties of the strong interaction introduce significant quantitative ambiguities in all aspects of this treatment. In support of a possible compelling QGP discovery claim, we must then identify the most striking qualitative predictions of theory, which survive the quantitative ambiguities, and we must look for a congruence of various observations that confirm such robust predictions. In this chapter, we provide a brief summary of the most important pieces of the theoretical framework, their underlying assumptions and quantitative limitations, and what we view as their most robust predictions. Some of these predictions will then be compared with RHIC experimental results in later chapters.

2.1 Features of the Phase Transition in Lattice QCD

The phase diagram of bulk thermally equilibrated strongly interacting matter should be described by QCD. At sufficiently high temperature one must expect hadrons to “melt”, deconfining quarks and gluons. The exposure of new (color) degrees of freedom would then be manifested by a rapid increase in entropy density, hence in pressure, with increasing temperature, and by a consequent change in the equation of state (EOS). In the limit where the deconfined quarks and gluons are non-interacting, and the quarks are massless, the (Stefan-Boltzmann) pressure P_{SB} of this partonic state, as a function of temperature T at zero chemical potential (*i.e.*, zero net quark density), would be simply determined by the number of degrees of freedom [2]:

$$\frac{P_{SB}}{T^4} = [2(N_c^2 - 1) + \frac{7}{2}N_c N_f] \frac{\pi^2}{90}, \quad (1)$$

where N_c is the number of colors, N_f the number of quark flavors, the temperature is measured in energy units (throughout this paper), and we have taken $\hbar = c = 1$. The two terms on the right in Eq. 1 represent the gluon and quark contributions, respectively. Refinements to this basic expectation, to incorporate effects of color interactions among the constituents, as well as

of non-vanishing quark masses and chemical potential, and to predict the location and nature of the transition from hadronic to partonic degrees of freedom, are best made via QCD calculations on a space-time lattice (LQCD).

In order to extract physically relevant predictions from LQCD calculations, these need to be extrapolated to the continuum (lattice spacing $\rightarrow 0$), chiral (actual current quark mass) and thermodynamic (large volume) limits. While computing power limitations have restricted the calculations to date to numbers of lattice points that are still considered somewhat marginal from the viewpoint of these extrapolations [2], enormous progress has been made in recent years. Within the constraints of computing cost, there have been important initial explorations of sensitivity to details of the calculations [2]: *e.g.*, the number and masses of active quark flavors included; the technical treatment of quarks on the lattice; the presence or absence of the $U_A(1)$ anomaly in the QGP state. Additional numerical difficulties have been partially overcome to allow first calculations at nonzero chemical potential and to improve the determination of physical quark mass scales for a given lattice spacing [2].

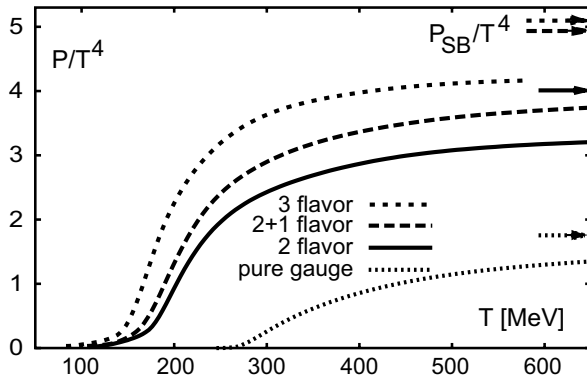


Fig. 1. LQCD calculation results from Ref. [14] for the pressure divided by T^4 of strongly interacting matter as a function of temperature, and for several different choices of the number of dynamical quark flavors. The arrows near the right axis indicate the corresponding Stefan-Boltzmann pressures for the same quark flavor assumptions.

Despite the technical complications, LQCD calculations have converged on the following predictions:

- There is indeed a predicted transition of some form between a hadronic and a QGP phase, occurring at a temperature in the vicinity of $T_c \simeq 160$ MeV for zero chemical potential. The precise value of the transition temperature depends on the treatment of quarks in the calculation.
- The pressure divided by T^4 rises rapidly above T_c , then begins to saturate by about $2T_c$, but at values substantially below the Stefan-Boltzmann limit (see Fig. 1) [14]. The deviation from the SB limit indicates substantial remaining interactions among the quarks and gluons in the QGP phase.
- Above T_c , the effective potential between a heavy quark-antiquark pair

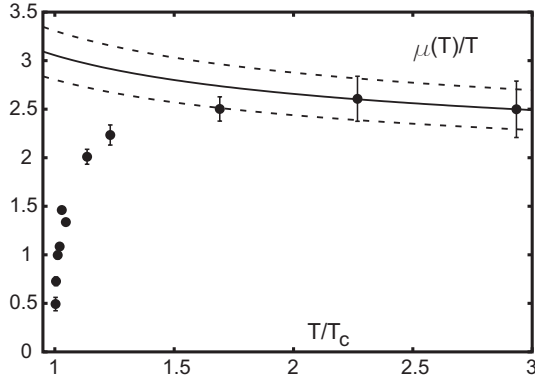


Fig. 2. *Temperature-dependence of the heavy-quark screening mass (divided by temperature) as a function of temperature (in units of the phase transition temperature), from LQCD calculations in Ref. [15]. The curves represent perturbative expectations of the temperature-dependence.*

takes the form of a screened Coulomb potential, with screening mass (or inverse screening length) rising rapidly as temperature increases above T_c (see Fig. 2) [15]. As seen in the figure, the screening mass deviates strongly from perturbative QCD expectations in the vicinity of T_c , indicating large non-perturbative effects. The increased screening mass leads to a shortening of the range of the $q\bar{q}$ interaction, and to an anticipated suppression of charmonium production, in relation to open charm [16]. The predicted suppression appears to set in at substantially different temperatures for J/ψ ($1.5 - 2.0T_c$) and ψ' ($\sim 1.0T_c$) [17].

- In most calculations, the deconfinement transition is also accompanied by a chiral symmetry restoration transition, as seen in Fig. 3 [14]. The reduction in the chiral condensate leads to significant predicted variations in in-medium meson masses. These are also affected by the restoration of $U_A(1)$ symmetry, which occurs at higher temperature than chiral symmetry restoration in the calculation of Fig. 3.
- The nature of the transition from hadronic to QGP phase is highly sensitive to the number of dynamical quark flavors included in the calculation and to the quark masses [18]. For the most realistic calculations, incorporating two light (u, d) and one heavier (s) quark flavor relevant on the scale of T_c , the transition is most likely of the crossover type (with no discontinuities in thermodynamic observables – as opposed to first- or second-order phase transitions) at zero chemical potential, although the ambiguities in tying down the precise values of quark masses corresponding to given lattice spacings still permit some doubt.
- Calculations at non-zero chemical potential, though not yet mature, suggest the existence of a critical point such as that illustrated in Fig. 4 [19]. The numerical challenges in such calculations leave considerable ambiguity about the value of μ_B at which the critical point occurs (*e.g.*, it changes from $\mu_B \approx 700$ to 350 MeV between Refs. [20] and [19]), but it is most likely above the value at which RHIC collision matter is formed, consistent with

the crossover nature of the transition anticipated at RHIC.

- Even for crossover transitions, the LQCD calculations still predict a rapid temperature-dependence of the thermodynamic properties, as revealed in all of the figures considered above. However, in basing experimental expectations on this feature, it must be kept in mind that the early collision temperature varies slowly with collision energy and is not directly measured by any of the probes studied most extensively to date.

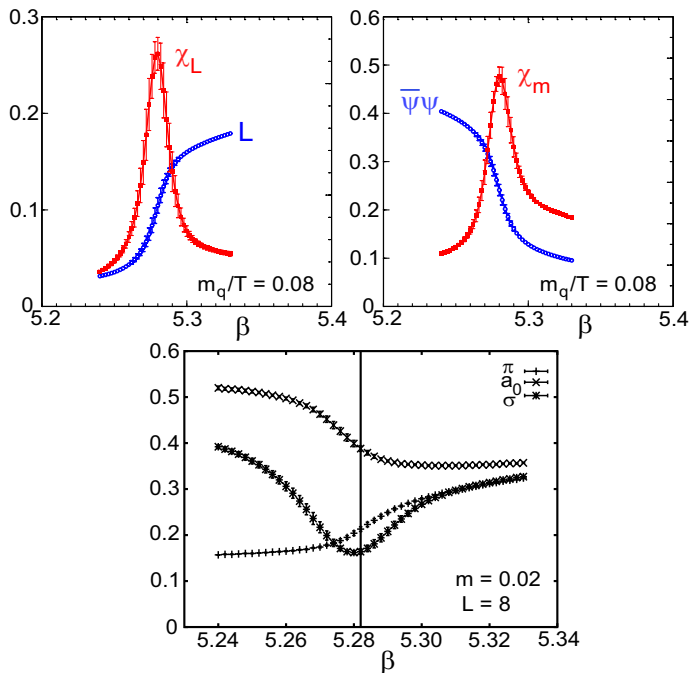


Fig. 3. LQCD calculations for two dynamical quark flavors [14] showing the coincidence of the chiral symmetry restoration (marked by the rapid decrease of chiral condensate $\langle\bar{\psi}\psi\rangle$ in the upper right-hand frame) and deconfinement (upper left frame) phase transitions. The lower plot shows that the chiral transition leads toward a mass degeneracy of the pion with scalar meson masses. All plots are as a function of the bare coupling strength β used in the calculations; increasing β corresponds to decreasing lattice spacing and to increasing temperature.

2.2 Hydrodynamic Signatures

In order to determine how the properties of bulk QGP matter, as determined in LQCD calculations, may influence observable particle production spectra from RHIC collisions, one needs to model the time evolution of the collision “fireball”. To the extent that the initial interactions among the constituents are sufficiently strong to establish local thermal equilibrium rapidly, and then to maintain it over a significant evolution time, the resulting matter may be treated as a relativistic fluid undergoing collective, hydrodynamic flow [3]. The application of hydrodynamics for the description of hadronic fireballs

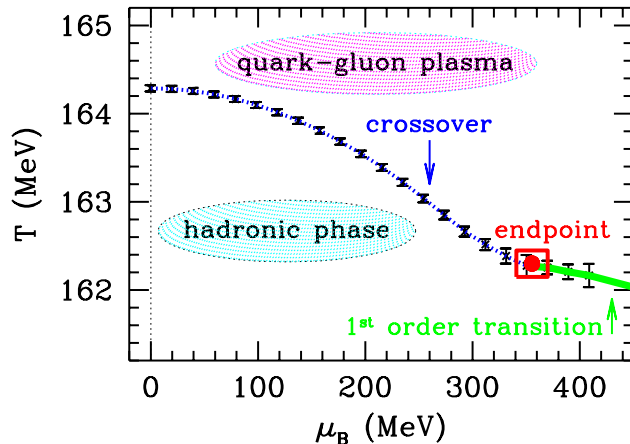


Fig. 4. *LQCD* calculation results for non-zero chemical potential [19], suggesting the existence of a critical point well above RHIC chemical potential values. The solid line indicates the locus of first-order phase transitions, while the dotted curve marks crossover transitions between the hadronic and QGP phases.

has a long history [21,22]. Relativistic hydrodynamics has been extensively applied to heavy ion collisions from BEVALAC to RHIC [3,22,23], but with the most striking successes at RHIC. The applicability of hydrodynamics at RHIC may provide the clearest evidence for the attainment of local thermal equilibrium at an early stage in these collisions. (On the other hand, there are alternative, non-equilibrium treatments of the fireball evolution that have also been compared to RHIC data [24].) The details of the hydrodynamic evolution are clearly sensitive to the EOS of the flowing matter, and hence to the possible crossing of a phase or crossover transition during the system expansion and cooling. It is critical to understand the relative sensitivity to the EOS as compared with that to other assumptions and parameters of the hydrodynamic treatment.

Traditional hydrodynamics calculations cannot be applied to matter not in local thermal equilibrium, hence they must be supplemented by more phenomenological treatments of the early and late stages of the system evolution. These parameterize the initial conditions for the hydrodynamic flow and the transition to freezeout, where the structureless matter flow is converted into final hadron spectra. Since longitudinal flow is especially sensitive to initial conditions beyond the scope of the theory, most calculations to date have concentrated on *transverse* flow, and have assumed longitudinal boost-invariance of the predictions [3]. Furthermore, it is anticipated that hadrons produced at sufficiently high transverse momentum in initial partonic collisions will not have undergone sufficient rescatterings to come to thermal equilibrium with the surrounding matter, so that hydrodynamics will be applicable at best only for the softer features of observed spectra. Within the time range and momentum range of its applicability, most hydrodynamics calculations to date have

treated the matter as an *ideal*, non-viscous fluid. The motion of this fluid is completely determined given the three components of the fluid velocity \vec{v} , the pressure (P) and the energy and baryon densities (e and n_B). The hydrodynamic equations of motion for an ideal fluid are derived from the exact local conservation laws for energy, momentum, and baryon number by assuming an ideal-fluid form for the energy-momentum tensor and baryon number current; they are closed by an equation of state $P(e, n_B)$ [21].

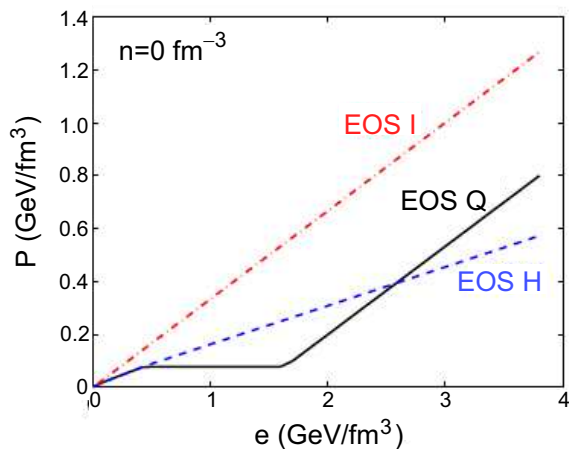


Fig. 5. Pressure as a function of energy density at vanishing net baryon density for three different equations of state of strongly interacting matter: a Hagedorn resonance gas (EOS H), an ideal gas of massless partons (EOS I) and a connection of the two via a first-order phase transition at $T_c=164$ MeV (EOS Q). These EOS are used in hydrodynamics calculations in Ref. [3], from which the figure is taken.

The EOS in hydrodynamics calculations for RHIC has been implemented using simplified models inspired by LQCD results, though not reproducing their details. One example is illustrated by the solid curve in Fig. 5, connecting an ideal gas of massless partons at high temperature to a Hagedorn hadron resonance gas [25] at low temperatures, via a first-order phase transition chosen to ensure consistency with ($\mu_B = 0$) LQCD results for critical temperature and net increase in entropy density across the transition [3]. In this implementation, the slope $\partial P/\partial e$ (giving the square of the velocity of sound in the matter) exhibits high values for the hadron gas and, especially, the QGP phases, but has a soft point at the mixed phase [3,22]. This generic softness of the EOS during the assumed phase transition has predictable consequences for the system evolution.

In heavy ion collisions, the measurable quantities are the momenta of the produced particles at the final state and their correlations. Transverse flow measures are key observables to compare quantitatively with model predictions in studying the EOS of the hot, dense matter. In non-central collisions, the reaction zone has an almond shape, resulting in azimuthally anisotropic

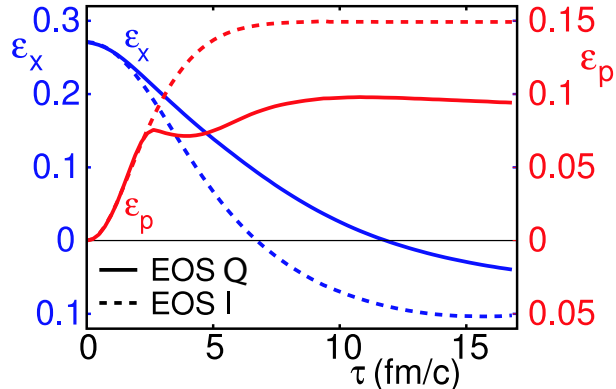


Fig. 6. *Hydrodynamics calculations for the time evolution of the spatial eccentricity ϵ_x and the momentum anisotropy ϵ_p for non-central (7 fm impact parameter) Au+Au collisions at RHIC [3]. The solid and dashed curves result, respectively, from use of EOS Q and EOS I from Fig. 5. The gradual removal of the initial spatial eccentricity by the pressure gradients that lead to the buildup of ϵ_p reflects the self-quenching aspect of elliptic flow. The time scale runs from initial attainment of local thermal equilibrium through freezeout in this calculation.*

pressure gradients, and therefore a nontrivial elliptic flow pattern. Experimentally, this elliptic flow pattern is usually measured using a Fourier decomposition of momentum spectra relative to the event-by-event reaction plane, in which the second Fourier component v_2 is the dominant contribution. The important feature of elliptic flow is that it is “self-quenching” [26,27], because the pressure-driven expansion tends to reduce the spatial anisotropy that causes the azimuthally anisotropic pressure gradient in the first place. This robust feature is illustrated in Fig. 6, which compares predictions for the spatial and resulting momentum eccentricities as a function of time during the system’s hydrodynamic evolution, for two different choices of EOS [3]. The self-quenching makes the elliptic flow particularly sensitive to earlier collision stages, when the spatial anisotropy and pressure gradient are the greatest. In contrast, hadronic interactions at later stages may contribute significantly to the radial flow [28,29].

The solid momentum anisotropy curve in Fig. 6 also illustrates that entry into the soft EOS mixed phase during a transition from QGP to hadronic matter stalls the buildup of momentum anisotropy in the flowing matter. An even more dramatic predicted manifestation of this stall is shown by the dependence of p_T -integrated elliptic flow on produced hadron multiplicity in Fig. 7, where a dip is seen under conditions where the phase transition occupies most of the early collision stage. Since the calculations are carried out for a fixed impact parameter, measurements to confirm such a dip would have to be performed as a function of collision energy. In contrast to early (non-hydrodynamic) projections of particle multiplicities at RHIC (represented by horizontal arrows in Fig. 7), we now know that the multiplicity at the predicted dip is approx-

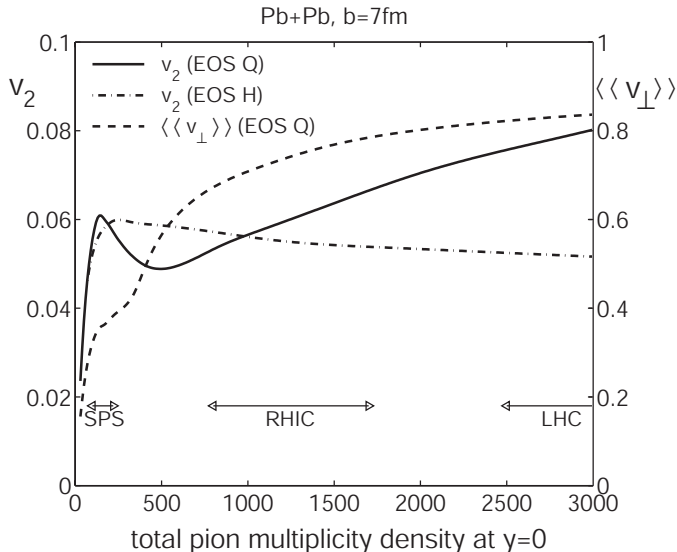


Fig. 7. Predicted hydrodynamic excitation function of p_T -integrated elliptic (v_2 , solid curve, left axis) and radial ($\langle\langle v_\perp \rangle\rangle$, dashed, right axis) flow for non-central Pb+Pb collisions [30]. The calculations assume a sharp onset for freezeout along a surface of constant energy density corresponding to temperature ≈ 120 MeV. The soft phase transition stage in EOS Q gives rise to a dip in the elliptic flow. The horizontal arrows at the bottom reflect early projections of particle multiplicity for different facilities, but we now know that RHIC collisions produce multiplicities in the vicinity of the predicted dip.

imately achieved for appropriate centrality in RHIC Au+Au collisions at full energy. However, comparisons of predicted with measured excitation functions for elliptic flow are subject to an overriding ambiguity concerning where and when appropriate conditions of initial local thermal equilibrium for hydrodynamic applicability are actually achieved. Hydrodynamics itself has nothing to say concerning this issue.

One can alternatively attain sensitivity to the EOS in measurements for given collision energy and centrality by comparing to the predicted dependence of elliptic flow strength on hadron p_T and mass (see Fig. 8). The mass-dependence is of simple kinematic origin [3], and is thus a robust feature of hydrodynamics, but its quantitative extent, along with the magnitude of the flow itself, depends on the EOS [3].

Of course, the energy- and mass-dependence of v_2 can also be affected by species-specific hadronic FSI at and close to the freezeout where the particles decouple from the system, and hydrodynamics is no longer applicable [28,29]. A combination of macroscopic and microscopic models, with hydrodynamics applied at the early partonic and mixed-phase stages and a hadronic transport model such as RQMD [31] at the later hadronic stage, may offer a more realistic description of the whole evolution than that achieved with a simplified sharp freezeout treatment in Figs. 6,7,8. The combination of hydrodynam-

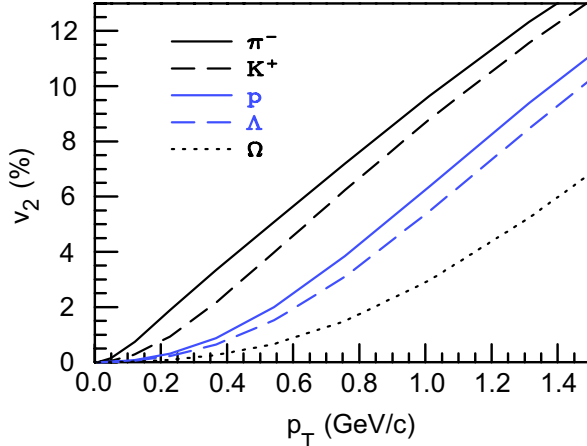


Fig. 8. *Hydrodynamics predictions [32] of the p_T and mass-dependences of the elliptic flow parameter v_2 for identified final hadrons from Au+Au collisions at $\sqrt{s_{NN}}=130$ GeV. The calculations employ EOS Q (see Fig. 5) and freezeout near 120 MeV.*

ics with RQMD [29] has, for example, led to predictions of a substantially different, and monotonic, energy-dependence of elliptic flow, as can be seen by comparing Fig. 9 to Fig. 7. The difference between the two calculations may result primarily [6] from the elimination in [29] of the assumption of ideal fluid expansion even in the hadronic phase. In any case, this comparison suggests that the energy dependence of elliptic flow in the quark-hadron transition region is at least as sensitive to the late hadronic interaction details as to the softening of the EOS in the mixed-phase region. Flow for multi-strange and charmed particles with small hadronic interaction cross sections may provide more selective sensitivity to the properties of the partonic and mixed phases [29,33,34]. There may be non-negligible sensitivity as well to the addition of such other complicating features as viscosity [35] and deviations from longitudinal boost-invariance, studies of the latter effect requiring computationally challenging (3+1)-dimensional hydrodynamics calculations [36]. Certainly, the relative sensitivities to EOS variations vs. treatments of viscosity, boost-invariance, and the evolution of the hadronic stage must be clearly understood in order to interpret agreement between hydrodynamics calculations and measured flow.

In addition to predicting one-body hadron momentum spectra as a function of many kinematic variables, hydrodynamic evolution of the matter is also relevant for understanding two-hadron Hanbury-Brown-Twiss (HBT) quantum correlation functions [5]. From these correlation measurements one can extract information concerning the size and shape of the emitting surface at freezeout, *i.e.*, at the end of the space-time evolution stage treated by hydrodynamics. While the detailed comparison certainly depends on improving models of the freezeout stage, it is reasonable to demand that hydrodynamics calculations consistent with the one-body hadron measurements be also at least roughly consistent with HBT results.

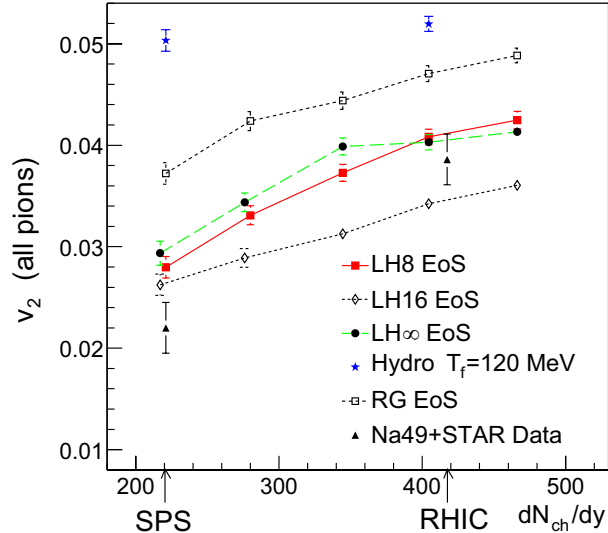


Fig. 9. Predictions [29] from a hybrid hydrodynamics-RQMD approach for the elliptic flow as a function of charged particle multiplicity in Pb+Pb collisions at an impact parameter $b = 6$ fm. Curves for different choices of EOS (LH8 is most similar to EOS Q in Fig. 7) are compared to experimental results derived [29] from SPS and RHIC measurements. The replacement of a simplified freezeout model for all hadron species and of the assumption of ideal hadronic fluid flow with the RQMD hadron cascade appears to remove any dip in v_2 values, such as seen in Fig. 7.

2.3 Statistical Models

The aim of statistical models is to derive the equilibrium properties of a macroscopic system from the measured yields of the constituent particles [37,38]. Statistical models, however, do not describe how a system approaches equilibrium [38]. Hagedorn [25] and Fermi [39] pioneered their application to computing particle production yield ratios in high energy collisions, where conserved quantities such as baryon number and strangeness play important roles [40]. Statistical methods have become an important tool to study the properties of the fireball created in high energy heavy ion collisions [37,41], where they succeed admirably in reproducing measured yield ratios. Can this success be taken as evidence that the matter produced in these collisions has reached thermal and chemical equilibrium before hadronization? Can the temperature and chemical potential values extracted from such statistical model fits be interpreted as the equilibrium properties of the collision matter?

The answer to both of the above questions is “not on the basis of fits to integrated yields alone.” The essential condition for applicability of statistical models is phase-space dominance in determining the distribution of a system with many degrees of freedom among relatively few observables [39,42], and this does not necessarily reflect a process of thermodynamic equilibration via interactions of the constituents. Indeed, statistical model fits can describe

the observed hadron abundances well (albeit, only by including a strangeness undersaturation factor, $\gamma_s < 1$) in p+p, $e^+ + e^-$ and p+A collisions, where thermal and chemical equilibrium are thought not to be achieved [37]. It is thus desirable to distinguish a system driven towards thermodynamic equilibrium from one born at hadronization with statistical phase space distributions, where “temperature” and “chemical potential” are simply Lagrange multipliers [43]. In order to make this distinction, it is necessary and sufficient to measure the extensive interactions among particles and to observe the change from canonical ensemble in a small system with the size of a nucleon (p+p, $e^+ + e^-$) and tens of produced particles, to grand canonical ensemble in a large system with extended volume and thousands of produced particles (central Au+Au) [37,40].

The evolution of the system from canonical to grand canonical ensemble can be observed, for example, via multi-particle correlations (especially of particles constrained by conservation laws [42]) or by the centrality dependence of the strangeness suppression factor γ_s . The interactions among constituent particles, necessary to attainment of *thermal* equilibrium, can be measured by collective flow of many identified particles [29,44] and by resonance yields [45] that follow their hadronic rescattering cross sections. (Collective flow and resonance formation could, in principle, proceed via the dominant hadronic interactions that do not change hadron species, and hence are not strictly sufficient to establish *chemical* equilibration among hadrons, which would have to rely on relatively weak *inelastic* processes [43].)

If other measurements confirm the applicability of a grand canonical ensemble, then the hadron yield ratios can be used to extract the temperature and chemical potential of the system [37] at chemical freezeout. The latter is defined as the stage where hadrons have been created and the net numbers of stable particles of each type no longer change in further system evolution. These values place constraints on, but do not directly determine, the properties of the matter when thermal equilibrium was first attained in the wake of the collision. Direct measurement of the temperature at this early stage requires characterization of the yields of particles such as photons that are produced early but do not significantly interact on their way out of the collision zone.

2.4 Jet Quenching and Parton Energy Loss

Partons from the colliding nuclei that undergo a hard scattering in the initial stage of the collision provide colored probes for the colored bulk matter that may be formed in the collision’s wake. It was Bjorken [46] who first suggested that partons traversing bulk partonic matter might undergo significant energy loss, with observable consequences on the parton’s subsequent fragmentation

into hadrons. More recent theoretical studies have demonstrated that the elastic parton scattering contribution to energy loss first contemplated by Bjorken is likely to be quite small, but that gluon radiation induced by passage through the matter may be quite sizable [4]. Such induced gluon radiation would be manifested by a significant softening and broadening of the jets resulting from the fragmentation of partons that traverse substantial lengths of matter containing a high density of partons – a phenomenon called “jet quenching”. As will be documented in later chapters, some of the most exciting of the RHIC results reveal jet quenching features quite strikingly. It is thus important to understand what features of this phenomenon may distinguish parton energy loss through a QGP from other possible sources of jet softening and broadening.

Several different theoretical evaluations of the non-Abelian radiative energy loss of partons in dense, but finite, QCD matter have been developed [47–50]. They give essentially consistent results, including the non-intuitive prediction that the energy loss varies with the square (L^2) of the thickness traversed through static matter, as a consequence of destructive interference effects in the coherent system of the leading quark and its first radiated gluon as they propagate through the matter. The overall energy loss is reduced, and the L -dependence shifted toward linearity, by the expansion of the matter resulting from heavy ion collisions. The significant deformation of the collision zone for non-central collisions, responsible for the observed elliptic flow (hence also for an azimuthal dependence of the rate of matter expansion), should give rise to a significant variation of the energy loss with angle with respect to the impact parameter plane. The scale of the net energy loss depends on factors that can all be related to the rapidity density of gluons (dN_g/dy) in the matter traversed.

The energy loss calculated via any of these approaches is then embedded in a perturbative QCD (pQCD) treatment of the hard parton scattering. The latter treatment makes the standard factorization assumption (untested in the many-nucleon environment) that the cross section for producing a given final-state high- p_T hadron can be written as the product of suitable initial-state parton densities, pQCD hard-scattering cross section, and final-state fragmentation functions for the scattered partons. Nuclear modifications must be expected for the initial parton densities as well as for the fragmentation functions. Entrance-channel modifications – including both nuclear shadowing of parton densities and the introduction by multiple scattering of additional transverse momentum to the colliding partons – are capable of producing some broadening and softening of the final-state jets. But these effects can, in principle, be calibrated by complementing RHIC A+A collision studies with p+A or d+A, where QGP formation is not anticipated.

The existing theoretical treatments of the final-state modifications attribute

the changes in effective fragmentation functions to the parton energy loss. That is, they assume vacuum fragmentation (as characterized phenomenologically from jet studies in more elementary systems) of the degraded parton and its spawned gluons [4]. This assumption may be valid in the high-energy limit, when the dilated fragmentation time should exceed the traversal time of the leading parton through the surrounding matter. However, its justification seems questionable for the soft radiated gluons and over the leading-parton momentum ranges to which it has been applied so far for RHIC collisions. In these cases, one might expect hadronization to be aided by the pickup of other partons from the surrounding QGP, and not to rely solely on the production of $q\bar{q}$ pairs from the vacuum. Indeed, RHIC experimental results to be described later in this document hint that the distinction between such recombination processes and parton fragmentation in the nuclear environment may not be clean. Furthermore, one of the developed models of parton energy loss [48] explicitly includes energy *gain* via absorption of gluons from the surrounding thermal QGP bath.

The assumption of vacuum fragmentation also implies a neglect of FSI effects for the hadronic fragmentation products, which might further contribute to jet broadening and softening. Models that attempt to account for *all* of the observed jet quenching via the alternative description of hadron energy loss in a hadronic gas environment are at this time still incomplete [51]. They must contend with the initial expectation of *color transparency* [52], *i.e.*, that high momentum hadrons formed in strongly interacting matter begin their existence as point-like color-neutral particles with very small color dipole moments, hence weak interactions with surrounding nuclear matter. In order to produce energy loss consistent with RHIC measurements, these models must then introduce *ad hoc* assumptions about the rate of growth of these “pre-hadron” interaction cross sections during traversal of the surrounding matter [51].

The above caveats concerning assumptions of the parton energy loss models may call into question some of their quantitative conclusions, but are unlikely to alter the basic qualitative prediction that substantial jet quenching is a *necessary* result of QGP formation. The more difficult question is whether the observation of jet quenching can also be taken as a *sufficient* condition for a QGP discovery claim? Partonic traversal of matter can, in principle, be distinguished from effects of *hadronic* traversal by detailed dependences of the energy loss, *e.g.*, on azimuthal angle and system size (reflecting the nearly quadratic length-dependence characteristic of gluon radiation), on p_T (since hadron formation times should increase with increasing partonic momentum [53]), or on type of detected hadron (since hadronic energy losses should depend on particle type and size, while partonic energy loss should be considerably reduced for heavy quarks [53,54]). However, the energy loss calculations do not (with the exception of the small quantitative effect of *ab-*

sorption of thermal gluons [48]) distinguish confined from deconfined quarks and gluons in the surrounding matter. Indeed, the same approaches have been applied to experimental results from semi-inclusive deep inelastic scattering [55] or Drell-Yan dilepton production [56] experiments on nuclear targets to infer quark energy losses in *cold*, confined nuclear matter [57]. Baier, *et al.* [58] have shown that the energy loss is expected to vary smoothly with energy density from cold hadronic to hot QGP matter, casting doubt on optimistic speculations [53] that the QGP transition might be accompanied by a rapid change in the extent of jet quenching with collision energy. Thus, the relevance of the QGP can only be inferred indirectly, from the magnitude of the gluon density dN_g/dy needed to reproduce jet quenching in RHIC collision matter, vis-a-vis that needed to explain the energy loss in cold nuclei. Is the extracted gluon density consistent with what one might expect for a QGP formed from RHIC collisions? To address this critical question, one must introduce new theoretical considerations of the initial state for RHIC collisions.

2.5 Saturation of Gluon Densities

In a partonic view, the initial conditions for the expanding matter formed in a RHIC collision are dominated by the scattering of gluons carrying small momentum fractions (Bjorken x) in the nucleons of the colliding nuclei. Gluon densities in the proton have been mapped down to quite small values of $x \sim 10^{-4}$ in deep inelastic scattering experiments at HERA [59]. When the measurements are made with high resolving power (*i.e.*, with large 4-momentum transfer Q^2), the extracted gluon density $xg(x, Q^2)$ continues to grow rapidly down to the lowest x values measured. However, at moderate $Q^2 \sim \text{few (GeV)}^2$, there are indications from the HERA data that $xg(x, Q^2)$ begins to saturate, as might be expected from the competition between gluon fusion ($g + g \rightarrow g$) and gluon splitting ($g \rightarrow g + g$) processes. It has been conjectured [60–63] that the onset of this saturation moves to considerably higher x values (for given Q^2) in a nuclear target, compared to a proton, and that a QGP state formed in RHIC collisions may begin with a saturated density of gluons. Indeed, birth within this saturated state might provide a natural mechanism for the rapid achievement of thermal equilibrium in such collisions [60].

The onset of saturation occurs when the product of the cross section for a QCD process (such as gluon fusion) of interest ($\sigma \sim \pi\alpha_s(Q^2)/Q^2$) and the areal density of partons (ρ) available to participate exceeds unity [66]. In this so-called Color Glass Condensate region (see Fig. 10), QCD becomes highly non-linear, but amenable to classical field treatments, because the coupling strength remains weak ($\alpha_s \ll 1$) while the field strength is large [60–63]. The borderline of the CGC region is denoted by the “saturation scale” $Q_s^2(x, A)$. It depends on both x and target mass number A , because the target gluon density

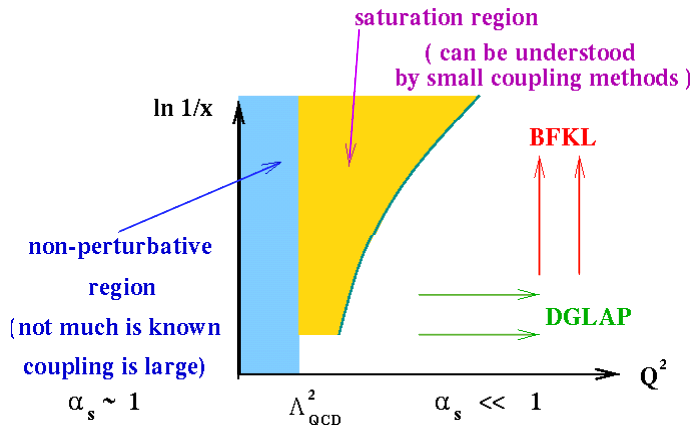


Fig. 10. Schematic layout of the QCD landscape in $x - Q^2$ space. The region at the right is the perturbative region, marked by applicability of the linear DGLAP[64] and BFKL[65] evolution equations for the Q^2 - and x -dependence, respectively, of the parton distribution functions. At $Q^2 < \Lambda_{QCD}^2$, the coupling constant is large and non-perturbative methods must be used to treat strongly interacting systems. The matter in RHIC collisions may be formed in the intermediate region, where gluon densities saturate, the coupling is still weak, but very strong color fields lead to non-linear behavior describable by classical field methods. The curve separating the saturation and perturbative regimes sets the saturation scale. Figure courtesy of Y. Kovchegov.

depends on both factors. In particular, at sufficiently low x and moderate Q^2 , ρ is enhanced for a nucleus compared to a nucleon by a factor $\sim A^{1/3}$: the target sees the probe as having a longitudinal coherence length ($\ell_c \sim 1/m_N x$) much greater, but a transverse size ($\sim 1/Q^2$) much smaller, than the nuclear diameter. The probe thus interacts coherently with all the target gluons within a small diameter cylindrical “core” of the nucleus. The HERA data [59] suggest a rather slow variation – $xg(x) \propto x^{-\lambda}$, with $\lambda \sim 0.3$ at $Q^2 \sim \text{few (GeV)}^2$ – of gluon densities with x at low x . Consequently, one would have to probe a proton at roughly two orders of magnitude lower x than a Au nucleus to gain the same factor growth in gluon densities as is provided by $A^{1/3}$.

Under the assumption that QGP formation in a RHIC collision is dominated by gluon-gluon interactions below the saturation scale, saturation models predict the density of gluons produced per unit area and unit rapidity [60]:

$$\frac{d^2 N}{d^2 b dy} = C \frac{N_c^2 - 1}{4\pi^2 \alpha_s(Q_s^2) N_c} Q_s^2(x, N_{part}), \quad (2)$$

where A has been replaced by N_{part} , the number of nucleons participating in an A+A collision at given impact parameter b , and $\hbar = c = 1$. The x -dependence of the saturation scale is taken from the HERA data,

$$Q_s^2(x) = Q_0^2 \left(\frac{x_0}{x}\right)^\lambda, \quad (3)$$

and the same values of $\lambda \sim 0.2 - 0.3$ are generally assumed to be valid inside the nucleus as well. However, the multiplicative factor C above, parameterizing the number of outgoing hadrons per initially present gluon, is typically adjusted to fit observed outgoing hadron multiplicities from RHIC collisions. (Variations in C are clearly not distinguishable, in the context of Eqn. (2), from changes to the overall saturation scale Q_0^2 .) Once this parameter is fixed, gluon saturation models should be capable of predicting the dependence of hadron multiplicity on collision energy, rapidity, centrality and mass number. Furthermore, the initial QGP gluon densities extracted can be compared with the independent values obtained from parton energy loss model fits to jet quenching observations or from hydrodynamics calculations of elliptic flow.

While it is predictable within the QCD framework that gluon saturation should occur under appropriate conditions, and the theoretical treatment of the CGC state is highly evolved [60–63], the dependences of the saturation scale are not yet fully exposed by supporting data. Eventual confirmation of the existence of such a scale must come from comparing results for a wide range of high energy experiments from Deep Inelastic Scattering in ep and eA (HERA, eRHIC) to pA and AA (RHIC, LHC) collisions.

2.6 Manifestations of Quark Recombination

The concept of quark recombination was introduced to describe hadron production in the forward region in p+p collisions [67]. At forward rapidity, this mechanism allows a fast quark resulting from a hard parton scattering to recombine with a slow anti-quark, which could be one in the original sea of the incident hadron, or one excited by a gluon [67]. If a QGP is formed in relativistic heavy ion collisions, then one might expect recombination of a different sort, namely, coalescence of the abundant thermal partons, to provide another important hadron production mechanism, active over a wide range of rapidity and transverse momentum [68]. In particular, at moderate p_T values (above the realm of hydrodynamics applicability), this hadron production “from below” (recombination of lower p_T partons from the thermal bath) has been predicted [69] to be competitive with production “from above” (fragmentation of higher p_T scattered partons). It has been suggested [70] that the need for substantial recombination to explain observed hadron yields and flow may be taken as a signature of QGP formation.

In order to explain observed features of RHIC collisions, the recombination models [68,69] make the central assumption that coalescence proceeds via *constituent* quarks, whose number in a given hadron determines its production rate. The constituent quarks are presumed to follow a thermal (exponential) momentum spectrum and to carry a collective transverse velocity distribution.

This picture leads to clear predicted effects on baryon and meson production rates, with the former depending on the spectrum of thermal constituent quarks and antiquarks at roughly one-third the baryon p_T , and the latter determined by the spectrum at one-half the meson p_T . Indeed, the recombination model was recently re-introduced in the RHIC context, precisely to explain an anomalous abundance of baryons vs. mesons observed at moderate p_T values [69]. If the observed (saturated) hadronic elliptic flow values in this momentum range result from coalescence of collectively flowing constituent quarks, then one can expect a similarly simple baryon vs. meson relationship [69]: the baryon (meson) flow would be 3 (2) times the quark flow at roughly one-third (one-half) the baryon p_T .

As will be discussed in later chapters, RHIC experimental results showing just such simple predicted baryon vs. meson features would appear to provide strong evidence for QGP formation. However, the models do not spell out the connection between the inferred spectrum and flow of constituent quarks and the properties of the essentially massless partons (predominantly gluons) in a chirally restored QGP, where the chiral condensate (hence most of the constituent quark mass) has vanished. One may guess that the constituent quarks themselves arise from an earlier coalescence of gluons and *current* quarks during the chiral symmetry breaking transition back to hadronic matter, and that the constituent quark flow is carried over from the partonic phase.

However, alternative guesses concerning the relation of partons to the recombination degrees of freedom are also conceivable. Perhaps it is valence current, rather than constituent, quarks that recombine to determine hadron flow and momentum in this moderate- p_T range. In that case, hadronization might proceed through the formation of “pre-hadrons” (*e.g.*, the pointlike color singlet objects discussed in connection with color transparency [52]) from the leading Fock (valence quark only) configurations, giving rise to the same 3-to-2 baryon-to-meson ratios as for constituent quarks. The internal pre-hadron wave functions would then subsequently evolve toward those of ordinary hadrons on their way out of the collision zone, so that the little-modified hadron momentum would in the end be shared substantially among sea quarks and gluons, as well as the progenitor valence quarks. Either of the above speculative (and quite possibly not orthogonal) interpretations of recombination would suggest that the hadron flow originates in, but is two steps removed from, *partonic* collectivity. But it is difficult to draw firm conclusions in light of the present ambiguity in connecting the effective degrees of freedom in coalescence models to the quarks and gluons treated by LQCD.

In addition, it is yet to be demonstrated that the coexistence of coalescence and fragmentation processes is quantitatively consistent with hadron angular correlations observed over p_T ranges where coalescence is predicted to dominate. These correlations exhibit prominent (near-side) peaks with angular

widths (at least in azimuthal difference between two moderate- p_T hadrons) and charge sign ordering characteristic of jets from vacuum fragmentation of hard partons [71]. The coalescence yield might simply contribute to the background underlying these peaks, but one should also expect contributions from the “fast-slow” recombination (hard scattered parton with QGP bath partons) [72] for which the model was first introduced, and these could produce charge sign ordering. The latter effects – part of in-medium, as opposed to vacuum, fragmentation – complicate the interpretation of the baryon/meson comparisons and, indeed, muddy the distinction between fragmentation and recombination processes.

Finally, the picture provided by recombination is distinctly different from ideal hydrodynamics at a hadronic level, where velocity (mass) of a hadron is the crucial factor determining flow, rather than the number of constituent (or valence) quarks. At low momentum, energy and entropy conservations become a serious problem for quark coalescence, placing an effective lower limit on the p_T range over which the models can be credibly applied. The solution of this problem would require a dynamical, rather than purely kinematic treatment of the recombination process [69]. Such parton dynamics at low momentum might account for the thermodynamic properties of the macroscopic system discussed earlier, but we do not yet have a unified partonic theoretical framework.

3 Bulk properties

The multiplicities, yields, momentum spectra and correlations of hadrons emerging from heavy-ion collisions, especially in the soft sector comprising particles at transverse momenta $p_T \lesssim 1.5$ GeV/c, reflect the properties of the bulk of the matter produced in the collision. In particular, we hope to infer constraints on its initial conditions, its degree of thermalization and its Equation of State from measurements of soft hadrons.

The measured hadron spectra reflect the properties of the bulk of the matter at kinetic freezeout, after elastic collisions among the hadrons have ceased. At this stage the system is already relatively dilute and “cold”. However from the detailed properties of the hadron spectra at kinetic freezeout, information about the earlier hotter and denser stage can be obtained. Somewhat more direct information on an earlier stage can be deduced from the integrated yields of the different hadron species, which change only via *inelastic* collisions. These inelastic collisions cease already (at so-called chemical freezeout) before kinetic freezeout.

The transverse momentum distributions of the different particles reflect a random and a collective component. The random component can be identified with the temperature of the system at kinetic freezeout. The collective component arises from the matter density gradient from the center to the boundary of the fireball created in high-energy nuclear collisions. Interactions among constituents push matter outwards; frequent interactions lead to a common constituent velocity distribution. This so-called *collective flow* is therefore sensitive to the strength of the interactions. The collective flow is additive and thus accumulated over the whole system evolution, making it potentially sensitive to the Equation of State of the expanding matter. At lower energies the collective flow reflects the properties of dense hadronic matter [73], while at RHIC energies a contribution from a pre-hadronic phase is anticipated.

In non-central heavy-ion collisions the initial transverse density gradient has an azimuthal anisotropy that leads to an azimuthal variation of the collective transverse flow velocity with respect to the impact parameter plane for the event. This azimuthal variation of flow is expected to be self-quenching (see Sec. 2.2), hence, especially sensitive to the interactions among constituents in the *early* stage of the collision [26,74], when the system at RHIC energies is anticipated to be well above the critical temperature for QGP formation.

Study of quantum (boson) correlations among pairs of emerging hadrons utilizes the Hanbury-Brown-Twiss effect to complement measurements of momentum spectra with information on the spatial size and shape of the emitting system. The measurement of more general two-particle correlations and

of event-wise fluctuations can illuminate the degree of equilibration attained in the final hadronic system, as well as the dynamical origin of any observed non-equilibrium structures. Such dynamical correlations are prevalent in high-energy collisions of more elementary particles – where even relatively soft hadrons originate in large part from the fragmentation of partons – but are expected to be washed out by thermalization processes that produce phase space dominance of the final distribution probabilities.

In this section, we review the most important implications and questions arising from RHIC’s vast body of data on soft hadrons. We also discuss some features of the transition region ($1.5 \lesssim p_T \lesssim 6$ GeV/c), where the spectra gradually evolve toward the characteristic behavior of the hard parton fragmentation regime. In the process of going through the measured features of hadron spectra in the logical sequence outlined above, we devote special attention to a few critical features observed *for the first time* for central and near-central Au+Au collisions at STAR, that bear directly on the case for the QGP:

- hadron yields suggestive of chemical equilibration across the u , d and s quark sectors;
- elliptic flow of soft hadrons attaining the strength expected for an ideal relativistic fluid thermalized very shortly after the collision;
- elliptic flow results at intermediate p_T that appear to arise from the flow of quarks in a pre-hadronic stage of the matter.

3.1 Rapidity Densities

Much has been made of the fact that predictions of hadron multiplicities in RHIC collisions before the year 2000 spanned a wide range of values, so that even the earliest RHIC measurements had significant discriminating power [7,75]. Mid-rapidity charged hadron densities measured in PHOBOS [76] and in STAR [77] are plotted in Fig. 11 as a function of collision centrality, as characterized by the number of participating nucleons, N_{part} , inferred from the fraction of the total geometric cross section accounted for in each analyzed bin. The solid curves in the figure represent calculations within a gluon saturation model [66], while the dashed curves in frames (a) and (b) represent two-component fits to the data [76] and in frames (c) and (d) represent an alternative model [78] assuming saturation of final-state mini-jet production. The apparent logarithmic dependence of the measured pseudorapidity densities on $\langle N_{part} \rangle$ is a characteristic feature of the gluon saturation model [66]. Consequently, the model’s ability to reproduce the measured centrality and energy dependences have been presented as evidence for the relevance of the Color Glass Condensate to the initial state for RHIC collisions, and used to

constrain the saturation scale for initial gluon densities. This scale is in fair agreement with the scale extrapolated from HERA e-p measurements at low Bjorken x [7].

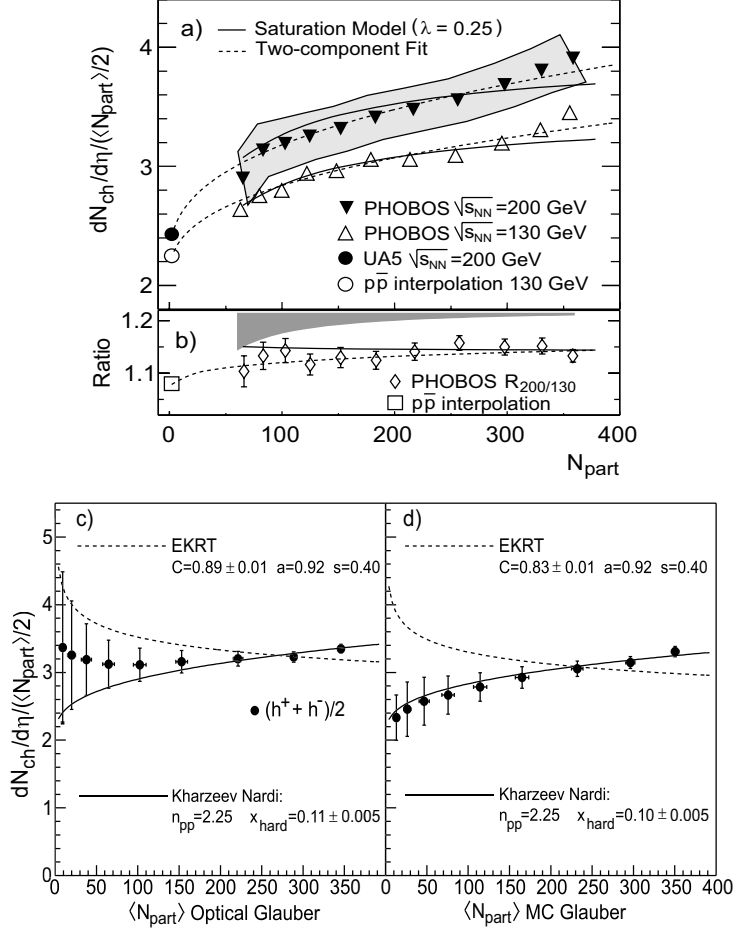


Fig. 11. Measured and calculated pseudorapidity densities $dN_{ch}/d\eta|_{|\eta| \leq 1}/(\langle N_{part} \rangle/2)$ of charged particles from RHIC Au+Au collisions as a function of N_{part} . PHOBOS data [76] at $\sqrt{s_{NN}} = 130$ GeV (open triangles) and 200 GeV (closed triangles) are shown in frame (a), and their ratio is plotted in (b). The open and solid circles in (a) are $\bar{p}p$ collision results. STAR data for 130 GeV [77] are shown in frames (c) and (d), plotted with two different Glauber model treatments to deduce $\langle N_{part} \rangle$. The data plotted in frames (a), (b) and (d) utilize the preferred Monte-Carlo Glauber approach. However, the initial-state gluon saturation model calculations [66] shown as solid curves in all frames have been carried out utilizing the questionable optical approximation to the Glauber treatment, which is applied as well to the experimental results only in frame (c). The dashed curves in frames (a) and (b) represent two-component fits to the data [76] and in frames (c) and (d) represent an alternative model [78] assuming saturation of final-state mini-jet production.

However, these arguments are compromised because the particle multiplicity appears not to have strong discriminating power once one allows for adjustment of theoretical parameters. Furthermore, $\langle N_{part} \rangle$, which affects the scale

on both axes in Fig. 11, is not a direct experimental observable. Glauber model calculations to associate values of $\langle N_{part} \rangle$ with given slices of the geometric cross section distribution have been carried out in two different ways, leading to an inconclusive theory *vs.* experiment comparison in Figs. 11(a) and (b). The preferred method for evaluating Glauber model cross sections in nucleus-nucleus collisions [79] invokes a Monte Carlo approach for integrating over all nucleon configurations, and has been used for the experimental results in frames (a), (b) and (d). However, the gluon saturation model calculations in *all* frames of Fig. 11 have employed the optical approximation, which ignores non-negligible correlation effects [79]. Comparison of the *experimental* results in frames (c) and (d), where the same STAR data have been plotted using these two Glauber prescriptions, illustrates the significant sensitivity to the use of the optical approximation. The “apples-to-apples” comparison of experiment and theory in frame (c) does not argue strongly in favor of initial-state gluon saturation, although an analogous “apples-to-apples” comparison within the Monte Carlo Glauber framework is clearly desirable.

Furthermore, over a much broader energy range, the charged particle multiplicity is found to vary quite smoothly from AGS energies ($\sqrt{s_{NN}} \approx \text{few GeV}$) to the top RHIC energy ($\sqrt{s_{NN}}=200 \text{ GeV}$)[80] (see Fig. 35). One would not expect CGC conditions to be dominant in collisions over this entire range [7], so the apparent success of CGC arguments for RHIC hadron multiplicities is less than compelling. Other evidence more directly relevant to CGC predictions will be discussed in Chap. 4.

Whatever physics ultimately governs the smooth increase in produced particle multiplicity with increasing collision energy and centrality seems also to govern the growth in total transverse energy per unit pseudorapidity ($dE_T/d\eta$). PHENIX measurements at $\sqrt{s_{NN}} = 130 \text{ GeV}$ [81] first revealed that RHIC collisions generate $\approx 0.8 \text{ GeV}$ of transverse energy per produced charged particle near mid-rapidity, independent of centrality – essentially the same value that is observed also in SPS collisions at an order of magnitude lower center-of-mass energy [82]. This trend persists to $\sqrt{s_{NN}} = 200 \text{ GeV}$ [83]. For RHIC central Au+Au collisions, this translates to the conversion of nearly 700 GeV per unit rapidity (dE_T/dy) from initial-state longitudinal to final-state transverse energy [81]. Under simplifying assumptions (longitudinal boost-invariance, free-streaming expansion in which the matter does no work) first suggested by Bjorken [84], one can extract from this observation a crude estimate of the initial spatial energy density of the bulk matter at the start of its transverse expansion:

$$e_{Bj} = \frac{dE_T}{dy} \frac{1}{\tau_0 \pi R^2}, \quad (4)$$

where τ_0 is the formation time and R the initial radius of the expanding system. With reasonable guesses for these parameter values ($\tau_0 \approx 1$ fm/c, $R \approx 1.2A^{1/3}$ fm), the PHENIX $dE_T/d\eta$ measurements suggest an initial energy density ~ 5 GeV/fm³ for central Au+Au collisions at RHIC, well above the critical energy density ~ 1 GeV/fm³ expected from LQCD for the transition to the QGP phase. This estimate of the initial energy density is larger than that in SPS collisions, since the particle multiplicity grows at RHIC, but by a modest factor (≈ 1.6 [81] at $\sqrt{s_{NN}} = 130$ GeV).

3.2 Hadron Yields and Spectra

Figure 12 compares STAR measurements of integrated hadron yield ratios for central Au+Au collisions to statistical model fits. In comparison to results from p+p collisions at similar energies, the relative yield of multi-strange baryons Ξ and Ω is considerably enhanced in RHIC Au+Au collisions [85,86]. The measured ratios are used to constrain the values of system temperature and baryon chemical potential at chemical freezeout, under the statistical model assumption that the system is in thermal and chemical equilibrium at that stage. The excellent fit obtained to the ratios in the figure, including stable and long-lived hadrons through multi-strange baryons, is consistent with the light flavors, u , d , and s , having reached chemical equilibrium (for central and near-central collisions only) at $T_{ch} = 163 \pm 5$ MeV [37,85–87]. (The deviations of the short-lived resonance yields, such as those for Λ^* and K^* collected near the right side of Fig. 12, from the statistical model fits, presumably result from hadronic rescattering after the chemical freezeout.)

Although the success of the statistical model in Fig. 12 might, in isolation, indicate hadron production mechanisms dominated by kinematic phase space in elementary collisions (see Sec. 2.3), other measurements to be discussed below suggest that true thermal and chemical equilibration is at least approximately achieved in heavy-ion collisions at RHIC by interactions among the system's constituents. The saturation of the strange sector yields, attained for the first time in near-central RHIC collisions, is particularly significant. The saturation is indicated quantitatively by the value obtained for the non-equilibrium parameter γ_s for the strange sector [88], included as a free parameter in the statistical model fits. As seen in the inset of Fig. 12, γ_s rises from ≈ 0.75 in peripheral Au+Au collisions to values statistically consistent with unity [85,86] for central collisions. The temperature deduced from the fits is essentially equal to the critical value for a QGP-to-hadron-gas transition predicted by LQCD [2,14], but is also close to the Hagedorn limit for a hadron resonance gas, predicted without any consideration of quark and gluon degrees of freedom [25].¹ If thermalization is indeed achieved by the bulk matter *prior*

¹ Note that Hagedorn himself considered the Hagedorn temperature and the LQCD

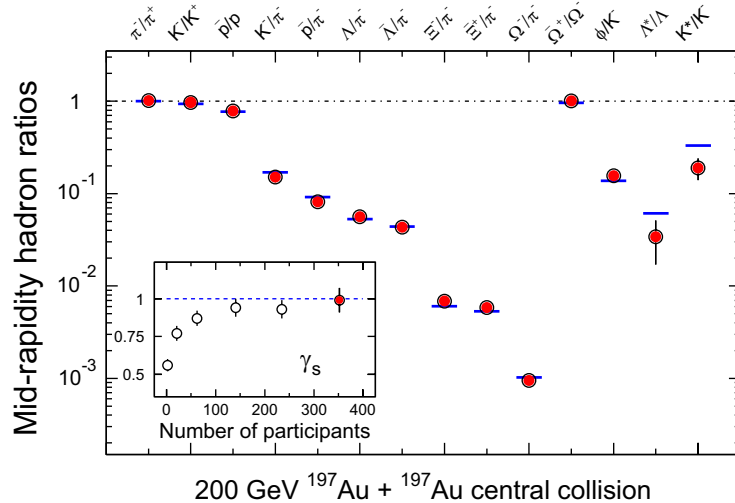


Fig. 12. Ratios of p_T -integrated mid-rapidity yields for different hadron species measured in STAR for central Au+Au collisions at $\sqrt{s_{\text{NN}}} = 200$ GeV. The horizontal bars represent statistical model fits to the measured yield ratios for stable and long-lived hadrons. The fit parameters are $T_{\text{ch}} = 163 \pm 4$ MeV, $\mu_B = 24 \pm 4$ MeV, $\gamma_s = 0.99 \pm 0.07$ [86]. The variation of γ_s with centrality is shown in the inset, including the value (leftmost point) from fits to yield ratios measured by STAR for 200 GeV $p+p$ collisions.

to chemical freezeout, then the deduced value of T_{ch} represents a lower limit on that thermalization temperature.

The characteristics of the system at *kinetic* freezeout can be explored by analysis of the transverse momentum distributions for various hadron species, some of which are shown in Fig. 13. In order to characterize the transverse motion, hydrodynamics-motivated fits [90] have been made to the measured spectra, permitting extraction of model parameters characterizing the random (generally interpreted as a kinetic freezeout temperature T_{fo}) and collective (radial flow velocity $\langle\beta_T\rangle$) aspects. Results for these parameters are shown for different centrality bins and different hadron species in Fig. 14. (While theoretical studies [90] suggest caution in interpreting spectrum fits made without correction for resonance feed-down, as is the case in Fig. 14, auxiliary STAR analyses show little quantitative effect of the feed-down within the STAR p_T coverage.)

As the collisions become more and more central, the bulk of the system, dominated by the yields of π , K , p , appears from Fig. 14 to grow cooler at kinetic freezeout and to develop stronger collective flow. These results may indicate a more rapid expansion after chemical freezeout with increasing collision centrality. On the other hand, even for the most central collisions, the spectra for multi-strange particles ϕ and Ω appear, albeit with still large uncertainties,

critical temperature to be identical [89].

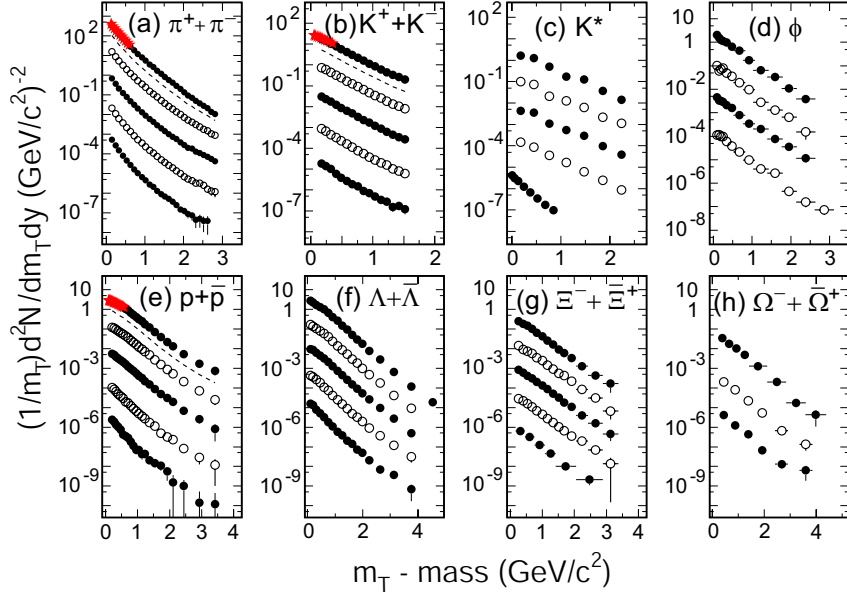


Fig. 13. Mid-rapidity hadron spectra from $\sqrt{s_{\text{NN}}} = 200$ GeV Au+Au collisions, as reported in Refs. [87,94–96]. The spectra are displayed for steadily decreasing centrality from the top downwards within each frame, with appropriate scaling factors applied to aid visual comparison of the results for different centralities. For K^* only, the lowest spectrum shown is for 200 GeV $p + p$ collisions. The dashed curves in frames (a), (b) and (e) represent spectra from minimum-bias collisions. The invariant spectra are plotted as a function of $m_T - \text{mass} \equiv \sqrt{p_T^2/c^2 + \text{mass}^2} - \text{mass}$.

to reflect a higher temperature [86]. The ϕ and Ω results suggest diminished hadronic interactions with the expanding bulk matter after chemical freezeout [85,86,91,92], as predicted [28,33,93] for hadrons containing no valence u or d quarks. If this interpretation is correct, the substantial radial flow velocity inferred for ϕ and Ω would have to be accumulated prior to chemical freezeout, giving the multi-strange hadrons perhaps greater sensitivity to collective behavior during earlier partonic stages of the system evolution.

As one moves beyond the soft sector, the p_T - and centrality dependences of the observed hadron spectra develop a systematic difference between mesons and baryons, distinct from the mass-dependence observed at lower p_T . This difference is illustrated in Fig. 15 by the binary-scaled ratio R_{CP} of hadron yields for the most central vs. a peripheral bin, corrected by the expected ratio of contributing binary nucleon-nucleon collisions in the two centrality bins [96]. The results are plotted as a function of p_T for mesons and baryons separately in panels (a) and (b), respectively, with the ratio of binary collision-scaled yields of all charged hadrons indicated in both panels by a dot-dashed curve to aid comparison. If the centrality-dependence simply followed the number of binary collisions, one would expect $R_{CP} = 1$. This condition is nearly achieved for baryons near $p_T \approx 2.5$ GeV/c, but is never reached for mesons. The initial results for ϕ -mesons and Ω -baryons included in Fig. 15 suggest that the

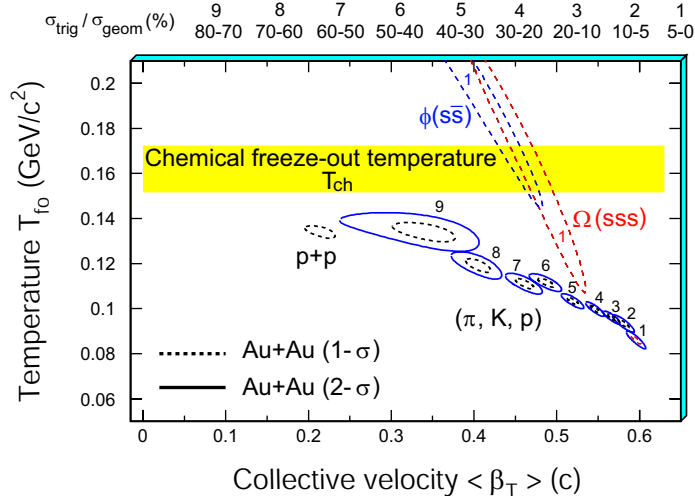


Fig. 14. The χ^2 contours, extracted from thermal + radial flow fits (without allowance for resonance feed-down), for copiously produced hadrons π, K and p and multi-strange hadrons ϕ and Ω . On the top of the plot, the numerical labels indicate the centrality selection. For π, K and p , 9 centrality bins (from top 5% to 70-80%) were used for $\sqrt{s_{NN}} = 200$ GeV Au+Au collisions [87]. The results from $p + p$ collisions are also shown. For ϕ and Ω , only the most central results [86] are presented. Dashed and solid lines are the 1- σ and 2- σ contours, respectively.

difference is not very sensitive to the mass of the hadron, but rather depends primarily on the number of valence quarks contained within it. The meson and baryon values appear to merge by $p_T \approx 5$ GeV/c, by which point $R_{CP} \approx 0.3$.

The origin of this significant shortfall in central high- p_T hadron production will be discussed at length in Sec. 4. Here, we want simply to note that the clear difference seen in the centrality dependence of baryon vs. meson production is one of the defining features of the intermediate p_T range from ~ 1.5 to ~ 6 GeV/c in RHIC heavy-ion collisions, and it cannot be understood from $p + p$ collision results [97]. Another defining feature of this medium p_T range, to be discussed further below, is a similar meson-baryon difference in elliptic flow. Both facets of the meson-baryon differences can be explained naturally in quark recombination models for hadron formation [69].

3.3 Hadron yields versus the reaction plane

In non-central heavy-ion collisions, the beam direction and the impact parameter define a reaction plane for each event, and hence a preferred azimuthal orientation. The orientation of this plane can be estimated experimentally by various methods, *e.g.*, using 2- or 4-particle correlations [98,99], with different sensitivities to azimuthal anisotropies not associated with collective flow. The observed particle yield versus azimuthal angle with respect to the event-

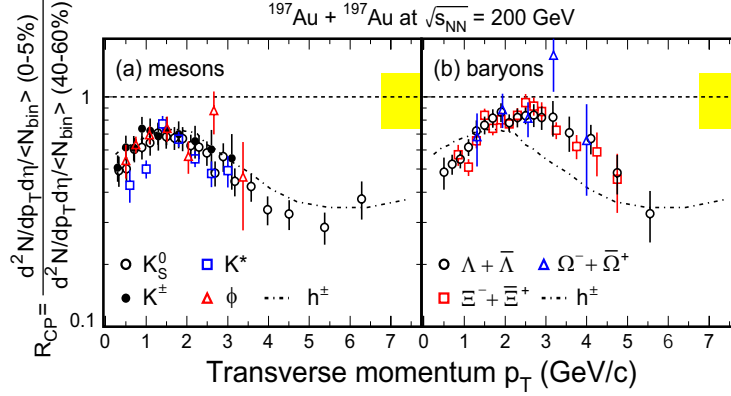


Fig. 15. *STAR* results [96] from $\sqrt{s_{NN}} = 200$ GeV Au+Au collisions for the ratio of mid-rapidity hadron yields R_{CP} in a central (0-5%) over a peripheral (40-60%) bin, plotted vs. p_T for mesons (a) and baryons (b). The yields are scaled in each centrality region by the calculated mean number $\langle N_{bin} \rangle$ of binary contributing nucleon-nucleon collisions, calculated within a Monte Carlo Glauber model framework. The width of the shaded band around the line at unity represents the systematic uncertainty in model calculations of the centrality dependence of $\langle N_{bin} \rangle$. R_{CP} for the sample of all charged hadrons is also shown by dot-dashed curves in both plots. The error bars on the measured ratios include both statistical and systematic uncertainties.

by-event reaction plane promises information on the early collision dynamics [27,74]. The anisotropy of the particle yield versus the reaction plane can be characterized in a Fourier expansion. Due to the geometry of the collision overlap region the second coefficient of this Fourier series – v_2 , often referred to as the elliptic flow – is expected to be the dominant contribution.

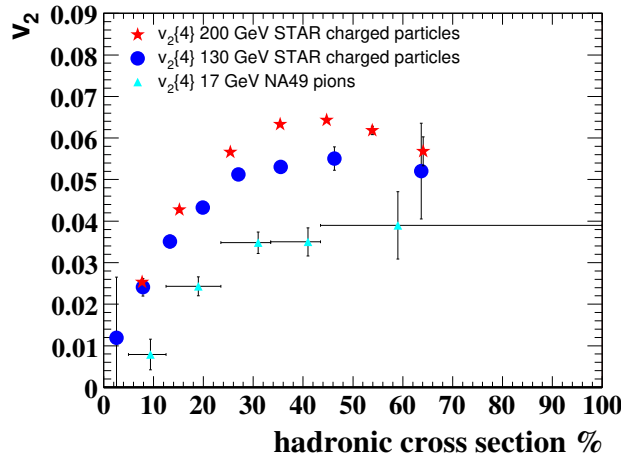


Fig. 16. Centrality dependence of v_2 , integrated over p_T . The triangles are the NA49 measurements for pions at $\sqrt{s_{NN}} = 17$ GeV [100]. The circles and crosses are *STAR* measurements for charged particles at $\sqrt{s_{NN}} = 130$ GeV [101] and 200 GeV [102], respectively. The 4-particle cumulant method has been used to determine v_2 in each case.

Figure 16 shows the mid-rapidity elliptic flow measurements, integrated over

transverse momentum, as a function of collision centrality for one SPS [100] and two RHIC [101,102] energies. One clearly observes a characteristic centrality dependence that reflects the increase of the initial spatial eccentricity of the collision overlap geometry with increasing impact parameter. The integrated elliptic flow value for produced particles increases about 70% from the top SPS energy to the top RHIC energy, and it appears to do so smoothly as a function of energy (see Fig. 34), so far exhibiting no obvious “dip” of the sort predicted [30] by ideal hydrodynamics in Fig. 7.

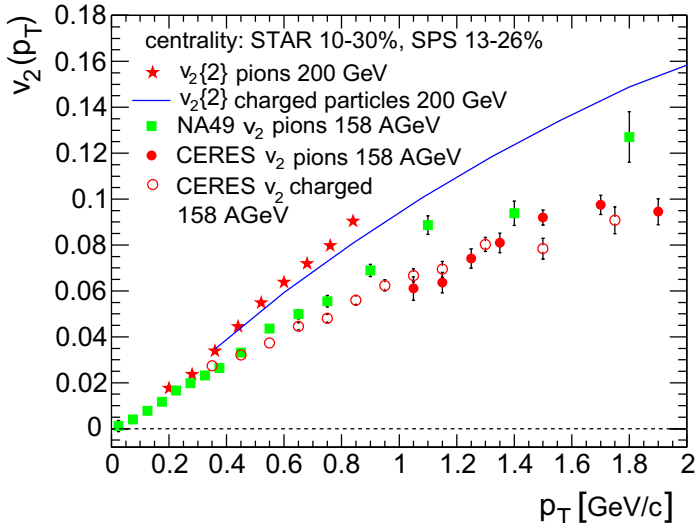


Fig. 17. $v_2(p_t)$ for one centrality (10-30%) range. The circles and squares are the CERES [103] and NA49 [100] measurements, respectively, at $\sqrt{s_{NN}} = 17$ GeV. The stars and the solid line are STAR measurements [102] for pions and for all charged particles, respectively, at $\sqrt{s_{NN}} = 200$ GeV (evaluated here by the 2-particle correlation method).

The origin of the energy dependence can be discerned by examining the differential $v_2(p_t)$, shown for the centrality selection 10–30% in Fig. 17. The comparison of the results for pions at $\sqrt{s_{NN}} = 200$ GeV and at the top SPS energy clearly reveals an increase in slope vs. p_T that accounts for part of the increase in p_T -integrated v_2 from SPS to RHIC. The remaining part of the change is due to the increase in $\langle p_t \rangle$. As measurements become available at more collision energies, it will be important to remove kinematic effects, such as the increase in $\langle p_t \rangle$, from comparisons of results, as they might mask finer, but still significant, deviations from smooth energy dependence.

Collective motion leads to predictable behavior of the shape of the momentum spectra as a function of particle mass, as reflected in the single inclusive spectra in Fig. 13. It is even more obvious in the dependence of $v_2(p_t)$ for the different mass particles. Figure 18 shows the measured low- p_T v_2 distributions from 200 and 130 GeV Au+Au minimum bias collisions. Shown are the measurements for charged pions, K_S^0 , antiprotons and Λ [104,105]. The clear, systematic

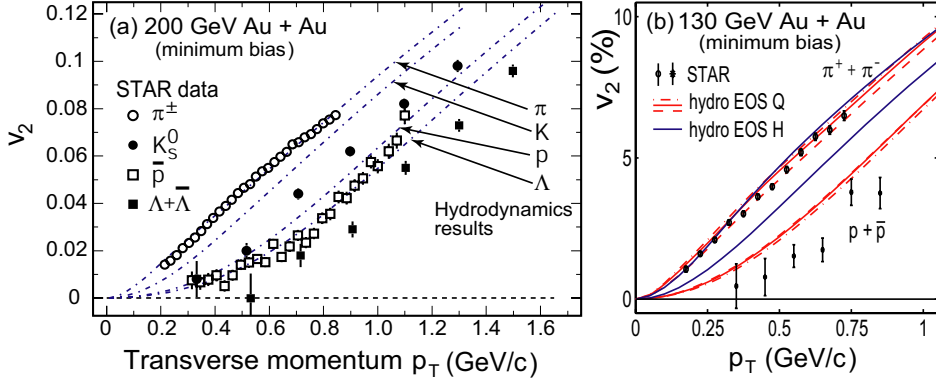


Fig. 18. (a) STAR experimental results of the transverse momentum dependence of the elliptic flow parameter in 200 GeV Au+Au collisions for charged $\pi^+ + \pi^-$, K_S^0 , \bar{p} , and Λ [104]. Hydrodynamics calculations [32,106] assuming early thermalization, ideal fluid expansion, an equation of state consistent with LQCD calculations including a phase transition at $T_c=165$ MeV (EOS Q in [32] and Fig. 5), and a sharp kinetic freezeout at a temperature of 130 MeV, are shown as dot-dashed lines. Only the lower p_T portion ($p_T \leq 1.5$ GeV/c) of the distributions is shown. (b) Hydrodynamics calculations of the same sort as in (a), now for a hadron gas (EOS H) vs. QGP (EOS Q) equation of state (both defined in Fig. 5) [3,32], compared to STAR v_2 measurements for pions and protons in minimum bias 130 GeV Au+Au collisions [105]. Predictions with EOS Q are shown for a wider variety of hadron species in Fig. 8.

mass-dependence of v_2 shown by the data is a strong indicator that a common transverse velocity field underlies the observations. This mass-dependence, as well as the absolute magnitude of v_2 , is reproduced reasonably well (*i.e.*, at the $\pm 30\%$ level) by the hydrodynamics calculations shown in Fig. 18. Parameters of these calculations have been tuned to achieve good agreement with the measured spectra for different particles, implying that they account for the observed radial flow and elliptic flow simultaneously. In particular, since the parameters are tuned for zero impact parameter, the theory-experiment comparison for v_2 as a function of centrality represents a significant test of these hydrodynamics calculations.

The agreement of these hydrodynamics calculations, which assume *ideal* relativistic fluid flow, with RHIC spectra and v_2 results is one of the centerpieces of recent QGP discovery claims [6–8]. The agreement appears to be optimized (though still with some quantitative differences, see Fig. 18) when it is assumed that local thermal equilibrium is attained very early ($\tau < 1$ fm/c) during the collision, and that the hydrodynamic expansion is characterized by an EOS (labeled Q in Fig. 18) containing a soft point roughly consistent with the LQCD-predicted phase transition from QGP to hadron gas [3,29,32]. When the expanding matter is treated as a pure hadron gas (EOS H in Fig. 18(b)), the mass-dependence of v_2 is significantly underpredicted. The inferred early thermalization suggests that the collision's early stages are dominated by very

strongly interacting matter with very short constituent mean free paths – essentially a “perfect liquid” [107], free of viscosity. Similar QGP-based calculations that invoke ideal hydrodynamics up to freezeout overpredict the elliptic flow for more peripheral RHIC collisions and for lower energies. One possible interpretation of this observation is that thermalized, strongly interacting QGP matter dominates near-central Au+Au collisions at or near the full RHIC energy.

In assessing these claims, it is critical to ask how unique and robust the hydrodynamics account is in detail for the near-central RHIC collision flow measurements (radial and elliptic). Might the observed v_2 result alternatively from a harder EOS (such as EOS H) combined with later achievement of thermalization or with higher viscosity [35] (both conditions impeding the development of collective flow)? How does the sensitivity to the EOS in the calculations compare quantitatively with the sensitivity to other ambiguities or questionable assumptions in the hydrodynamics treatments? For example, the particular calculations in Fig. 18 [32,106] invoke a simplified treatment with a sharp onset of kinetic freezeout along a surface of constant energy density corresponding to $T_{fo} \approx 130$ MeV. The sensitivity to the assumed value of T_{fo} , if it is kept within the range spanned by the measurements in Fig. 14, is relatively weak [32]. However, alternative approaches combining ideal hydrodynamics for the partonic stage with a hadron transport (RQMD) treatment of the presumably viscous hadronic stage [29] yield similar success in accounting for RHIC results, but certainly predict a dependence of v_2 on collision energy differing significantly from the sharp-freezeout predictions (compare Fig. 7 and Fig. 9). While the combination of partonic hydrodynamics and hadron transport offers the promise of a reasonable QGP-based account for the observed smooth energy dependence of p_T -integrated v_2 (see Figs. 9,34), it also serves to emphasize that quantitative ambiguities of scale comparable to the EOS sensitivity remain to be understood.

In addition to questions about the thermalization time, viscosity and freezeout treatment, one also needs to address the robustness of the standard assumption of longitudinal boost-invariance in hydrodynamics calculations [3]. There is growing evidence at RHIC for significant deviations from boost-invariance. This is illustrated by PHOBOS results for v_2 as a function of pseudorapidity in Fig. 19, where one sees no evidence for a mid-rapidity plateau in elliptic flow strength [108]. Thus, while the successes of QGP-based hydrodynamics calculations at RHIC are tantalizing, substantially greater systematic investigation of their sensitivities – including computationally challenging full three-dimensional treatments – would be needed to make a compelling QGP claim on their basis alone.

At higher p_T values, as shown by experimental results from 200 GeV Au+Au minimum bias collisions in Fig. 20, the observed values of v_2 saturate and the

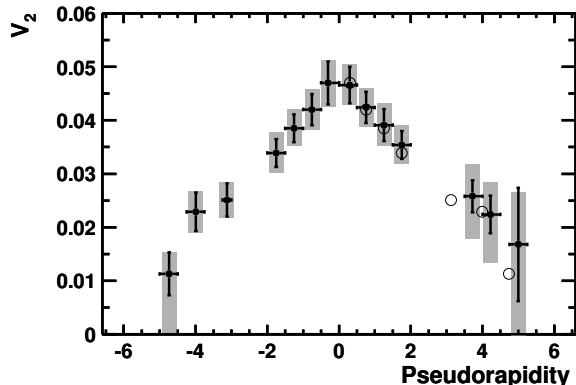


Fig. 19. Azimuthal anisotropies v_2 measured by the PHOBOS collaboration [108] for Au+Au collisions at $\sqrt{s_{\text{NN}}}=130$ GeV, as a function of pseudorapidity. Within each pseudorapidity bin, the results are averaged over all charged particles, over all centralities and over all p_T . The black error bars are statistical and the grey bands systematic uncertainties. The points on the negative side are reflected about $\eta = 0$ and plotted as open circles on the positive side, for comparison. Figure taken from Ref. [108].

level of the saturation differs substantially between mesons and baryons. Hydrodynamics calculations overpredict the flow in this region. The dot-dashed curves in Fig. 20(a)-(c) represent simple analytical function fits to the measured K_S^0 and $\Lambda + \bar{\Lambda}$ v_2 distributions [104,109]. It is seen in Fig. 20 (a) and (b) that STAR's most recent v_2 results for the multi-strange baryons Ξ and Ω [110] are consistent with that of Λ 's, but within still sizable statistical uncertainties.

In Fig. 20 (c), particle-identified elliptic flow measurements for the 200 GeV Au+Au minimum-bias sample are combined by dividing both v_2 and p_T by the number of valence quarks (n_q) in the hadron of interest. The apparent scaling behavior seen in this figure for $p_T/n_q > 1$ GeV/c is intriguing, as the data themselves seem to be pointing to constituent quarks (or at least to valence quarks sharing the full hadron momentum, see Sec. 2.6) as the most effective degree of freedom in determining hadron flow at intermediate p_T values. The data need to be improved in statistical precision and p_T extent for more identified mesons and baryons in order to establish this scaling more definitively. Within error bars the size of those for $p_T/n_q > 1$ GeV/c, the low p_T data would also look as though they scale with the number of constituent quarks, whereas we already have seen in Fig. 18 that there is rather a clear hydrodynamic mass-dependence in the low p_T region. (Note that the pion data barely extend into the scaling region at $p_T/n_q > 1$ GeV/c.)

If the scaling behavior at intermediate p_T is confirmed with improved data, it will provide a very important clue to the origin of the meson-baryon differences (see also Fig. 15) that characterize this p_T range. In particular, both the v_2 scaling and the meson-baryon R_{CP} differences can be explained [69,112]

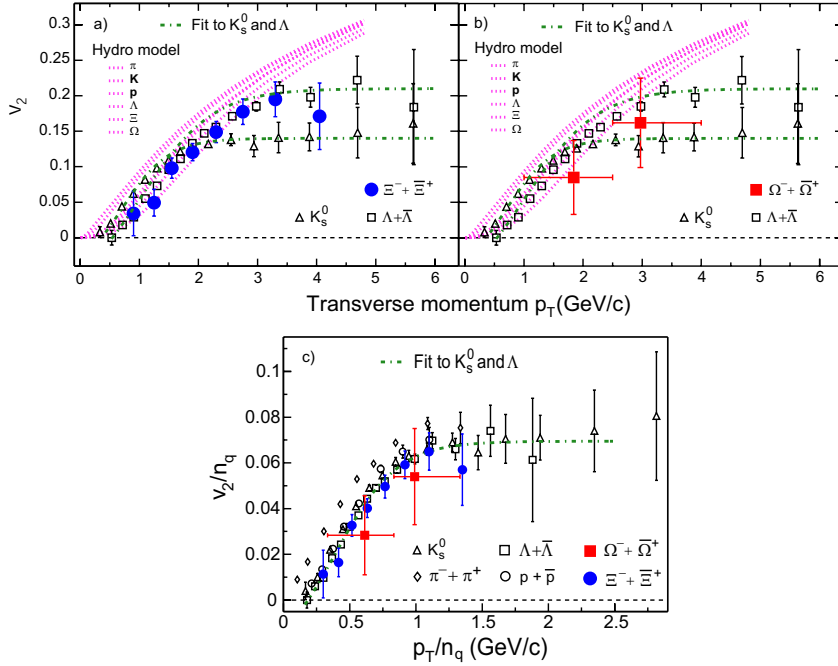


Fig. 20. *Experimental results on the transverse momentum dependence of the event elliptic anisotropy parameter for various hadron species produced in minimum-bias Au+Au collisions at $\sqrt{s_{NN}} = 200$ GeV. STAR results [104] for K_S^0 and $\Lambda + \bar{\Lambda}$ are shown in all frames, together with simple analytic function fits (dot-dashed lines) to these data. Additional data shown are STAR multi-strange baryon elliptic flow [110] for Ξ (in frames (a) and (c)) and Ω ((b) and (c)), and PHENIX results [111] for π and $p + \bar{p}$ (frame (c)). Hydrodynamics calculations are indicated by dotted curves in frames (a) and (b). In (c), the flow results for all of the above hadrons are combined by scaling both v_2 and p_T by the number of valence quarks (n_q) in each hadron. The figure is an update of one in [109].*

(see Fig. 21) by assuming that hadron formation at moderate p_T proceeds via two competing mechanisms: the coalescence of n_q constituent quarks at transverse momenta $\sim p_T/n_q$, drawn from a thermal (exponential) spectrum [69], plus more traditional fragmentation of hard-scattered partons giving rise to a power-law component of the spectrum. Note that, as discussed in section 2.6, these models are not expected to apply at low p_T . It is not yet clear that the same models could simultaneously account as well for another observed feature characteristic of this intermediate p_T range, namely, a jet-like azimuthal correlation of hadron pairs that will be discussed further in Sec. 4.

In these coalescence models, the constituent quarks carry their own substantial azimuthal anisotropy, which is then summed to give the hadron v_2 . The establishment of clearer evidence for such pre-hadronic collective flow would be an important milestone in elucidating the nature of the matter produced in RHIC collisions. In interpreting such evidence, it must be kept in mind that constituent quarks are not partons: they are effective degrees of freedom nor-

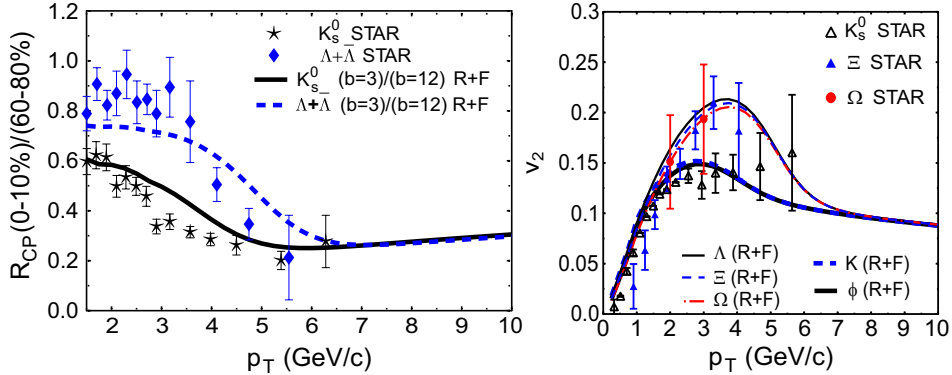


Fig. 21. Comparisons of calculations in the Duke quark recombination model [69,112] with STAR measurements [104,110] of (a) R_{CP} and (b) v_2 for strange mesons and baryons. “R+F” denotes the sum of recombination and fragmentation contributions. Comparison of the solid and broken curves in (b) reveals a weak mass-dependence in the calculations, superimposed on the predominant meson-baryon differences. The figures are taken from Ref. [70], and they include preliminary STAR data for multi-strange baryons that differ slightly from the values shown in Fig. 20.

mally associated with chiral symmetry breaking and confinement, rather than with the deconfinement of a QGP. Until the mechanism for the emergence of these effective degrees of freedom from a QCD plasma of current quarks and gluons is clarified (see Sec. 2.6), collectively flowing constituent quarks should not be taken as definitive proof of a QGP stage, as we have defined it in Sec. 1. It is unclear, for example, whether the characteristic time scale for constituent quarks to coalesce from current quarks and gluons might not be shorter than that for the establishment of thermalization in the collision (leading to a sort of “constituent quark plasma”, as opposed to a QGP). Furthermore, the constituent quark v_2 values needed to account for the observed hadron v_2 saturation might arise in part from differential energy loss of their progenitor partons in traversing the spatially anisotropic matter of non-central collisions [47], rather than strictly from the partonic hydrodynamic flow assumed in [112]. The unanticipated RHIC results in this intermediate p_T range thus raise a number of important and fascinating questions that should be addressed further by future measurements and theoretical calculations.

In summary, the measured yields with respect to the reaction plane are among the most important results to date from RHIC: they provide critical hints of the properties of the bulk matter at early stages. They indicate that it behaves collectively, and is consistent with rapid (*i.e.*, very short mean free path) attainment of at least approximate local thermal equilibrium in a QGP phase. Hydrodynamic accounts for the mass- and p_T -dependence of v_2 for soft hadrons appear to favor system evolution through a soft, mixed-phase EOS. The saturated v_2 values observed for identified mesons and baryons in the range $1.5 \lesssim p_T \lesssim 6$ GeV/c suggest that hadronization in this region

occurs largely via coalescence of collectively flowing constituent quarks. What has yet to be demonstrated is that these interpretations are unique and robust against improvements to both the measurements and the theory. In particular, it must be demonstrated more clearly that the sensitivity to the role of the QGP outweighs that to other, more mundane, ambiguities in the theoretical treatment.

3.4 Quantum Correlation Analyses

Two-hadron correlation measurements in principle should provide valuable information on the phase structure of the system at freezeout. From the experimentally measured momentum-space two-particle correlation functions, a Fourier transformation is then performed in order to extract information on the space-time structure [113]. Bertsch-Pratt parameterization [114] is often used to decompose total momentum in such measurements into components parallel to the beam (*long*), parallel to the pair transverse component (*out*) and along the remaining third direction (*side*). In this Cartesian system, information on the source duration time is mixed into the *out* components. Hence, the ratio of inferred emitting source radii R_{out}/R_{side} is sensitive to the time duration of the source emission. For example, if a QGP is formed in collisions at RHIC, a long duration time and consequently large value of R_{out}/R_{side} are anticipated [115].

Measured results for Hanbury-Brown-Twiss (HBT) pion interferometry, exploiting the boson symmetry of the two detected particles at low relative momenta, are shown in Figs. 22 and 23. A clear dependence of the ‘size’ parameters on the pair transverse momentum k_T is characteristic of collective expansion of the source [116,117], so the results are plotted vs. k_T in Fig. 22. As indicated by the set of curves in the figure, hydrodynamics calculations that can account for hadron spectra and elliptic flow at RHIC systematically over-predict R_{out}/R_{side} [116,118]. One possible implication of this discrepancy is that the collective expansion does not last as long in reality as in the hydrodynamics accounts. However, shorter expansion times are difficult to reconcile with the observed magnitude of R_{side} , and are not supported by a recent systematic study of HBT correlations relative to the event-by-event reaction plane [117]. The source eccentricity at freezeout inferred from these azimuthally sensitive measurements is shown in Fig. 23 to retain a significant fraction of the initial spatial eccentricity characteristic of the impact parameter for each centrality bin. The observed eccentricity retention is, in fact, quantitatively consistent with hydrodynamics expectations for the *time-integrated* pion emission surface to which HBT is sensitive [119]. Thus, the deformations in Fig. 23 tend to support the hydrodynamics view of the expansion pressure and timeline (see Fig. 6), which lead to an eventual complete quenching of the

initial configuration-space anisotropy by the end of the freezeout process.

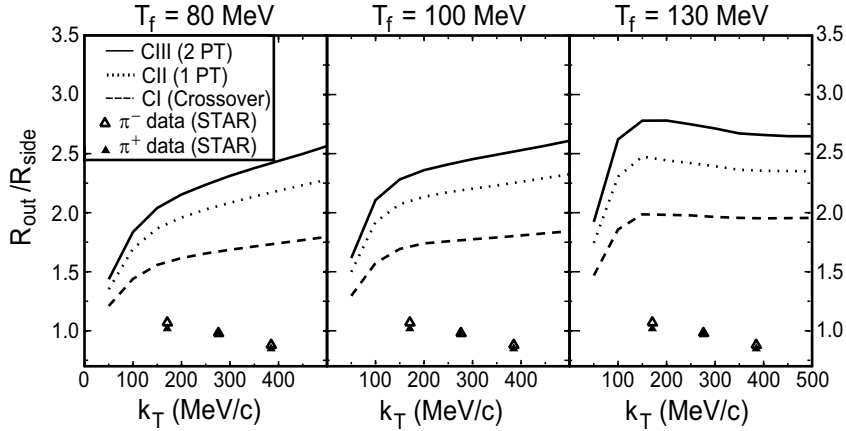


Fig. 22. STAR measurements [116] of R_{out}/R_{side} from pion HBT correlations for central Au+Au collisions, plotted as a function of the pion pair transverse momentum k_T . The experimental results are identical in the three frames, but are compared to hydrodynamics calculations [118] performed for a variety of parameter values.

The failure of the hydrodynamics calculations to account for the HBT results in Fig. 22 raises another significant issue regarding the robustness of the hydrodynamics success in reproducing v_2 and radial flow data. Although the HBT interference only emerges after the freezeout of the strong interaction, whose treatment is beyond the scope of hydrodynamics, the measured correlation functions receive contributions from all times during the collision process. Furthermore, these HBT results are extracted from the low p_T region, where soft bulk production dominates. It is thus reasonable to expect the correct hydrodynamics account of the collective expansion to be consistent with the HBT source sizes. If improved treatment of the hadronic stage and/or the introduction of finite viscosity during the hydrodynamic expansion [35] are necessary to attain this consistency, then it is important to see how those improvements affect the agreement with elliptic flow and spectra.

STAR has also measured two-hadron momentum-space correlation functions for *non-identical* particles [121]. These are sensitive to differences in the average emission time and position for the different particle species. Such differences are very clearly revealed by the measured correlations between pions and kaons [121], and provide additional strong evidence for a collective transverse flow of the produced hadrons.

3.5 Correlations and fluctuations

A system evolving near a phase boundary should develop significant dynamical fluctuations away from the mean thermodynamic properties of the matter. For

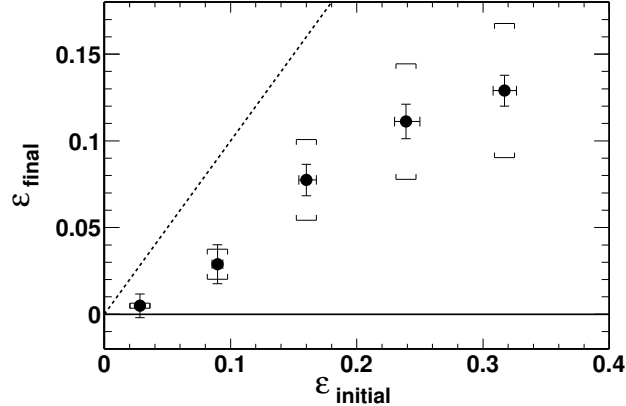


Fig. 23. The eccentricity ϵ_{final} of the time-integrated emitting source of soft pions, inferred from STAR HBT correlations measured with respect to the reaction plane, plotted versus the initial spatial eccentricity $\epsilon_{\text{initial}}$ deduced from a Glauber calculation for five different Au+Au centrality bins. The dotted line represents $\epsilon_{\text{final}} = \epsilon_{\text{initial}}$. See [117] for details.

high-energy heavy ion collisions, it has been predicted that the general study of two-particle correlations and event-wise fluctuations might provide evidence for the formation of matter with partonic degrees of freedom [122–127]. In addition, nonstatistical correlations and fluctuations may be introduced by incomplete equilibrium [128]. With its large acceptance and complete event-by-event reconstruction capabilities, the STAR detector holds great potential for fluctuation analyses of RHIC collisions.

An approach that has been used previously [129,130] to search for the presence of dynamical correlations involves extraction of measures of the excess variance of some observable above the statistical fluctuations that show up even in mixed-event samples. An example shown in Fig. 24 utilizes the square root of the covariance in p_T for charged-particle pairs from collisions at SPS (CERES [129]) and at STAR [131]. The presence of dynamical 2-particle correlations is revealed by non-zero values of this quantity, whose gross features exhibit a magnitude and a smooth centrality-dependence that are essentially independent of collision energy, once the variations of the inclusive mean p_T values ($\langle\langle p_T \rangle\rangle$) with centrality and energy have been divided out. However, the detailed nature of the dynamical correlations is best probed by fully exploiting the impressive statistical precision at STAR to investigate finer, multi-dimensional aspects of the correlation densities themselves, rather than of the integrals of correlation densities represented by excess variance measures.

For example, emerging STAR angular correlation results are already suggesting that there is appreciable soft hadron emission before the attainment of local thermal equilibrium, even in the most central RHIC collisions. The evidence resides in remnants of jet-like behavior observed [132] even in soft

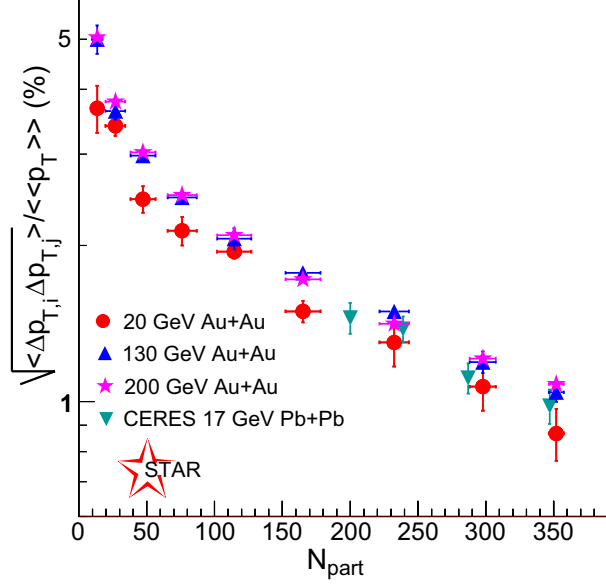


Fig. 24. The square root of the transverse momentum covariance for charged particle pairs, scaled by the inclusive mean p_T value for each centrality and collision energy, plotted vs. centrality for SPS [129] and RHIC [131] data at several energies. Both the centrality-dependence (nearly $\propto 1/N_{part}$) and magnitude of this quantity are essentially unchanged from SPS to RHIC energies, but its implicit integration of correlation densities over the full detector acceptance masks other interesting correlation features.

($0.15 \leq p_T \leq 2.0$ GeV/c) hadron pair correlations on the angular difference variables $\Delta\eta \equiv \eta_1 - \eta_2$ (pseudorapidity) and $\Delta\phi \equiv \phi_1 - \phi_2$ (azimuthal angle), presented for peripheral and central Au+Au collisions in Fig. 25. The equivalent correlations for p+p collisions at RHIC [132] emphasize the central role of parton fragmentation, even down to hadron transverse momenta of 0.5 GeV/c, resulting in a prominent near-side jet peak symmetric about $\Delta\eta = \Delta\phi = 0$ and a broad $\Delta\eta$ -independent away-side ($\Delta\phi = \pi$) jet ridge. One certainly anticipates some remnants of these correlations to survive in heavy-ion collisions at sufficiently high hadron p_T , and these correlations will be discussed in the next chapter. In the soft sector, however, attainment of a fully equilibrated state of all emerging hadrons at freezeout would wash out such initial hard-scattering dynamical correlations.

Instead, the observed soft-hadron-pair correlation for central Au+Au collisions shown in the upper right-hand frame of Fig. 25, after removal of multipole components representing elliptic flow (v_2) and momentum conservation (v_1) [132], exhibits a substantially modified remnant of the jet correlation on the near side, affecting typically 10-30% of the detected hadrons. Contributions to this near-side peak from HBT correlations and Coulomb final-state interactions between hadrons have been suppressed by cuts to remove pairs at very low relative momentum, reducing the overall strength of the correlation near $\Delta\eta = \Delta\phi = 0$ by $\sim 10\%$ [132]. Simulations demonstrate that resonance de-

cays make no more than a few percent contribution to the remaining near-side correlation strength. (The lack of evidence for any remaining away-side correlation in central collisions will be discussed further in the high- p_T context in Sec. 4. Its absence even for more peripheral collisions in the upper left frame of Fig. 25 can be attributed to the broad centrality bin used here to compensate for limited statistics in the 130 GeV Au+Au data sample, and to the v_1 subtraction that removes thermalized soft hadrons balancing the near-side jet's momentum.)

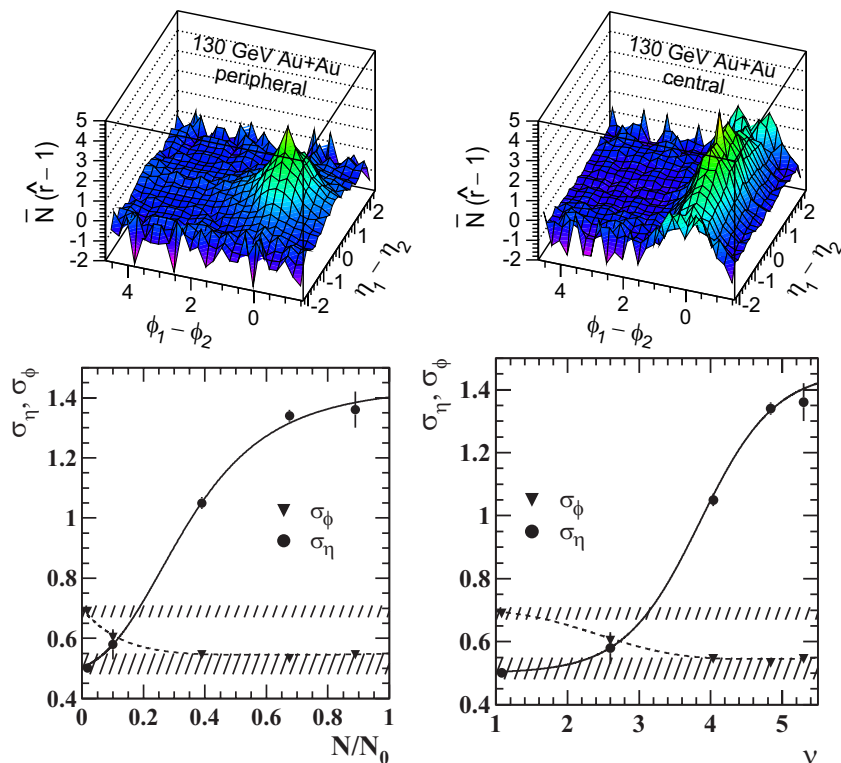


Fig. 25. Upper frames: joint autocorrelations measured by STAR, as a function of the hadron pair angle differences $\eta_1 - \eta_2$ and $\phi_1 - \phi_2$, for $0.15 \leq p_T \leq 2.0$ GeV/c charged hadrons detected in 130 GeV Au+Au collisions [132]. The right frame contains data for central collisions, while the left frame spans a broad range of centralities for more peripheral collisions. The quantity $\overline{N}(\hat{r}-1)$ plotted on the vertical axes represents the average multiplicity for the selected centrality bin multiplied by the relative difference in charged particle pair yields between same events and mixed events. Elliptic flow and momentum conservation long-range correlations have been subtracted, as explained in [132]. Lower frames: centrality-dependence of the Au+Au pseudorapidity and azimuthal widths from two-dimensional gaussian fits to the near-side correlation structure seen for two centrality bins in the upper frames. The same extracted widths for Au+Au collisions are plotted vs. two different measures of centrality: the observed charged-particle multiplicity divided by its maximum value (on the left), and the mean number ν of nucleons encountered by a typical participant nucleon (right). The hatched bands indicate the widths observed for p+p collisions, and the curves guide the eye.

The observed near-side correlation in central Au+Au is clearly much broader in $\Delta\eta$ than that in p+p or peripheral Au+Au collisions. The pseudorapidity spread, as characterized by the $\Delta\eta$ width of a two-dimensional gaussian function fitted to the structure (ignoring the $\Delta\eta = \Delta\phi = 0$ bin, where conversion electron pairs contribute), grows rapidly with increasing collision centrality, as revealed in the lower frames of Fig. 25. This trend suggests that while some parton fragments are not yet fully equilibrated in the soft sector, they are nonetheless rather strongly coupled to the longitudinally expanding bulk medium. The onset of this coupling appears especially dramatic when the results are plotted (lower right-hand frame) *vs.* the alternative centrality measure $\nu \equiv (N_{part}/2)^{1/3}$ (estimating the mean number of nucleons encountered by a typical participant nucleon along its path through the other nucleus), rather than the more traditional charged-particle multiplicity (lower left frame). The latter comparison serves as a reminder that, as we seek evidence for a transition in the nature of the matter produced in RHIC collisions, it is important to consider carefully the optimal variables to use to characterize the system.

The coupling to the longitudinal expansion can be seen more clearly as an equilibration mechanism from measurements of the power spectra P^λ of local fluctuations in the density of charged hadrons with respect to a mixed-event counterpart P_{mix}^λ . The λ superscript distinguishes different directions (modes) of density variation, orthogonal in the wavelet decomposition used [134] for the analysis: along η , along ϕ , and along the diagonal $\eta\phi$. The so-called “dynamic texture” [133] of the event, used to characterize the non-statistical excess in density fluctuations, is defined as $P_{dyn}^\lambda/P_{mix}^\lambda/N$, where $P_{dyn}^\lambda = P^\lambda - P_{mix}^\lambda$ and N is the average number of tracks in a given p_T interval per event. The dynamic texture is shown as a function of p_T for three different modes and for both central and peripheral collisions in Fig. 26 [134]. HIJING simulations [136] shown in the figure cannot account for the observed fluctuations, even when jet quenching is included, although they do suggest qualitatively that the rising trends in the data with increasing p_T are signals of “clumpiness” in the particle density caused by jets. In the absence of a successful model for these fluctuations, we can at least search for interesting centrality dependences. The box symbols in the figure represent what we would expect for the dynamic texture in central collisions, based on what STAR measures for peripheral collisions, if the correlation structure were independent of centrality. The strong suppression observed with respect to this expectation for the central collision η -mode fluctuations is interpreted as another manifestation of the coupling of parton fragments to the longitudinally expanding bulk medium [134].

The results in Figs. 25 and 26 are averaged over all charged hadrons without consideration of the sign of the charge. Detailed information on the hadronization of the medium can be obtained from the study of charge-*dependent* (CD) correlations, *e.g.*, by examining the difference between angle-dependent correlations of like- *vs.* unlike-sign pairs. One method focuses on the “balance

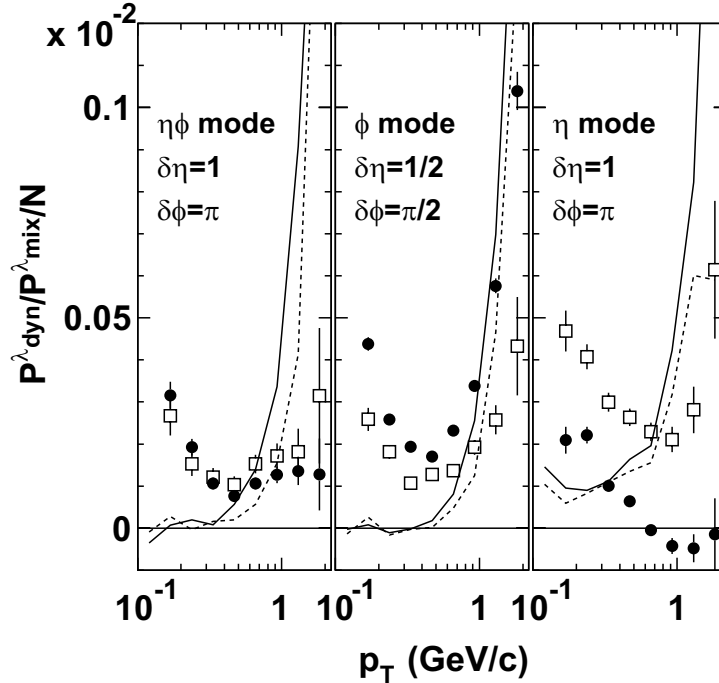


Fig. 26. *STAR* measurements (filled circles) of dynamic texture for the 4% most central Au+Au collisions at $\sqrt{s_{\text{NN}}} = 200$ GeV, compared to *STAR* peripheral (60-84%) collision data (boxes) renormalized for direct comparison, and to HIJING calculations with (dashed curves) and without (solid curves) inclusion of jet quenching. The dynamic texture measures the non-statistical excess in point-to-point fluctuations in the local density of charged hadrons in an event, averaged over the event ensemble. Figure taken from Ref. [134].

function”, constructed [126,135] to measure the excess of unlike- over like-sign pairs as a function of their (pseudo)rapidity difference $\Delta\eta$. The results in Fig. 27 show that the width of this function in $\Delta\eta$ steadily decreases with increasing Au+Au centrality [131,135], in contrast to HIJING simulations [136]. A related trend is observed in the CD two-dimensional autocorrelation [132] (not plotted) analogous in format to the charge-independent results shown in Fig. 25. The CD peak amplitude increases, and its width decreases, dramatically with increasing centrality. These trends indicate a marked change in the formation mechanism of charged hadron pairs in central Au+Au, relative to p+p, collisions. The implications of that change for the nature of the medium produced are now under intensive study with a growing array of correlation techniques.

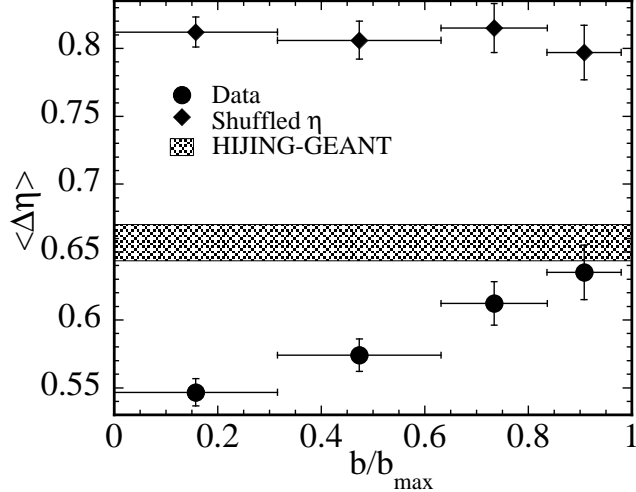


Fig. 27. Width $\langle \Delta\eta \rangle$ of the measured charged hadron balance function from Au+Au (filled circles) collisions at $\sqrt{s_{\text{NN}}}=130$ GeV, plotted as a function of the relative impact parameter deduced from the charged particle multiplicities for each analyzed centrality bin. The cross-hatched band represents the centrality-independent results of HIJING simulations [136] of the balance function width measured within STAR for 130 GeV Au+Au collisions. The diamond-shaped points illustrate constraints imposed on the balance function by global charge conservation and the STAR detector acceptance, when dynamical correlations are removed by randomly shuffling the association of pseudorapidities with detected particles within each analyzed event. The figure is from Ref. [135].

3.6 Summary

In this chapter, we have presented important results on the bulk matter properties attained in Au+Au collisions at RHIC. The measured hadron spectra, yield ratios, and low p_T v_2 , are all consistent from all experiments at RHIC. STAR, in particular, has made pioneering measurements of elliptic flow, of multi-strange baryons, and of dynamical hadron correlations that bear directly on the matter properties critical to establishing QGP formation. The yield ratios are consistent with chemical equilibration across the u , d and s sectors. The spectra and v_2 clearly reveal a collective velocity field in such collisions. The combined evidence for near-central Au+Au collisions at RHIC suggests that thermal equilibrium is largely, though not quite completely, attained, and that collective flow is established, at an early collision stage when sub-hadronic degrees of freedom dominate the matter. However, the quality of some of the data, and the constraints on ambiguities in some of the theoretical models used for interpretation, are not yet sufficient to demonstrate convincingly that thermalized, deconfined matter has been produced.

In particular, the unprecedented success of hydrodynamics in providing a reasonable quantitative account for collective flow at RHIC, and of the statistical

model in reproducing hadron yields through the strange sector, together argue for an early approach toward thermalization spanning the u , d and s sectors. On the other hand, measurements of angle difference distributions for soft hadron pairs reveal that some (admittedly heavily modified) remnants of jet-like dynamical correlations survive the thermalization process, and indicate its incompleteness. The fitted parameters of the statistical model analyses, combined with inferences from the produced transverse energy per unit rapidity, suggest attainment of temperatures and energy densities at least comparable to the critical values for QGP formation in LQCD calculations of bulk, static strongly interacting matter.

The data in this chapter provide two hints of deconfinement that need to be sharpened in future work. One is the improvement in hydrodynamics accounts for measured low- p_T flow when the calculations include a soft point in the EOS, suggestive of a transition from partonic to hadronic matter. It needs to be better demonstrated that comparable improvement could not be obtained alternatively by addressing other ambiguities in the hydrodynamics treatment. One indication of such other ambiguities is the failure of hydrodynamics calculations to explain the emitting source sizes inferred from pion interferometry. The second hint is the apparent relevance of (constituent or valence) quark degrees of freedom in determining the observed meson-baryon differences in flow and yield in the intermediate- p_T region. Here the data need improved precision to establish more clearly the quark scaling behavior expected from coalescence models, while the theory needs to establish a clearer connection between the effective quarks that seem to coalesce and the current quarks and gluons of QCD.

4 Hard Probes

Due to the transient nature of the matter created in high energy nuclear collisions, external probes cannot be used to study its properties. However, the dynamical processes that produce the bulk medium also produce energetic particles through hard scattering processes. The interaction of these energetic particles with the medium provides a class of unique, penetrating probes that are analogous to the method of computed tomography (CT) in medical science.

For $p_T \gtrsim 5$ GeV/c the observed hadron spectra in Au+Au collisions at RHIC exhibit the power-law falloff in cross section with increasing p_T that is characteristic of perturbative QCD hard-scattering processes [137]. The parameters of this power-law behavior vary systematically with collision centrality, in ways that reveal important properties of the matter traversed by these penetrating probes [137]. While we focus for the most part in this chapter on hadrons of p_T above 5 GeV/c, we do also consider data in the intermediate p_T range down to 2 GeV/c, when those data allow more statistically robust measurements of effects we associate with hard scattering.

4.1 Inclusive hadron yields at high p_T

There are several results to date from RHIC exhibiting large and striking effects of the traversed matter on hard probes in central collisions. Figures 28 and 29 show the most significant high p_T measurements made at RHIC thus far. Both figures incorporate measurements of $\sqrt{s_{NN}}=200$ GeV p+p, d+Au and centrality-selected Au+Au collisions at RHIC, with the simpler p+p and d+Au systems providing benchmarks for phenomena seen in the more complex Au+Au collisions.

Figure 28 shows $R_{AB}(p_T)$, the ratio of inclusive charged hadron yields in A+B (either Au+Au or d+Au) collisions to p+p, corrected for trivial geometric effects via scaling by $\langle N_{bin} \rangle$, the calculated mean number of binary nucleon-nucleon collisions contributing to each A+B centrality bin:

$$R_{AB}(p_T) = \frac{dN_{AB}/d\eta d^2p_T}{T_{AB} d\sigma_{NN}/d\eta d^2p_T}. \quad (5)$$

where the overlap integral $T_{AB} = \langle N_{bin} \rangle / \sigma_{inelastic}^{pp}$. A striking phenomenon is seen: large p_T hadrons in central Au+Au collisions are suppressed by a factor ≈ 5 relative to naive (binary scaling) expectations. Conventional nuclear effects, such as nuclear shadowing of the parton distribution functions and

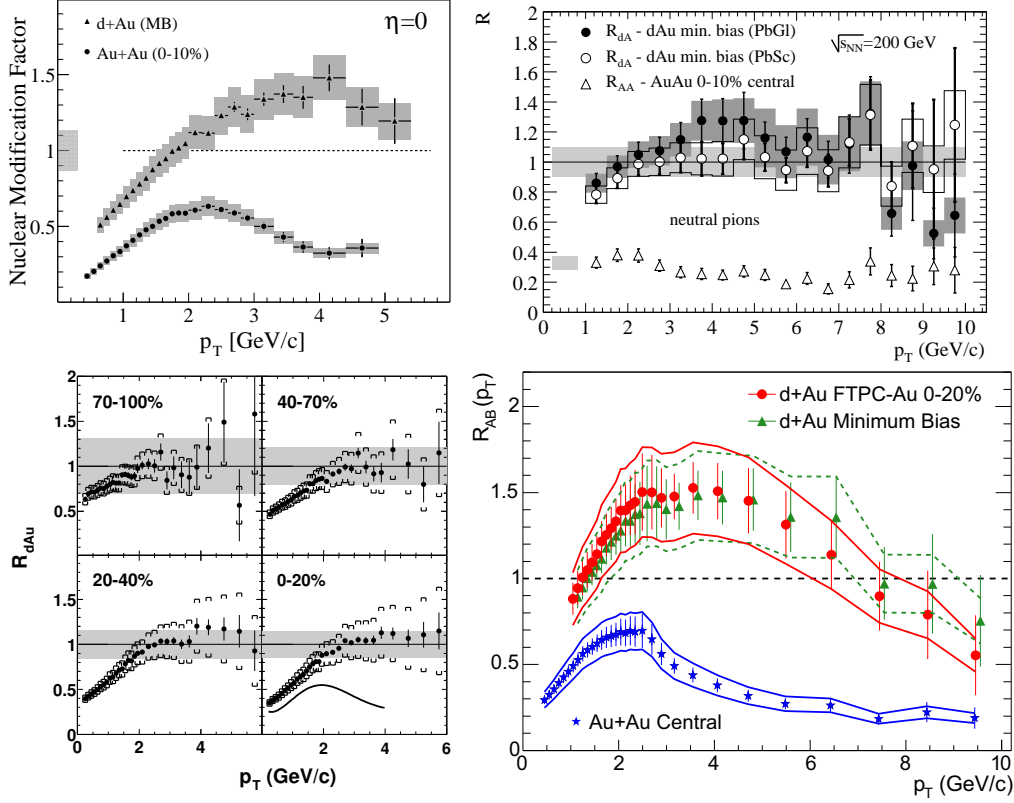


Fig. 28. Binary-scaled ratio $R_{AB}(p_T)$ (Eq. 5) of charged hadron and π^0 inclusive yields from 200 GeV Au+Au and d+Au relative to that from p+p collisions, from BRAHMS[138] (upper left), PHENIX[139] (upper right), PHOBOS[140] (lower left) and STAR[141] (lower right). The PHOBOS data points in the lower left frame are for d+Au, while the solid curve represents PHOBOS central (0-6%) Au+Au data. The shaded horizontal bands around unity represent the systematic uncertainties in the binary scaling corrections.

initial state multiple scattering, cannot account for the suppression. Furthermore, the suppression is not seen in d+Au but is unique to Au+Au collisions, proving experimentally that it results not from nuclear effects in the initial state (such as gluon saturation), but rather from the final state interaction (FSI) of hard scattered partons or their fragmentation products in the dense medium generated in Au+Au collisions [138–141].

These dominant FSI in Au+Au are presumably superimposed on a variety of interesting initial-state effects revealed by the d+Au results. The enhancement seen in Fig. 28 in R_{dAu} for moderate p_T and mid-rapidity, known as the Cronin effect [142], is generally attributed [143] to the influence of multiple parton scattering through cold nuclear matter *prior* to the hard scattering that produces the observed high- p_T hadron. Other effects, revealed by the strong *rapidity*-dependence of R_{dAu} , will be discussed in Sec. 4.4.

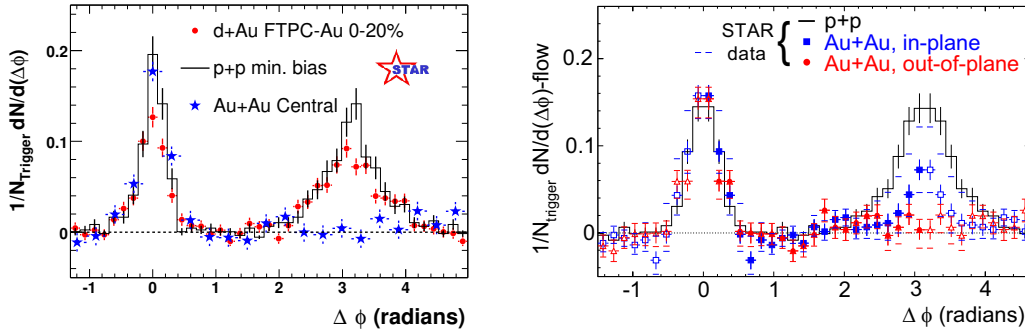


Fig. 29. Dihadron azimuthal correlations at high p_T . Left panel shows correlations for $p+p$, central $d+Au$ and central $Au+Au$ collisions (background subtracted) from STAR [141,71]. Right panel shows the background-subtracted high p_T dihadron correlation for different orientations of the trigger hadron relative to the $Au+Au$ reaction plane [144].

4.2 Dihadron azimuthal correlations

Figure 29 shows seminal STAR measurements of correlations between high p_T hadrons. The left panel shows the azimuthal distribution of hadrons with $p_T > 2$ GeV/c relative to a trigger hadron with $p_T^{\text{trig}} > 4$ GeV/c. A hadron pair drawn from a single jet will generate an enhanced correlation at $\Delta\phi \approx 0$, as observed for $p+p$, $d+Au$ and $Au+Au$, with similar correlation strengths, widths and (not shown) charge-sign ordering (the correlation is stronger for oppositely charged hadron pairs [71]). A hadron pair drawn from back-to-back dijets will generate an enhanced correlation at $\Delta\phi \approx \pi$, as observed for $p+p$ and for $d+Au$ with somewhat broader width than the near-side correlation peak. However, the back-to-back dihadron correlation is strikingly, and uniquely, absent in central $Au+Au$ collisions, while for peripheral $Au+Au$ collisions the correlation appears quite similar to that seen in $p+p$ and $d+Au$. If the correlation is indeed the result of jet fragmentation, the suppression is again due to the FSI of hard-scattered partons or their fragmentation products in the dense medium generated in $Au+Au$ collisions [141]. In this environment, the hard hadrons we do see (and hence, the near-side correlation peak) would arise preferentially from partons scattered outward from the surface region of the collision zone, while the away-side partons must burrow through significant lengths of dense matter.

The qualification concerning the dominance of jet fragmentation is needed in this case, because the correlations have been measured to date primarily for hadrons in that intermediate p_T range (2-6 GeV/c) where sizable differences in meson vs. baryon yields have been observed (see Fig. 15), in contrast to expectations for jets fragmenting in vacuum. The systematics of the meson-baryon differences in this region suggest sizable contributions from softer mechanisms, such as quark coalescence [69]. Where the azimuthal correlation measurements

have been extended to trigger particles above 6 GeV/c, they show a similar pattern to the results in Fig. 29, but with larger statistical uncertainties [145]. This suggests that the peak structures in the correlations do, indeed, reflect dijet production, and that the back-to-back suppression is indeed due to jet quenching. Coalescence processes in the intermediate p_T range may contribute predominantly to the smooth background, with only long-range (*e.g.*, elliptic flow) correlations, that has already been subtracted from the data in Fig. 29.

It remains an open challenge for the quark coalescence models to account for the observed $\Delta\phi$ distributions at moderate p_T at the same time as the meson *vs.* baryon yield and elliptic flow differences discussed in Sec. 3 (see Fig. 21 and associated discussion). Can the size of the jet peaks seen in Fig. 29 be reconciled with the modest fragmentation contributions implied by the coalescence fits near $p_T \approx 4$ GeV/c (Fig. 21)? Do the jet $\Delta\phi$ peaks rather require substantial contributions also from recombination of a hard-scattered parton with thermal partons from the bulk matter [72]? Are models of the latter type of contributions, of constituent quark coalescence in a thermal ensemble [112] and of vacuum fragmentation [4] mutually compatible? They would appear to contain non-orthogonal contributions and to employ incompatible degrees of freedom. Until these questions are successfully addressed, some ambiguity remains in physics conclusions drawn from the intermediate- p_T region, including the dihadron correlations in Fig. 29.

A more differential probe of partonic energy loss is the measurement of high p_T dihadron correlations relative to the reaction plane orientation. The right panel of Fig. 29 shows a study from STAR of the high p_T dihadron correlation from 20-60% centrality Au+Au collisions, with the trigger hadron situated in the azimuthal quadrants centered either in the reaction plane (“in-plane”) or orthogonal to it (“out-of-plane”) [144]. The same-side dihadron correlation in both cases is similar to that in p+p collisions. In contrast, the suppression of the back-to-back correlation depends strongly on the relative angle between the trigger hadron and the reaction plane. This systematic dependence is consistent with the picture of partonic energy loss: the path length in medium for a dijet oriented out of the reaction plane is longer than in the reaction plane, leading to correspondingly larger energy loss. The dependence of parton energy loss on path length is predicted [4] to be substantially stronger than linear. The orientation-dependence of the energy loss should be further affected by different rates of matter expansion in-plane *vs.* out-of-plane.

The energy lost by away-side partons traversing the collision matter must appear, in order to conserve transverse momentum, in the form of an excess of softer emerging hadrons. An analysis of azimuthal correlations between hard and *soft* hadrons has thus been carried out for both 200 GeV p+p and Au+Au collisions [146] in STAR, as a first attempt to trace the degree of degradation on the away side. With trigger hadrons still in the range $4 < p_T^{trig} < 6$ GeV/c,

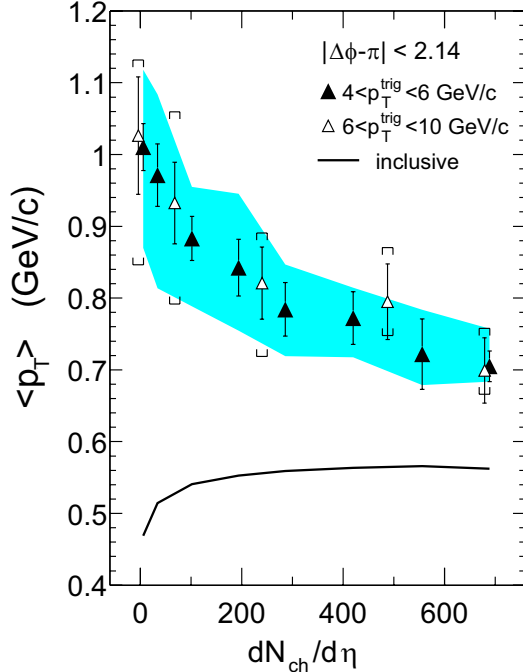


Fig. 30. Associated charged hadron $\langle p_T \rangle$ from the away-side in 200 GeV $p+p$ (two leftmost points) and Au+Au collisions at various centralities, in each case opposite a trigger hadron with p_T in the 4–6 GeV/c (filled triangles) or 6–10 GeV/c (open triangles) range [146]. The shaded band and the horizontal caps represent the systematic uncertainties for the filled and open symbols, respectively. $\langle p_T \rangle$ for inclusive hadron production in the Au+Au collisions is indicated by the solid curve.

but the associated hadrons now sought over $0.15 < p_T < 4$ GeV/c, combinatorial coincidences dominate these correlations, and they must be removed statistically by a careful mixed-event subtraction, with an elliptic flow correlation correction added by hand [146]. The results demonstrate that, in comparison with $p+p$ and peripheral Au+Au collisions, the momentum-balancing hadrons opposite a high- p_T trigger in central Au+Au are greater in number, much more widely dispersed in azimuthal angle, and significantly softer. The latter point is illustrated in Fig. 30, showing the centrality dependence of $\langle p_T \rangle$ of the associated away-side charged hadrons in comparison to that of the bulk inclusive hadrons. While in peripheral collisions the values of $\langle p_T \rangle$ for the away-side hadrons are significantly larger than that of inclusive hadrons, the two values approach each other with increasing centrality. These results are again subject to the ambiguity arising from possible soft (*e.g.*, coalescence) contributions to the observed correlations, as the away-side strength shows little remnant of jet-like behavior [146]. But again, preliminary results for higher trigger-hadron p_T values, shown in Fig. 30, appear to be consistent within larger uncertainties. If a hard-scattering interpretation framework turns out to be valid, the results suggest that even a moderately hard parton traversing a significant path length through the collision matter makes substantial progress toward equilibration with the bulk. The rapid attainment of thermalization via the

multitude of softer parton-parton interactions in the earliest collision stages would then not be surprising.

4.3 Theoretical interpretation of hadron suppression

Figure 31 shows $R_{CP}(p_T)$, the binary scaled ratio of yields from central relative to peripheral collisions for charged hadrons from 200 GeV Au+Au interactions. $R_{CP}(p_T)$ is closely related to $R_{AB}(p_T)$, using as reference the binary-scaled spectrum from peripheral Au+Au collisions rather than p+p collisions. The substitution of the reference set allows a slight extension in the p_T range for which useful ratios can be extracted. The error bars at the highest p_T are dominated by statistics and are therefore, to a large extent, uncorrelated from point to point. The suppression for central collisions is again seen to be a factor ≈ 5 relative to the most peripheral collisions, and for $p_T \gtrsim 6$ GeV/c it is independent of p_T within experimental uncertainties. Also shown in Fig. 31 are results from theoretical calculations based on pQCD incorporating partonic energy loss in dense matter (pQCD-I [147], pQCD-II [148]) and on suppression at high p_T due to gluon saturation effects (Saturation [150], with implications discussed further in the following subsection). The negligible p_T -dependence of the suppression at high p_T is a prediction of the pQCD models [147,148], resulting from the subtle interplay of partonic energy loss, Cronin (initial-state multiple scattering) enhancement, and nuclear shadowing. The variation in the suppression for $p_T \lesssim 5$ GeV/c is related to differences in suppression in this region for mesons and baryons (see Fig. 15). It is accounted for in the pQCD-I calculation by the introduction of an additional non-fragmentation production mechanism for kaons and protons [147]. The magnitude of the hadron suppression in the pQCD calculations is adjusted to fit the measurements for central collisions, as discussed further below.

In order to deduce the magnitude of *partonic* energy loss in the medium it is essential to establish the degree to which *hadronic* interactions, specifically the interaction of hadronic jet fragments with the medium, can at least in part generate the observed high p_T phenomena and contribute substantially to the jet quenching [51,152,153]. Simple considerations already argue against this scenario. The dilated formation time of hadrons with energy E_h and mass m_h is $t_f = (E_h/m_h)\tau_f$, where the rest frame formation time $\tau_f \sim 0.5 - 0.8$ fm/c. Thus, a 10 GeV/c pion has formation time ~ 50 fm/c and is unlikely to interact as a fully formed pion in the medium. Since the formation time depends on the boost, the suppression due to hadronic absorption with constant or slowly varying cross section should turn off with rising p_T , at variance with observations (Fig. 31). A detailed hadronic transport calculation [51] leads to a similar conclusion: the absorption of formed hadrons in the medium fails by a large factor to account for the observed suppression. Rather, this calculation

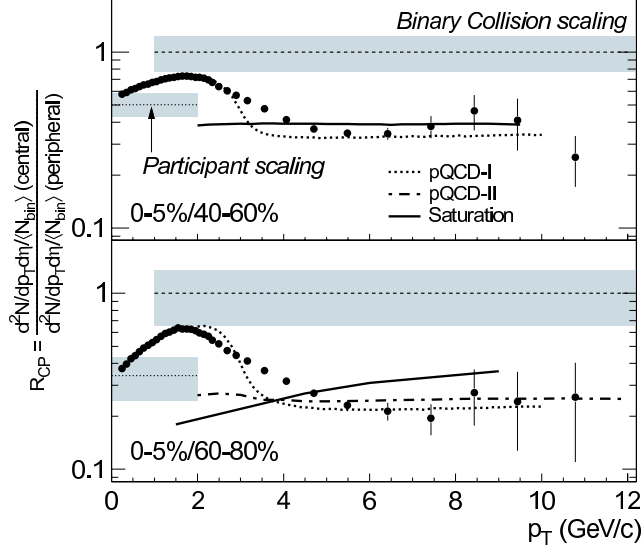


Fig. 31. Binary-scaled yield ratio $R_{CP}(p_T)$ for central (0-5%) relative to peripheral (40-60%, 60-80%) collisions for charged hadrons from 200 GeV Au+Au collisions [151]. The shaded bands show the multiplicative uncertainty of the normalization of $R_{CP}(p_T)$ relative to binary collision and participant number scaling.

attributes the suppression to *ad hoc* medium interactions of “pre-hadrons” with short formation time and constant cross section. The properties of these “pre-hadrons” are thus similar to those of colored partons [51], and not to the expected color transparency of hadronic matter to small color singlet particles that might evolve into normal hadrons [52].

Additional considerations of the available high p_T data [53] also support the conclusion that jet quenching in heavy ion collisions at RHIC is the consequence of partonic energy loss. In particular, large v_2 values observed at high p_T and the systematics of the small-angle dihadron correlations are difficult to reconcile with the hadronic absorption scenario. While further theoretical investigation of this question is certainly warranted, we conclude that there is no support in the data for *hadronic* absorption as the dominant mechanism underlying the observed suppression phenomena at high p_T and we consider *partonic* energy loss to be well established as its primary origin. It is conceivable that there may be minor hadronic contributions from the fragments of soft gluons radiated by the primary hard partons during their traversal of the collision matter. In any case, we emphasize that while the jet quenching results seem to favor partons over hadrons *losing* energy, they do not allow any direct conclusion regarding whether the energy is lost *to* partonic or hadronic matter.

The magnitude of the suppression at high p_T in central collisions is fit to the data in the pQCD-based models with partonic energy loss, by adjusting the initial gluon density of the medium. The agreement of the calculations with the measurements at $p_T > 5$ GeV/c is seen in Fig. 31 to be good. In order to

describe the observed suppression, these models require an initial gluon density about a factor 50 greater than that of cold nuclear matter [147–149]. This is the main physics result of the high p_T studies carried out at RHIC to date. It should be kept in mind that the actual energy loss inferred for the rapidly expanding Au+Au collision matter is not very much larger than that inferred for static, cold nuclear matter from semi-inclusive deep inelastic scattering data [57]. But in order to account for this slightly larger energy loss *despite* the rapid expansion, one infers the much larger *initial* gluon density at the start of the expansion [147,148]. Certainly, then, the quantitative extraction of gluon density is subject to uncertainties from the theoretical treatment of the expansion and of the energy loss of partons in the entrance-channel cold nuclear matter before they initially collide.

The gluon density derived from energy loss calculations is consistent with estimates from the measured rapidity density of charged hadrons [154] using the Bjorken scenario [84], assuming isentropic expansion and duality between the number of initial gluons and final charged hadrons. Similar values are also deduced under the assumption that the initial state properties in central Au+Au RHIC collisions, and hence the measured particle multiplicities, are determined by gluon-gluon interactions below the gluon density saturation scale in the initial-state nuclei [66]. Additionally, the energy density is estimated from global measurements of transverse energy (see Sec. 3.1) to be of order 50-100 times that in cold nuclear matter, consistent with the values inferred from hydrodynamics accounts of measured hadron spectra and flow. The consistency among all these estimates, though only semi-quantitative at present, is quite significant. These inferred densities fall well into the regime where LQCD calculations predict equilibrated matter to reside in the QGP phase.

4.4 Rapidity-dependence of high p_T hadron yields in d+Au collisions

It had been proposed recently [150] that gluon saturation effects can extend well beyond the saturation momentum scale Q_s , resulting in hadron suppression relative to binary scaling ($R_{AB}(p_T) < 1$) for $p_T \sim 5 - 10$ GeV/c mid-rapidity hadron production at RHIC energies, in apparent agreement with the data in Fig. 31. However, since this predicted suppression originates in the properties of the incoming nuclear wave function, hadron production in d+Au collisions should also be suppressed by this mechanism [150]. Experimentally, an *enhancement* in mid-rapidity hadron production in d+Au is seen instead (Fig. 28 [138–141]), even in central d+Au collisions [141] where saturation effects should be most pronounced. The observed enhancement is at variance with saturation model expectations at high p_T [150].

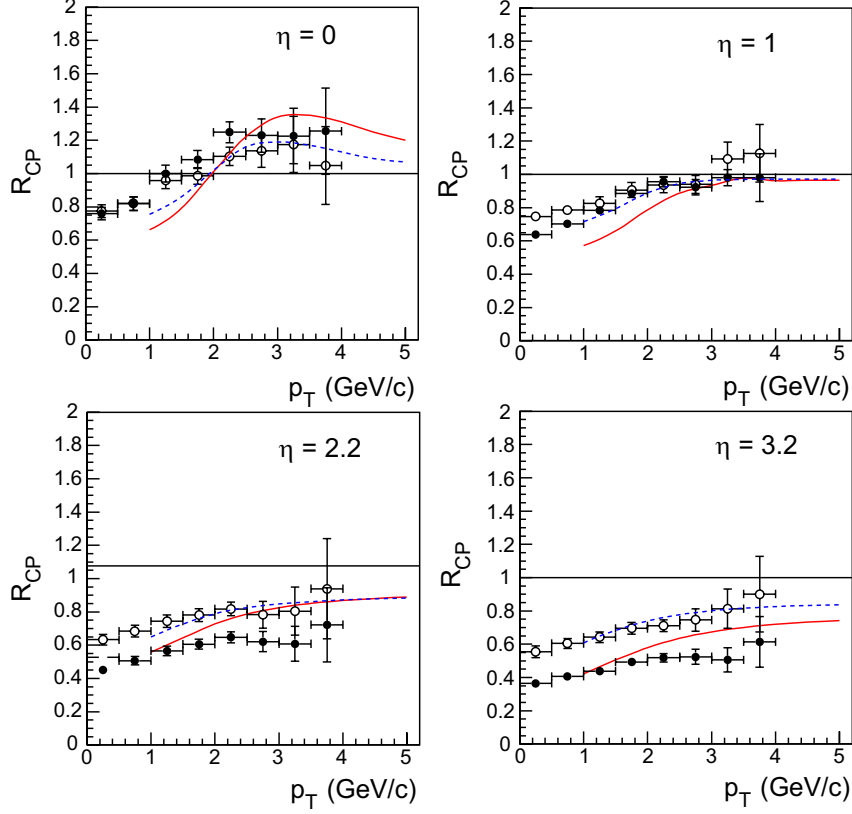


Fig. 32. The ratio R_{CP} of binary-scaled central to peripheral hadron yields for $d+Au$ collisions at $\sqrt{s_{NN}}=200$ GeV, plotted as a function of p_T for four different pseudo-rapidity bins, centered at $\eta = 0$, $\eta = 1$, $\eta = 2.2$ and $\eta = 3.2$. The measurements are from the Brahms Collaboration [155], for all charged hadrons (negative hadrons only) in the case of the former (latter) two η bins. The curves represent gluon saturation model fits from [157]. The filled circles and solid curves compare yields in the 0-20% to 60-80% centrality bins, while the open circles and dashed curves compare 30-50% to 60-80%. The figure is taken from Ref. [157].

However, at large rapidities in the deuteron direction, a suppression of the highest p_T hadrons studied is indeed observed in $d+Au$ collisions, as revealed by the results from the Brahms experiment in Fig. 32 [155]. This is not true of large rapidities in the Au direction [158,159]. This distinct behavior is consistent with gluon saturation models, as seen by the fits [157] to these results in Fig. 32. High- p_T hadrons produced at small angles with respect to the deuteron beam arise preferentially from asymmetric partonic collisions involving gluons at low Bjorken x in the Au nucleus. (For example, in a next-to-leading order leading-twist perturbative QCD calculation, the mean x -value of partons probed in the Au nucleus has been found to be 0.03-0.05 when selecting on hadrons at $\eta = 3.2$ and $p_T = 1.5$ GeV/c [156]. Note, however, that such a calculation may have limited validity in the regime of strong gluonic fields.) It is precisely at low x in heavy nuclei that gluon saturation, and the resultant suppression in high- p_T hadron production, should set in. Thus, gluon satura-

tion models predicted the qualitative behavior of increasing suppression with increasing rapidity in the deuteron direction before the experimental results became available [160], although parameter values had to be tuned after the fact [157] to adjust the saturation scale to obtain the fits shown in Fig. 32.

At the moderate p_T values kinematically accessible at large pseudorapidity, one may worry legitimately that softer hadron production mechanisms (*e.g.*, quark recombination) and initial-state multiple scattering of partons before hard collisions complicate the interpretation of the d+Au results. The same basic suppression of hadrons in the deuteron, relative to the Au, direction can be seen extending to higher p_T in the mid-rapidity backward/forward yield ratios from STAR [159], shown in Fig. 33. The same gluon saturation model calculations [157] shown in Fig. 32 are seen in Fig. 33 to be qualitatively, but not quantitatively, consistent with the observed dependences of the hadron yields on pseudorapidity, p_T and centrality. In particular, both measurements and calculations suggest that the mid-rapidity suppression fades away at transverse momenta above 5-6 GeV/c, as one probes higher- x partons in the Au nucleus.

The results in Fig. 32 and 33 represent the strongest evidence yet available for the applicability of Color Glass Condensate concepts within the kinematic range spanned by RHIC collisions. Nonetheless, more mundane origins of this forward hadron suppression in d+Au have not been ruled out. Di-hadron correlation measurements involving these forward hadrons in d+Au collisions may help to distinguish between CGC and other explanations [161]. A critical characteristic of the CGC is that it can be treated as a classical gluon field. Forward hadrons that result from the interaction of a quark from the deuteron beam with this gluon field may have their transverse momentum balanced not by a single recoiling parton (and therefore a jet), but rather by a number of relatively soft hadrons with a much more smeared angular correlation than is characteristic of di-jet processes. Such a “mono-jet” signature would not be expected from more conventional sources of shadowing of gluon densities in the Au nucleus [162], which still allow individual quark-gluon, rather than quark-gluon field, scattering. On the other hand, kinematic limits on the accessible p_T values for forward hadrons imply that one is dealing, even in a di-jet framework, with unconventional away-side jets of only a few GeV/c [163]. In this regime, a suitable reference is needed, using p+p or d+A with a sufficiently light nucleus A to place the contributing parton x -range above the anticipated gluon saturation regime. The discriminating power of di-hadron correlations for CGC mono-jets must be demonstrated by modifications in d+Au with respect to this reference.

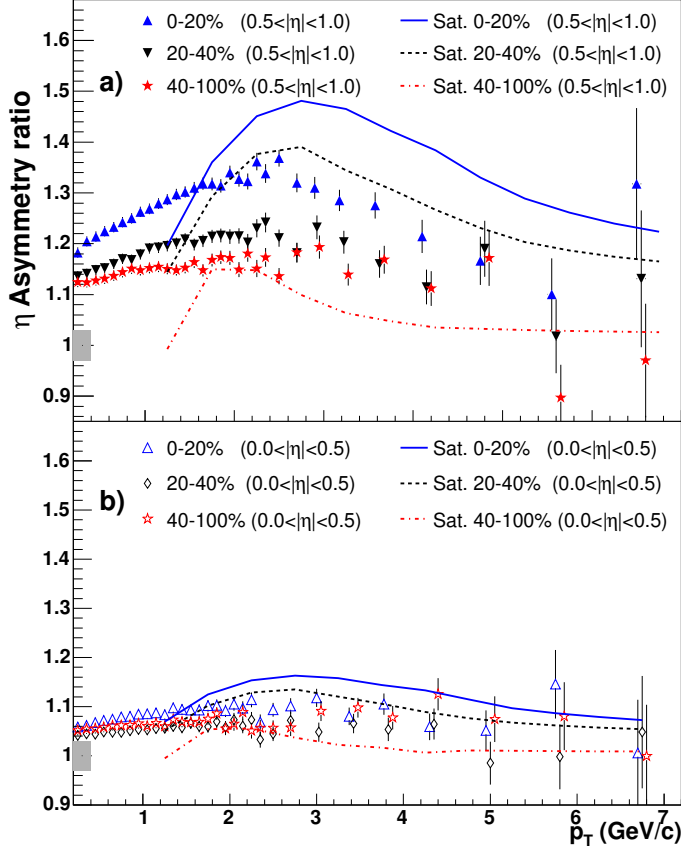


Fig. 33. Comparison of STAR measurements [159] with gluon saturation model calculations [157] for backward (Au side) to forward (d side) charged hadron yield ratios at mid-rapidity in $d+Au$ collisions at $\sqrt{s_{NN}}=200$ GeV. Results are shown as a function of hadron p_T for two different pseudorapidity ranges, (a) $0.5 < |\eta| < 1.0$ and (b) $0.0 < |\eta| < 0.5$, and three different centrality ranges. Centrality is determined experimentally from the measured charged particle multiplicity in the forward Au direction, for $-3.8 < \eta < -2.8$. Figure is taken from Ref. [159].

4.5 Outlook

While large effects have been observed and the phenomenon of jet quenching in dense matter has been firmly established, precision data in a larger p_T range are needed to fully explore the jet quenching phenomena and their connection to properties of the dense matter. The region $2 < p_T < 6$ GeV/c has significant contributions from non-perturbative processes other than vacuum fragmentation of partons, perhaps revealing novel hadronization mechanisms. Most studies to date of azimuthal anisotropies and correlations of “jets” have by necessity been constrained to this region, with only the inclusive spectra extending to the range where hard scattering is expected to dominate the inclusive yield. High statistics data sets for much higher p_T hadrons are needed to fully exploit azimuthal asymmetries and correlations as measurements of partonic energy loss. Dihadron measurements probing the details of the frag-

mentation process may be sensitive to the *energy* density, in addition to the gluon density that is probed with the present measurements. Heavy quark suppression is theoretically better controlled, and measurement of it will provide a critical check on the understanding of partonic energy loss. The *differential* measurement of energy loss through measurement of the emerging away-side jet and the recovery of the energy radiated in soft hadrons is still in its initial phase of study. A complete mapping of the modified fragmentation with larger initial jet energy and with a direct photon trigger will crosscheck the energy dependence of energy loss extracted from single inclusive hadron suppression. Experiments at different colliding energies are also useful to map the variation of jet quenching with initial energy density and the lifetime of the dense system.

At the same time as we extend the p_T range for jet quenching studies on the high side, it is crucial also to pursue further (particle-identified) hadron correlation measurements in the soft sector, in order to understand better how jets are modified by interactions with the dense bulk matter. Measurements such as those presented in Figs. 25 and 30 are just beginning to illuminate the processes leading to thermalization of parton energy. The properties of particles that have been substantially degraded, but not completely thermalized, by passage through the bulk may provide particularly fertile ground for exposing possible fundamental modifications (*e.g.*, symmetry violations or restoration) of strong interactions in RHIC collision matter.

5 Some Open Issues

It should be clear from the detailed discussions of experimental and theoretical results in the preceding chapters that some open questions need to be addressed before we can judge the evidence in favor of QGP formation at RHIC to be compelling. In this chapter we collect a number of such open questions for both experiment and theory. Convincing answers to even a few of these questions might tip the balance in favor of a QGP discovery claim. But even then, it will be important to address the remaining questions to solidify our understanding of the properties of the matter produced in RHIC collisions.

Lattice QCD calculations suggest that a confined state is impossible in bulk, thermodynamically equilibrated matter at the energy densities apparently achieved at RHIC. Indeed, several experimental observations are *consistent* with the creation of deconfined matter. However, a discovery as important as the observation of a fundamentally new state of matter surely demands proof beyond circumstantial evidence for deconfinement. Can we do better?

One response that has been offered is that the EOS of strongly interacting matter is already known from lattice QCD calculations, so that only the conditions initially attained in heavy-ion collisions, and the degree of thermalization in the matter produced, are open to doubt. Such a view tends to trivialize the QGP search by presuming the answer. Indeed, an important aspect of the original motivation for the experimental program at RHIC was to explore the Equation of State of strongly interacting matter under these extreme conditions of energy density. Lattice QCD, in addition to its technical difficulties and attendant numerical uncertainties, attempts to treat bulk, static, thermodynamically equilibrated quark-gluon systems. The relationship of such idealized matter to the finite, rapidly evolving systems produced in relativistic heavy-ion collisions is not *a priori* clear. One would prefer, then, to take LQCD calculations as guideposts to the transition properties to search for experimentally, but not as unassailable truth. On the other hand, there are sufficient complexities in the theoretical treatment of heavy-ion collisions that one would like to apply all credible constraints in parameterizing the problem. This dichotomy leads to our first question:

- **To what extent should LQCD results be used to constrain the Equations of State considered in model treatments of RHIC collisions? How does one allow for independent checks of the applicability of LQCD to the dynamic environment of a RHIC collision?**

Experimentally, to verify the creation of a fundamentally new state of matter at RHIC one would like crosschecks demonstrating that the matter behaves

qualitatively *differently* than “normal” (hadronic) matter in a system known or believed to be in a confined state. Although such a demonstration might be straightforward in bulk matter, it becomes an enormous challenge with the limited experimental control one has over thermodynamic variables in heavy-ion collisions. The finite size and lifetime of the matter produced in the early collision stages, coupled with the absence of global thermal equilibrium and of measurements (to date) of local temperature, all work to obscure the hallmark of QGP formation predicted by lattice QCD: a rapid transition around a critical temperature leading to deconfinement and, quite possibly, chiral symmetry restoration (the latter considered here as a sufficient, but not necessary, QGP manifestation). Given these complications, the underlying challenge to theory and experiment is:

- **Can we make a convincing QGP discovery claim without clear evidence of a rapid transition in the behavior of the matter produced? Can we devise probes with sufficient sensitivity to early, local system temperature to facilitate observation of such an onset at RHIC? Can we predict, based on what we now know from SPS and RHIC collisions, at what energies or under what conditions we might produce matter below the critical temperature, and which observables from those collisions should not match smoothly to SPS and RHIC results?**

At the most basic level, it is conceivable that there is no rapid deconfinement transition in nature (or at least in the matter formed fleetingly in heavy-ion collisions), but rather a gradual evolution from dominance of hadronic toward dominance of partonic degrees of freedom. It is not yet clear that we could distinguish such behavior of QCD matter from the blurring of a well-defined QGP transition by the use of tools with insufficient resolution or control.

5.1 What experimental crosschecks can be performed on apparent QGP signatures at RHIC?

Below we briefly discuss some of the key observations that underlie theoretical claims [6–8] that deconfined matter has been produced at RHIC, and ask what crosschecks might be carried out to test this hypothesis.

5.1.1 Jet quenching

As discussed in Sec. 4, inclusive hadron spectra and two-particle azimuthal correlations at moderate and high p_T clearly demonstrate that jets are suppressed in central RHIC Au+Au collisions, relative to scaled NN collisions. The lack

of suppression (indeed, the enhancement, due to the Cronin effect) in d+Au collisions at RHIC provides a critical crosscheck that the quenching is not an initial-state effect. Measurements with respect to the event reaction plane orientation (see Fig. 29) provide another important crosscheck, demonstrating that the magnitude of the suppression depends strongly on the amount of matter traversed. Such jet quenching was first predicted [46] within the framework of parton energy loss in traversing a QGP. However, more recent theoretical work [58] casts doubt that deconfinement of the medium is essential to the phenomenon, or would be manifested clearly in the energy-dependence of quenching. Nonetheless, experimental hints of a possibly interesting energy dependence to quenching phenomena should be pursued as a potential cross-check on formation of a new state of matter.

Moderate- p_T (up to 4 GeV/c) yields from Pb-Pb collisions at the SPS [164] appear to show an enhancement over a scaled *parameterized* p-p reference spectrum. However, questions raised about the p-p parameterization [165], combined with the unavailability of measurements constraining the initial-state (Cronin) enhancement at these energies, leave open the possibility that even at SPS, jets in central A+A collisions may turn out to be suppressed *relative to expectations*. Indeed, the data in [164] do demonstrate hadron suppression in central relative to semi-peripheral collisions. Also, it is unclear whether the suppression of away-side two-particle correlations out of the reaction plane, observed at RHIC (see Fig. 29), might be of similar origin as the away-side out-of-plane broadening observed at the SPS [103]. These ambiguities are amplified by the limited p_T range covered in SPS measurements, spanning only a region where RHIC results suggest that hard parton scattering and fragmentation may not yet be the dominant contributing hadron production mechanism. These observations lead to the following question:

- **Is there a qualitative change in the yield of high- p_T hadrons in A+A collisions between SPS and RHIC energies? Or does hadron suppression rather evolve smoothly with energy, reflecting a gradual growth in initial gluon density and parton energy loss? Is it feasible to make meaningful measurements of hard probes at sufficiently low collision energy to test for the absence or gross reduction of jet quenching in matter believed to be in a hot hadronic (*i.e.*, confined) gas state?**

5.1.2 Constituent-quark scaling of yields and anisotropies

The baryon *vs.* meson systematics of R_{CP} (Fig. 15) and the apparent scaling of elliptic flow with the number of constituent quarks (Fig. 20) in the intermediate p_T range strongly suggest collective behavior at a pre-hadronic level, a necessary aspect of QGP formation and thermalization in heavy-ion collisions.

Once again, one would like to observe the *absence* of this behavior for systems in which QGP is not formed. High-quality, particle-identified elliptic flow data do not yet exist at SPS (or lower) energies in this p_T region.

- **Should constituent-quark scaling of v_2 in the intermediate p_T sector be broken if a QGP is *not* formed? If so, is an appropriate statistically meaningful, particle-identified measurement of v_2 at intermediate p_T feasible at $\sqrt{s_{NN}}$ below the QGP formation threshold?**

Alternatively, we could seek to establish the role of constituent quarks more convincingly by additional predictions of the quark coalescence models introduced to characterize this intermediate p_T region. For this purpose it may be helpful to integrate the coalescence models with other (e.g., gluon saturation or hydrodynamics) models that might serve to constrain the anticipated initial conditions and coalescence parameters as a function of centrality or collision energy.

- **Coalescence models have provided a simple ansatz to recognize the possible importance of constituent quark degrees of freedom in the hadronization process in A+A collisions at RHIC, and to suggest that these constituent quarks exhibit collective flow. Once model parameters have been adjusted to account for the observed ratios of yields and elliptic flow strengths for baryons vs. mesons, can integration of key features from other models enhance predictive power? For example, can the centrality-dependence of these ratios, or meson vs. baryon correlations (angular or otherwise) at moderate p_T be predicted?**

5.1.3 Strong elliptic flow in agreement with hydrodynamics

In contrast to the above signatures, which require access to moderate-to-high p_T values, observables in the soft sector have already been extensively explored, even from Bevalac energies. The only soft-sector observable selected as a “pillar” of the QGP claim at RHIC, in Ref. [6], is the strong elliptic flow, whose magnitude, mass and p_T -dependence for mid-central collisions are in reasonable agreement with expectations based on ideal hydrodynamic flow (see Fig. 18). Furthermore, the agreement appears better for an Equation of State that includes passage through a phase transition from partonic to hadronic matter.

This success leads to the claim [3,6] that the elliptic flow has finally, in near-central collisions at RHIC energies, reached the ideal hydrodynamic “limit,” suggesting creation of equilibrated, low-viscosity matter at an early stage in

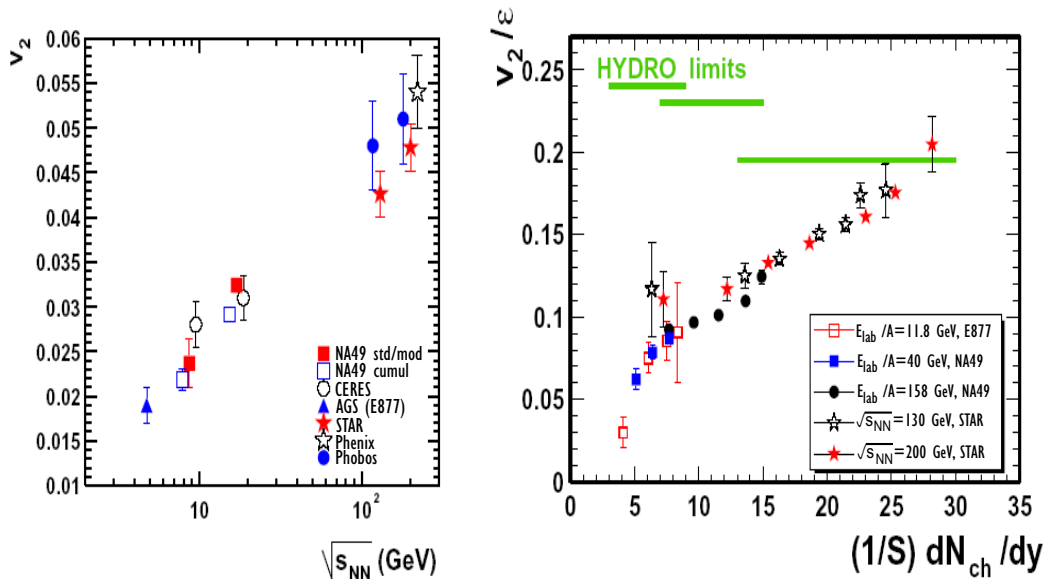


Fig. 34. (a) Energy dependence of elliptic flow measured near mid-rapidity for mid-central collisions ($\sim 12 - 34\%$ of the geometric cross section) of $A \sim 200$ nuclei at the AGS, SPS and RHIC. (b) Mid-rapidity elliptic flow measurements from various energies and centralities combined in a single plot of v_2 divided by relevant initial spatial eccentricity vs. charged-particle rapidity density per unit transverse area in the $A + A$ overlap region. The figures, taken from Ref. [100], highlight the smooth behavior of flow vs. energy and centrality. The rightmost points represent near-central STAR results, where the observed v_2/ϵ ratio becomes consistent with limiting hydrodynamic expectations for an ideal relativistic fluid. The hydrodynamic limits are represented by horizontal lines [100] drawn for AGS, SPS and RHIC energies (from left to right), for one particular choice of EOS that assumes no phase transition in the matter produced.

the collision (when geometric anisotropy is still large). However, the results from many experiments clearly indicate a smoothly rising $v_2(\sqrt{s_{NN}})$, while the hydrodynamic limit for given initial spatial eccentricity and fixed EOS is falling with increasing energy (see Fig. 34). It is thus unclear from the available data whether we are observing at RHIC the interesting onset of saturation of a simple physical limit particularly relevant to QGP matter, or rather an accidental crossing point of experiment with a necessarily somewhat simplified theory. It is of major significance that ideal hydrodynamics appears to work at RHIC for the first time. This conclusion – and in particular the evidence for an Equation of State containing a phase change – would be much strengthened if the hydrodynamic limit were demonstrated to be relevant as well under conditions far removed from those in RHIC measurements to date. Future measurements in central collisions of heavier and highly deformed nuclei (*e.g.*, U+U [3]) possible after a planned upgrade of the ion source for RHIC, or at significantly lower or higher energy (the latter awaiting LHC turn-on) will

provide the possibility of additional crosschecks of this important conclusion.

- **Is the ideal hydrodynamic limit for elliptic flow relevant to heavy-ion collisions over a broad range of conditions, within which near-central Au+Au collisions at full RHIC energy represent merely a first “sighting”? Will v_2 at LHC energies surpass the hydrodynamic limit? Is thermalization likely to be sufficiently established in collisions below $\sqrt{s_{\text{NN}}} \approx 100$ GeV to permit meaningful tests of hydrodynamics? If so, will measurements at lower RHIC energies reveal a non-trivial energy dependence of v_2 , such as that predicted in Fig. 7 by ideal hydrodynamics incorporating a phase transition? Can one vary the initial spatial eccentricity of the bulk matter independently of centrality and degree of thermalization, via controlled changes in the relative alignment of deformed colliding nuclei such as uranium?**

5.1.4 *Dependence of observables on system size*

The above questions focused on excitation function measurements, which traditionally have played a crucial role in heavy-ion physics. It is also desirable to explore the appearance and disappearance of possible QGP signatures as a function of system size. To date, system size variations have been examined at RHIC primarily via the centrality dependence of many observables. A number of variables have been observed to change rapidly from the most peripheral to mid-peripheral collisions, and then to saturate for mid-central and central collisions. Examples of this type of behavior include: the strength (I_{AA} in Ref. [71]) and $\Delta\eta$ width (Fig. 25) of near-side di-hadron correlations; the ratio of measured v_2 to the hydrodynamic limit for relevant impact parameter [105]; the strangeness saturation parameter γ_s deduced from statistical model fits to measured hadron yield ratios (inset in Fig. 12) [86]. Do these changes reflect a (QGP) transition with increasing centrality in the nature of the matter first produced, or merely the gradual growth in importance of hadronic initial- and final-state interactions, and in the degree of thermalization achieved, as the number of nucleon participants increases? One’s answer to this question may depend on how rapid the variation with centrality appears, but this in turn depends on what measure one uses for centrality, as emphasized in the lower frames of Fig. 25.

As the centrality changes for given colliding nuclei, so, unavoidably, does the initial shape of the overlap region. In order to unravel the influence of different initial conditions on the evolution of the matter formed in heavy-ion collisions, it will be important to measure as well the dependence of observables such as those above on the size of the colliding nuclei.

- **Do RHIC measurements as a function of centrality already contain hints of the onset of QGP formation in relatively peripheral regions? Will future measurements for lighter colliding nuclei permit more definitive delineation of these apparently rapid changes with system size?**

5.2 *Do the observed consistencies with QGP formation demand a QGP-based explanation?*

Because it is difficult to control the degree of thermalization achieved in heavy-ion collisions, and to measure directly the temperature at which it is initially achieved, it is possible that none of the crosschecks discussed in the preceding subsection for RHIC energies and below may provide definitive experimental resolution concerning QGP formation. In this case, our reliance on the comparison with theory would be significantly increased, and the questions posed below become especially important. Here, we question the *uniqueness* of a QGP-based explanation. In other words, do the data *demand* a scenario characterized by thermalized, deconfined matter?

5.2.1 *Strong elliptic flow*

The hydrodynamic overestimate of elliptic flow at energies below RHIC has been attributed either to a failure to achieve complete thermalization in those collisions [3] or to their earlier transition to a viscous hadronic phase [6]. These interpretations suggest that the observed energy-dependence of flow (Fig. 34) is dominated by the complex dynamics of early thermalization and late hadronic interactions. While application of hydrodynamics relies on local thermal equilibrium, it is not obvious that agreement with data after parameter adjustment necessarily proves thermalization. The following question is posed in this light.

- **The unprecedented success of hydrodynamics calculations assuming ideal relativistic fluid behavior in accounting for RHIC elliptic flow results has been interpreted as evidence for both early attainment of local thermal equilibrium and an Equation of State with a soft point, characteristic of the predicted phase transition. How do we know that the observed elliptic flow can't result, alternatively, from a harder EOS coupled with incomplete or late thermalization and/or significant viscosity in the produced matter?**

Even if we *assume* thermalization (and hence the applicability of hydrodynamics), it is clear that a complete evaluation of the “theoretical error bars”

has yet to be performed. When parameters are adjusted to reproduce spectra, agreement with v_2 measurements in different centrality bins is typically at the 20-30% level. The continuing systematic discrepancies from HBT results, and from the energy dependence of elliptic flow when simplified freezeout parameterizations are applied, suggest some level of additional ambiguity from the treatment of late-stage hadronic interactions and from possibly faulty assumptions of the usual hydrodynamics calculations (see Sec. 2.2). When theoretical uncertainties within hydrodynamics are fairly treated, does a convincing signal for an EOS with a soft point survive?

- **The indirect evidence for a phase transition of some sort in the elliptic flow results comes primarily from the sensitivity in hydrodynamics calculations of the magnitude and hadron mass-dependence of v_2 to the EOS. How does the level of this EOS sensitivity compare quantitatively to that of uncertainties in the calculations, gleaned from the range of parameter adjustments, from the observed deviations from the combination of elliptic flow, spectra and HBT correlations, and from the sensitivity to the freezeout treatment and to such normally neglected effects as viscosity and boost non-invariance?**

5.2.2 *Jet quenching and high gluon density*

The parton energy loss treatments do not directly distinguish passage through confined vs. deconfined systems. Although effects of deconfinement must exist at some level, *e.g.*, on the propagation of radiated soft gluons, their inclusion in the energy loss models might well be quantitatively masked by other uncertainties in the calculations. Evidence of deconfinement must then be indirect, via comparison of the magnitude of inferred gluon or energy densities early in the collision to those suggested by independent partonic treatments such as gluon saturation models. The actual energy loss inferred from fits to RHIC data, through the rapidly expanding collision matter, is only slightly larger than that indicated through static cold nuclei by fits to semi-inclusive deep inelastic scattering data. The significance of the results is then greatly magnified by the correction to go from the expanding collision matter to an equivalent static system at the time of the initial hard scattering. The quantitative uncertainties listed in the question below will then be similarly magnified. What, then, is a reasonable guess of the range of initial gluon or energy densities that can be accommodated, and how does one demonstrate that those densities can only be reached in a deconfined medium?

- **Does the magnitude of the parton energy loss inferred from RHIC hadron suppression observations *demand* an explanation in terms of traversal through deconfined matter? The answer must take**

into account quantitative uncertainties in the energy loss treatment arising, for example, from the uncertain applicability of factorization in-medium, from potential differences (other than those due to energy loss) between in-medium and vacuum fragmentation, and from effects of the expanding matter and of energy loss of the partons through cold matter preceding the hard scattering.

Gluon saturation models set a QCD scale for anticipated gluon densities, that can then be compared to values inferred from parton energy loss treatments, modulo the questions asked above and below. An important question, given that RHIC multiplicity data are used as input to the models (*e.g.*, to fix the proportionality between gluon density and hadron yields) is whether they provide information truly independent from the initial energy density inferred via the simple Bjorken hydrodynamic expansion scenario (Eq. 4) from measured rapidity densities of transverse energy.

- **If there is a truly universal gluon density saturation scale, determined already from HERA e-p deep inelastic scattering measurements, why can't RHIC A+A particle multiplicities be predicted a priori without input from RHIC experimental data? Is not the A- (or N_{part} -) dependence of the gluon densities at the relevant Bjorken x-ranges predicted in gluon saturation treatments? Can saturated entrance-channel gluon densities in overlapping cold nuclei be directly compared to the early gluon densities in thermalized hot matter, inferred from parton energy loss treatments of jet quenching?**

6 Overview and Outlook

6.1 What have we learned from the first three years of RHIC measurements?

Already in their first three years, all four RHIC experiments have been enormously successful in producing a broad array of high-quality data illuminating the dynamics of heavy-ion collisions in a new regime of very high energy densities. STAR, in particular, has established a number of seminal, striking results highlighted in Secs. 3 and 4 of this document. In parallel, there have been significant advances in the theoretical treatment of these collisions. The theory-experiment comparison indicates that central Au+Au collisions at RHIC produce a unique form of strongly interacting matter, with some dramatic and surprisingly simple properties. A number of the most striking experimental results have been described to a reasonable quantitative level, and in some cases even predicted beforehand, using theoretical treatments inspired by QCD and based on QGP formation in the early stages of the collisions.

The observed hadron spectra and correlations at RHIC reveal three transverse momentum ranges with distinct behavior: a soft range ($p_T \lesssim 1.5$ GeV/c) containing the vast majority of produced hadrons, representing most of the remnants of the bulk collision matter; a hard-scattering range ($p_T \gtrsim 6$ GeV/c), providing partonic probes of the early collision matter; and an intermediate range ($1.5 \lesssim p_T \lesssim 6$ GeV/c) where hard processes coexist with softer ones. The behavior in each of these ranges is quite different than would be expected from an incoherent sum of independent nucleon-nucleon collisions; for the hard sector, in particular, this is one of the most important new observations at RHIC. Below we summarize the major findings described in earlier chapters within each of these three ranges, in each case listing them in approximate decreasing order of what we judge to be their level of robustness with respect to current experimental and theoretical ambiguities. This is not intended necessarily to represent order of importance, as some of the presently model-dependent conclusions are among the strongest arguments in favor of QGP formation.

6.1.1 Soft sector

- The matter produced exhibits **strong collective flow**: most hadrons at low p_T reflect a communal transverse velocity field resulting from conditions early in the collision, when the matter was clearly expanding rapidly under high, azimuthally anisotropic, pressure gradients and frequent interactions among the constituents. The commonality of the velocity is clearest from

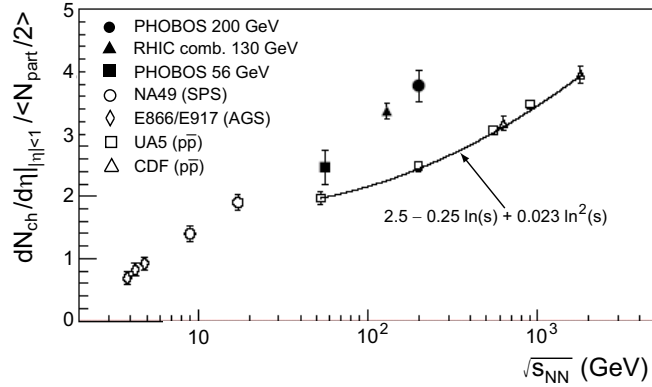


Fig. 35. Measured mid-rapidity charged particle densities, scaled by the calculated number of participant nucleons, for central collisions of $A \sim 200$ nuclei at AGS, SPS and RHIC, plotted as a function of the center-of-mass energy. Results for $\bar{p}+p$ collisions are shown for comparison. Figure from [80].

the systematic dependence of elliptic flow strength on hadron mass at low p_T (see Fig. 18), from the common radial flow velocities extracted by fitting observed spectra (Fig. 14), and from the measurements of HBT and non-identical particle correlations [121]. All of these features fit naturally, at least in a qualitative way, within a hydrodynamic description of the system evolution.

- Most bulk properties measured appear to fall on quite smooth curves with similar results from lower-energy collisions. Examples shown include features of integrated two-hadron p_T correlations (Fig. 24), elliptic flow (Fig. 34), charged particle density (Fig. 35) and emitting source radii inferred from HBT analyses (Fig. 36). Similarly, the centrality-dependences observed at RHIC are generally smooth (but see Fig. 25 for a possible exception). These experimental results contrast with theoretical speculations and predictions made before RHIC start-up, which often [11,30,166] suggested strong energy dependences accompanying the hadron-to-QGP transition. The observed smooth general behavior has been primarily attributed to the formation of matter over a range of initial local conditions, even at a given collision energy or centrality, and to the absence of any direct experimental determination of early temperature. In any case, the results clearly highlight **the difficulty of observing any rapid “smoking-gun” onset of a transition to a new form of matter.**
- Despite the smoothness of the energy and centrality dependences, two important milestones related to the attainment of thermal equilibrium appear to be reached for the first time in near-central RHIC collisions at or near full energy. The first is that **the yields of different hadron species, up to and including multi-strange hadrons, become consistent with a Grand Canonical statistical distribution** at a chemical freezeout temperature of 160 ± 10 MeV and a baryon chemical potential ≈ 25 MeV

(see Fig. 12). This result places an effective lower limit on the temperatures attained if thermal equilibration is reached during the collision stages preceding this freezeout. This lower limit is **essentially equal to the QGP transition temperature predicted by lattice QCD calculations** (see Fig. 1).

- At the same time (*i.e.*, for near-central RHIC collisions) the mass- and p_T -dependence of the observed hadron spectra and of the strong elliptic flow in the soft sector become **consistent, at the $\pm 20 - 30\%$ level, with hydrodynamic expectations for an *ideal* relativistic fluid** formed with an initial eccentricity characteristic of the impact parameter. These hydrodynamic calculations have not yet succeeded in also quantitatively explaining the emitting hadron source size inferred from measured HBT correlations (see Fig. 22). Nonetheless, their overall success suggests that the interactions among constituents in the initial stages of these near-central collisions are characterized by very short mean free paths, leading to **quite rapid ($\tau \lesssim 1$ fm/c) attainment of at least approximate local thermal equilibrium**. The short mean free path in turn suggests a very dense initial system.
- Based on the rapid attainment of thermal equilibrium, and making the assumption of longitudinal boost-invariant expansion, one can extract [84] a rough lower bound on the initial energy density from measured rapidity densities [81,83] of the total transverse energy (dE_T/dy) produced in the collisions. These estimates suggest that in central Au+Au collisions at RHIC, **matter is formed at an initial energy density well above the critical density (~ 1.0 GeV/fm³)** predicted by LQCD for a transition to the QGP.
- Measurements of two-hadron angular correlations and of the power spectrum of local charged-particle density fluctuations reveal strong near-side correlations surviving in the soft sector, reminiscent of jet-like behavior in some aspects, but with a strong pseudorapidity broadening introduced by the presence of the collision matter. The observed structure (see Fig. 25) suggests that **soft jet fragments are not fully thermalized with the bulk matter, but nonetheless show the effects of substantial coupling to that matter** in a considerable broadening of the jet “peak” in pseudorapidity difference between two hadrons.
- Hydrodynamics calculations are best able to reproduce RHIC results for hadron spectra and the magnitude and mass-dependence of elliptic flow (Fig. 18) by utilizing **an Equation of State incorporating a soft LQCD-inspired phase transition from QGP to hadronic matter**. However, the calculations also exhibit comparable sensitivity to other *a priori* unknown features, *e.g.*, the details of the hadronic final-state interactions and the time at which thermal equilibrium is first attained. In light of these competing sensitivities, it is not yet clear if the experimental results truly *demand* an EOS with a soft point.

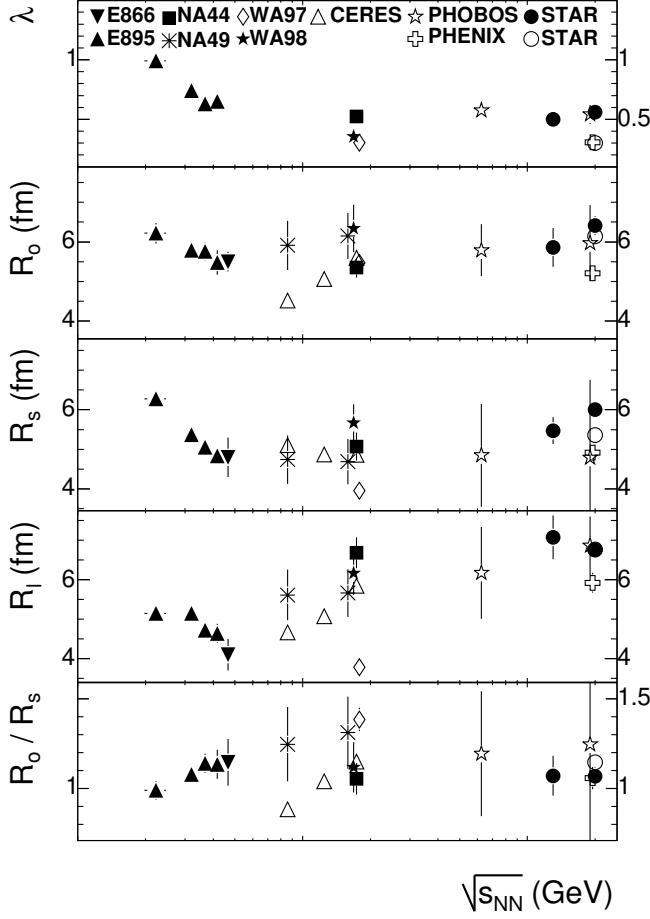


Fig. 36. Energy dependence of HBT parameters extracted from pion pair correlations in central $A + A$ ($A \sim 200$) collisions at mid-rapidity and pair $k_T \approx 0.2$ GeV/c. The data span the AGS, SPS and RHIC. Figure from [167].

6.1.2 Intermediate sector

- In the intermediate p_T range, the elliptic flow strength v_2 saturates and we see systematic meson vs. baryon differences (rather than a systematic mass-dependence) in both yield (see Fig. 15) and v_2 value (Figs. 20). In the same region we also observe clear jet-like angular correlation peaks in the near-side azimuthal difference distributions between pairs of hadrons (see Fig. 29). The most natural interpretation for this combination of characteristics is that **the intermediate- p_T yield arises from a mixture of partonic hard-scattering (responsible for the jet-like correlations) and softer processes (responsible for the meson-baryon differences)**.
- **The saturated v_2 values appear to scale with the number of constituent (or valence) quarks n in the hadron studied, i.e., v_2/n vs. p_T/n falls on a common curve for mesons and baryons (see Fig. 20).** If this trend persists as the particle-identified intermediate- p_T data are improved in

statistical precision for a suitable variety of hadron types, it would provide direct experimental evidence for the relevance of sub-hadronic degrees of freedom in determining flow for hadrons produced at moderate p_T in RHIC collisions.

- Quark recombination models are able to provide a reasonable account of the observed meson and baryon spectra, as well as the v_2 systematics, in the intermediate sector by **a sum of contributions from coalescence of thermalized constituent quarks following an exponential p_T spectrum and from fragmentation of initially hard-scattered partons with a power-law spectrum** [70]. It is not yet clear if the same mixture can also account quantitatively for the azimuthal dihadron correlation (including background under the jet-like peaks) results as a function of p_T . Other models [69,72] mix the above contributions by also invoking recombination of hard-scattered with thermal partons.

6.1.3 Hard sector

- The dominant characteristic of the hard regime is **the strong suppression of hadron yields in central Au+Au collisions**, in comparison to expectations from p+p or peripheral Au+Au collisions, scaled by the number of contributing binary (nucleon-nucleon) collisions (see Fig. 31). Such suppression sets in already in the intermediate sector, but saturates and remains constant as a function of p_T throughout the hard region explored to date. Such suppression was not seen in d+Au collisions at RHIC, indicating that it is **a final-state effect associated with the collision matter produced in Au+Au**. It is consistent with effects of parton energy loss in traversing dense matter, predicted before the data were available [147,148].
- Azimuthal correlations of moderate- (see Fig. 29) and high- p_T [145] hadrons exhibit clear jet-like peaks on the near side. However, **the anticipated away-side peak associated with dijet production is suppressed** by progressively larger factors as the Au+Au centrality is increased, and for given centrality, as the amount of (azimuthally anisotropic) matter traversed is increased (see Fig. 29). Again, no such suppression is observed in d+Au collisions. The suppression of hadron yields and back-to-back correlations firmly establish that **jets are quenched by very strong interactions with the matter produced in central Au+Au collisions**. The jet-like near-side correlations survive presumably because one observes preferentially hard fragments of partons scattered outward from the surface region of the collision zone. Effects of interaction with the bulk matter are nonetheless still seen on the near side, primarily by the broadened distribution in pseudorapidity of softer correlated fragments (see Fig. 25 and Ref. [146]).
- Many features of the observed suppression of high- p_T hadrons, including the centrality-dependence and the p_T -independence, can be described efficiently by **perturbative QCD calculations incorporating parton en-**

ergy loss in a thin, dense medium (see Fig. 31). To reproduce the magnitude of the observed suppression, despite the rapid expansion of the collision matter the partons traverse, these treatments need to assume that **the initial gluon density when the collective expansion begins is more than an order of magnitude greater than that characteristic of cold, confined nuclear matter** [147]. The inferred gluon density is consistent, at a factor ~ 2 level, with the saturated densities needed to account for RHIC particle multiplicity results in gluon saturation models (see Fig. 11).

- The yields of hadrons at moderate-to-high p_T in central d+Au collisions exhibit a systematic dependence on pseudorapidity, marked by **substantial suppression, with respect to binary scaling expectations, of products near the deuteron beam direction, in contrast to substantial enhancement of products at mid-rapidity and near the Au beam direction** (see Figs. 32 and 33). This pattern suggests a depletion of gluon densities at low Bjorken x in the colliding Au nucleus, and is **qualitatively consistent with predictions of gluon saturation models**. Measurements to date cannot yet distinguish interactions with a classical gluon field (Color Glass Condensate) from interactions with a more conventionally shadowed density of individual gluons.
- Angular correlations between moderate- p_T and soft hadrons have been used to explore how transverse momentum balance is achieved, in light of jet quenching, opposite a high- p_T hadron in central Au+Au collisions. The results show the balancing hadrons to be significantly larger in number, softer (see Fig. 30) and more widely dispersed in angle compared to p+p or peripheral Au+Au collisions, with **little remnant of away-side jet-like behavior**. To the extent that hard scattering dominates these correlations at moderate and low p_T , the results could signal an approach of the away-side parton toward thermal equilibrium with the bulk matter it traverses. As mentioned earlier, progress toward thermalization of jet fragments on the near-side is also suggested by soft-hadron correlations.
- The hard sector was not accessed in SPS experiments, so any possible energy dependence of jet quenching can only be explored via the hadron nuclear modification factor in the intermediate- p_T range. While the results (see Fig. 37) leave open the possibility of a rapid transition [53], one is not expected on the basis of theoretical studies of parton energy loss [58]. Furthermore, serious questions have been raised [165] about the validity of the p+p reference data used to determine the SPS result in the figure.

In summary, the RHIC program has enabled dramatic advances in the study of hot strongly interacting matter, for two basic reasons. With the extended reach in initial energy density, the matter produced in the most central RHIC collisions appears to have attained conditions that considerably simplify its theoretical treatment: essentially ideal fluid expansion, and approximate local thermal equilibrium beyond the LQCD-predicted threshold for QGP formation. With the extended reach in particle momentum, the RHIC experiments

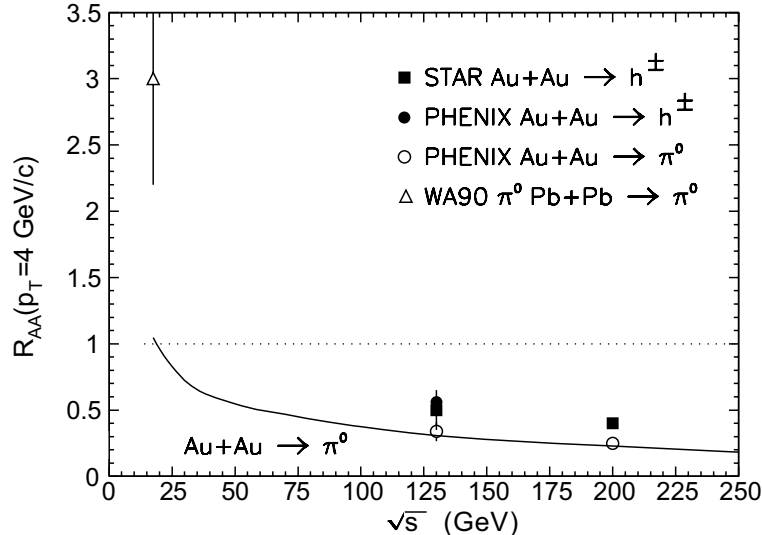


Fig. 37. The nuclear modification factor measured for 4 GeV/c hadrons in central $A + A$ ($A \sim 200$) collisions at SPS and two RHIC energies, showing (Cronin) enhancement at the lower energy and clear jet-quenching suppression at RHIC. The small difference between RHIC charged hadron and identified π^0 results reflects meson vs. baryon differences in this p_T range. The solid curve represents a parton energy loss calculation under simplifying assumptions concerning the energy-dependence, as described in [147].

have developed probes for behavior that was difficult to access at lower collision energies: jet quenching and apparent constituent quark scaling of elliptic flow. These results indicate, with fairly modest reliance on theory, that RHIC collisions produce highly opaque and dense matter that behaves collectively. The magnitude of the density inferred from parton energy loss treatments, together with the hints of constituent quark collective flow, argue against the effectiveness of a purely hadronic treatment of this unique strongly interacting matter. It appears from the most robust signals to evolve for a significant fraction of its lifetime as a low-viscosity, pre-hadronic liquid.

If one takes seriously all of the theoretical successes mentioned above, they suggest the following more detailed overall picture of RHIC collisions: Interactions of very short mean free path within the gluon density saturation regime lead to a rapidly thermalized partonic system at energy densities and temperatures above the LQCD critical values. This thermalized matter expands collectively and cools as an ideal fluid, until the phase transition back to hadronic matter begins, leading to a significant pause in the build-up of elliptic flow. During the phase transition, constituent quarks emerge as the effective degrees of freedom in describing hadron formation at medium p_T out of this initially partonic matter. Initially hard-scattered partons (with lower color interaction cross sections than the bulk partons) traversing this matter lose substantial energy to the medium via gluon radiation, and thereby approach, but do not quite reach, equilibration with the bulk matter. Thus,

some evidence of degraded jets survives (*e.g.*, see Fig. 29), depending on the amount of matter traversed. Any claim of QGP discovery based on RHIC results to date requires an assessment of the robustness, internal consistency, quantitative success and predictive power of this emerging picture.

6.2 *Are we there yet?*

The consistency noted above of many RHIC results with a QGP-based theoretical framework is an important and highly non-trivial statement! Indeed, it is the basis of some claims [6–8] that the Quark-Gluon Plasma has already been discovered at RHIC. However, these claims are associated with QGP definitions [6,7] that do not specifically highlight deconfinement as an essential property to be demonstrated. In our judgment, for reasons mentioned below, and also reflected in the list of open questions provided in Chap. 5 of this document, it is premature to conclude definitively that the matter produced in central RHIC collisions is a Quark-Gluon Plasma, as this term has been understood by the scientific community for the past 20 years (see Appendix B).

- The RHIC experiments have not yet produced *direct* evidence for deconfinement, or indeed for any clear transition in thermodynamic properties of the matter produced. It may be unreasonable to expect a clear onset of deconfinement in heavy-ion systems as a function of collision energy, because the matter, even if locally thermalized, is presumably formed over a range of initial temperatures at any given collision energy. Thus, in the emerging theoretical picture, the matter produced in heavy-ion collisions at SPS was probably also formed in part above the critical energy density, but over a smaller fraction of the volume and with shorter-lived (or perhaps never attained) thermal equilibrium, in comparison with RHIC collisions. At still lower collision energies, where the critical conditions might never be reached, various aspects of the theoretical framework applied at RHIC become inapplicable, precluding a simple theory-experiment comparison over a range from purely hadronic to allegedly QGP-dominated matter.
- The indirect evidence for a thermodynamic transition and for attainment of local thermal equilibrium in the matter produced at RHIC are intertwined in the hydrodynamics account for observed hadron spectra and elliptic flow results. The uniqueness of the solution involving early thermalization and an EOS with a soft mixed phase is not yet demonstrated. Nor is its robustness against changes in the treatment of the late hadronic stage of the evolution, including the introduction of viscosity and other modifications that might be needed to reduce discrepancies from HBT measurements.
- The indirect evidence for deconfinement rests primarily on the large initial gluon densities inferred from parton energy loss fits to the observed hadron

suppression at high p_T , and on the supposition that such high densities could only be achieved in deconfined matter. The latter supposition has yet to be demonstrated in a compelling theoretical argument. The agreement with initial gluon densities suggested by Color Glass Condensate approaches is encouraging, but is still at a basically qualitative level. The measurements suggest that matter is formed at initial temperatures and energy densities at or above the critical values predicted by LQCD for a deconfinement transition. But they do not establish the detailed relevance of the lattice calculations to the fleeting dynamic matter produced in heavy-ion collisions.

- The role of collectively flowing constituent quarks in hadron formation at intermediate p_T is not yet well established experimentally. If it becomes so established by subsequent measurements and analyses, this will hint at the existence of a collective, thermalized partonic stage in the system evolution. However, that hint will fall short of a conclusive QGP demonstration until some interpretational ambiguities are resolved: Is it really *constituent*, rather than *current* (valence) quarks that coalesce? If the former, do the constituent quarks then merely represent the effective degrees of freedom for hadronization of a QGP, or do they indicate an intermediate, pre-hadronic evolutionary stage, after the abundant gluons and current quarks have coalesced and dynamical chiral symmetry breaking has been re-introduced? If there is a distinct constituent quark formation stage, is thermalization achieved before, or only during, that stage?
- The theory remains a patchwork of different treatments applied in succession to each stage of the collision evolution, without yet a clear delineation of the different aspects as distinct limits of one overarching, seamless theory. The theoretical claims of QGP discovery in [8], considered together, rely on five “pillars of wisdom” for RHIC central Au+Au collisions, and each invokes a separate model or theoretical approach for its interpretation: (i) statistical model fits to measured hadron yields to infer possible chemical equilibrium across the u , d and s sectors; (ii) hydrodynamics calculations of elliptic flow to suggest early thermalization and soft EOS; (iii) quark recombination models to highlight the role of thermalized constituent quarks in intermediate-sector v_2 scaling; (iv) parton energy loss models to infer an initial gluon density from high- p_T hadron suppression observations; (v) gluon saturation model fits to observed hadron multiplicities and yields at large rapidity, to suggest how high-density QCD may predetermine the achieved initial gluon densities. Each movement of the theoretical suite has its own assumptions, technical difficulties, adjusted parameters and quantitative uncertainties, and they fit together somewhat uneasily. Until they are assimilated into a more self-consistent whole with only a few overall parameters fitted to existing data, it may be difficult to assess theoretical uncertainties quantitatively or to make non-trivial quantitative predictions whose comparison with future experimental results have the potential to prove the theory wrong.

The bottom line is that in the absence of a direct “smoking gun” signal of deconfinement revealed by experiment alone, a QGP discovery claim must rest on the comparison with a promising, but still not yet mature, theoretical framework. In this circumstance, clear predictive power with quantitative assessments of theoretical uncertainties are necessary for the present appealing picture to survive as a lasting one. The matter produced in RHIC collisions is fascinating and unique. The continuing delineation of its properties will pose critical tests for the theoretical treatment of non-perturbative QCD. But we judge that a QGP discovery claim based on RHIC measurements to date would be premature. We do not propose that a comprehensive theoretical understanding of all observed phenomena must be attained before a discovery claim is warranted, but only that at least some of the serious open questions posed above and in Sec. 5 be successfully answered.

6.3 What are the critical needs from future experiments?

The above comments make it clear what is needed most urgently from theory. But how can future measurements, analyses and heavy-ion collision facilities bring us to a clearer delineation of the fundamental properties of the unique matter produced, and hopefully to a more definitive conclusion regarding the formation of a Quark-Gluon Plasma? We briefly describe below the goals of some important anticipated programs, separated into short-term and long-term prospects, although the distinction in time scale is not always sharp. In the short term, RHIC measurements should concentrate on verifying and extending its new observations of jet quenching and v_2 scaling; on testing quantitative predictions of theoretical calculations incorporating a QGP transition at lower energies and for different system sizes; on measuring charmed-hadron and charmonium yields and flow to search for other evidence of deconfinement; and on testing more extensive predictions of gluon saturation models for forward hadron production. Some of the relevant data have already been acquired during the highly successful 2004 RHIC run – which has increased the RHIC database by an order of magnitude – and simply await analysis, while other measurements require anticipated near-term upgrades of the detectors. In the longer term, the LHC will become available to provide crucial tests of QGP-based theoretical extrapolations to much higher energies, and to focus on very high p_T probes of collision matter that is likely to be formed deep into the gluon saturation regime. Over that same period, RHIC should provide the extended integrated luminosities and upgraded detectors needed to undertake statistically challenging measurements to probe directly the initial system temperature, the pattern of production yields among various heavy quarkonium species, the quantitative energy loss of partons traversing the early collision matter, and the fate of strong-interaction symmetries in that

matter.

Important short-term goals include the following:

- **Establish v_2 scaling more definitively.** Extend the particle-identified flow measurements for hadrons in the medium- p_T region over a broader p_T range, a wider variety of hadron species, and as a function of centrality. Does the universal curve of v_2/n vs. p_T/n remain a good description of all the data? How is the scaling interpretation affected by anticipated hard contributions associated with differential jet quenching through spatially anisotropic collision matter? Can the observed di-hadron angular correlations be quantitatively accounted for by a 2-component model attributing hadron production in this region to quark coalescence (with correlations reflecting only the collective expansion) plus fragmentation (with jet-like correlations)? Do hadrons such as ϕ -mesons or Ω -baryons, containing no valence u or d quarks, and hence with quark-exchange contributions to hadronic interaction cross sections suppressed in normal nuclear matter, follow the same flow trends as other hadrons? Do the measured v_2 values for resonances reflect their constituent quark, or rather their hadron, content? These investigations have the potential to establish more clearly that constituent quarks exhibiting collective flow are the relevant degrees of freedom for hadronization at medium p_T .
- **Establish that jet quenching is an indicator of parton, and not hadron, energy loss.** Extend the measurements of hadron energy loss and di-hadron correlations to higher p_T , including particle identification in at least some cases. Do the meson-baryon suppression differences seen at lower p_T truly disappear? Does the magnitude of the suppression remain largely independent of p_T , in contrast to expectations for hadron energy loss [53]? Does one begin to see a return of away-side jet behavior, via punch-through of correlated fragments opposite a higher- p_T trigger hadron? Improve the precision of di-hadron correlations with respect to the reaction plane, and extend jet quenching measurements to lighter colliding nuclei, to observe the non-linear dependence on distance traversed, expected for radiating partons [4]. Measure the nuclear modification factors for charmed meson production, to look for the “dead-cone” effect predicted [54] to reduce energy loss for heavy quarks.
- **Extend RHIC Au+Au measurements down toward SPS measurements in energy, to test quantitative predictions of the energy-dependence.** Does the suppression of high- p_T hadron yields persist, and does it follow the gentle energy-dependence predicted in Fig. 37? Do the gluon densities inferred from parton energy loss model fits to hadron yields follow energy-dependent trends expected from gluon saturation models? Does elliptic flow remain in agreement with calculations that couple expansion of an ideal partonic fluid to a late-stage, viscous hadron cascade? Do meson-baryon differences and indications of constituent-quark scaling

persist in hadron yields and flow results at intermediate p_T ? Do quark coalescence models remain viable, with inferred thermal quark spectra that change sensibly with the (presumably) slowly varying initial system temperatures? The study of the evolution with collision energy of differential measurements such as those in Fig. 25 promises to yield important insight into the dynamical processes which occur during system evolution.

- **Measure charmonium yields and open charm yields and flow, to search for signatures of color screening and partonic collectivity.** Use particle yield ratios for charmed hadrons to determine whether the apparent thermal equilibrium in the early collision matter at RHIC extends even to quarks with mass significantly greater than the anticipated system temperature. From the measured p_T spectra, constrain the relative contributions of coalescence vs. fragmentation contributions to charmed-quark hadron production. Compare D-meson flow to the trends established in the u , d and s sectors, and try to extract the implications for flow contributions from coalescence vs. possibly earlier partonic interaction stages of the collision. Look for the extra suppression of charmonium, compared to open charm, yields expected to arise from the strong color screening in a QGP state (see Fig. 2).
- **Measure angular correlations with far forward high-energy hadrons in d+Au or p+Au collisions.** Search for the mono-jet signature anticipated for quark interactions with a classical (saturated) gluon field, as opposed to di-jets from quark interactions with individual gluons. Correlations among two forward hadrons are anticipated to provide the best sensitivity to the gluon field at sufficiently low Bjorken x to probe the possible saturation regime.

Longer-term prospects, requiring much greater integrated luminosities (as anticipated at RHIC II) or other substantial facility developments, include:

- **Develop thermometers for the early stage of the collisions, when thermal equilibrium is first established.** In order to pin down experimentally where a thermodynamic transition may occur, it is critical to find probes with direct sensitivity to the temperature well before chemical freeze-out. Promising candidates include probes with little final-state interaction: direct photons – measured down to low momentum, for example, via $\gamma - \gamma$ HBT, which is insensitive to the large π^0 background – and thermal dileptons. The former would require enhanced pair production tracking and the latter the introduction of hadron-blind detectors and techniques.
- **Measure the yields and spectra of various heavy quarkonium species.** Recent LQCD calculations [17] predict the onset of charmonium melting – which can be taken as a signature for deconfinement – at quite different temperatures above T_c for J/ψ vs. ψ' . Similar differences are anticipated for the various Υ states. While interpretation of the yield for any one quarkonium species may be complicated by competition in a QGP state between

enhanced heavy quark production rates and screened quark-antiquark interactions, comparison of a measured hierarchy of yields with LQCD expectations would be especially revealing. They would have to be compared to measured yields for open charm and beauty, and to the corresponding quarkonium production rates in p+p and p+A collisions. Clear identification of ψ' and separation of Υ states require upgrades to detector resolution and vertexing capabilities.

- **Quantify parton energy loss by measurement of mid-rapidity jet fragments tagged by a hard direct photon, a heavy-quark hadron, or a far forward energetic hadron.** Such luminosity-hungry coincidence measurements will elucidate the energy loss of light quarks vs. heavy quarks vs. gluons, respectively, through the collision matter. They should thus provide more quantitative sensitivity to the details of parton energy loss calculations.
- **Test quantitative predictions for elliptic flow in U+U collisions.** The large size and deformation of uranium nuclei make this a considerable extrapolation away from RHIC Au+Au conditions, and a significant test for the details of hydrodynamics calculations that are consistent with the Au+Au results [3]. If the relative alignment of the deformation axes of the two uranium nuclei can be experimentally controlled, one would be able to vary initial spatial eccentricity largely independently of centrality and degree of thermalization of the matter.
- **Measure hadron multiplicities, yields, correlations and flow at LHC and GSI energies, and compare to quantitative predictions based on models that work at RHIC.** By fixing parameters and ambiguous features of gluon saturation, hydrodynamics, parton energy loss and quark coalescence models to fit RHIC results, and with guidance from LQCD calculations regarding the evolution of strongly interacting matter with initial temperature and energy density, theorists should make quantitative predictions for these observables at LHC and GSI before the data are collected. The success or failure of those predictions will represent a stringent test of the viability of the QGP-based theoretical framework.
- **Devise tests for the fate of fundamental QCD symmetries in the collision matter formed at RHIC.** If the nature of the QCD vacuum is truly modified above the critical temperature, then chiral and $U_A(1)$ symmetries may be restored, while parity and CP may conceivably be broken [168]. Testing these symmetries in this unusual form of strongly interacting matter is of great importance, even if we do not have a crisp demonstration beforehand that the matter is fully thermalized and deconfined. Indeed, if evidence were found for a clear change in the degree of adherence to one of the strong interaction symmetries, in comparison with normal nuclear matter, this would likely provide the most compelling “smoking gun” for production of a new form of matter in RHIC collisions. Approaches that have been discussed to date include looking for meson mass shifts in dilepton spectra as a signal of chiral symmetry restoration, and searching for

CP violation via $\Lambda - \bar{\Lambda}$ spin correlations or electric dipole distributions of produced charge with respect to the reaction plane [168]. It may be especially interesting to look for evidence among particles emerging opposite an observed high- p_T hadron tag, since the strong suppression of away-side jets argues that the fate of the away-side particles may reflect strong interactions with a maximal amount of early collision matter. These tests will begin in the short term, but may ultimately need the higher statistics available in the longer term to distinguish subtle signals from dominant backgrounds.

6.4 Outlook

The programs we have outlined above for desirable advances in theory and experiment represent a decade's worth of research, not all of which must, or are even expected to, *precede* a discovery announcement for the Quark-Gluon Plasma. We can imagine several possible scenarios leading to a more definitive QGP conclusion. Identification of a single compelling experimental signature is still conceivable, but the most promising prospects are long-term: establishment of a telling pattern of quarkonium suppression *vs.* species; observation of clear parity or CP violation, or of chiral symmetry restoration, in the collision matter; extraction of a transition signal as a function of measured early temperature. It is also possible that a single theoretical development could largely seal the case: *e.g.*, a compelling argument that gluon densities more than an order of magnitude higher than those in cold nuclear matter really do *demand* deconfinement; or sufficient hydrodynamics refinement to demonstrate that RHIC flow results really do *demand* a soft point in the EOS. Perhaps the most likely path would involve several additional successes in theory-experiment comparisons, leading to a preponderance of evidence that RHIC collisions have produced thermalized, deconfined quark-gluon matter.

In any scenario, however, RHIC has been, and should continue to be, a tremendous success in its broader role as an instrument for discovery of new features of QCD matter under extreme conditions. The properties already delineated, with seminal contributions from STAR, point toward a dense, opaque, non-viscous, pre-hadronic liquid state that was not anticipated before RHIC. Determining whether the quarks and gluons in this matter reach thermal equilibrium with one another before they become confined within hadrons, and eventually whether chiral symmetry is restored, are two among many profound questions one may ask. Further elaboration of the properties of this matter, with eyes open to new unanticipated features, remains a vital research mission, independent of the answer that nature eventually divulges to the more limited question that has been the focus of this document.

7 Appendix A: Charge

This report was prepared for the STAR Collaboration in response to the following charge from the Spokesperson, delivered to a drafting committee on March 18, 2004.

“Thank you very much for agreeing to help in preparing a draft whitepaper to serve as the starting point for a focused discussion by the STAR Collaboration of the experimental evidence regarding the role of the Quark-Gluon Plasma in RHIC heavy ion collisions.”

“The charge to this panel is to make a critical assessment of the presently available evidence to judge whether it warrants a discovery announcement for the QGP, using any and all experimental and theoretical results that address this question. The white paper should pay particular attention to identifying the most crucial features of the QGP that need to be demonstrated experimentally for a compelling claim to be made. It should summarize those data that may already convincingly demonstrate some features, as well as other data that may be suggestive but with possible model-dependence, and still other results that raise questions about a QGP interpretation. If the conclusion is that a discovery announcement is at present premature, the paper should outline critical additional measurements and analyses that would make the case stronger, and the timeline anticipated to produce those new results.”

“The white paper should be of sufficient quality and scientific integrity that, after incorporation of collaboration comments, it may be circulated widely within the RHIC and larger physics communities as a statement of STAR’s present assessment of the evidence for the QGP.”

8 Appendix B: Definitions of the Quark-Gluon Plasma in Nuclear Physics Planning Documents

One's conclusion concerning the state of the evidence in support of Quark-Gluon Plasma formation is certainly influenced by the definition one chooses for the QGP state. Recent positive claims have been based on definitions different from that chosen in this work (see Sec. 1), leaning more toward either an operational definition based on actual RHIC measurements [6], or a demonstration that experiments have reached conditions under which lattice QCD calculations predict a QGP state [7]. We have rather chosen to extract what we believe to be the consensus definition built up in the physics community from the past 20 years' worth of planning documents and proposals for RHIC. In this section, we collect relevant quotes concerning the QGP from a number of these documents.

A relativistic heavy-ion collider facility was first established as the highest priority for new construction by the 1983 Nuclear Science Advisory Committee (NSAC) Long Range Plan [169]. In discussing the motivation for such a facility, that document states:

“Finally, under conditions of very elevated energy density, nuclear matter will exist in a wholly new phase in which there are no nucleons or hadrons composed of quarks in individual bags, but an extended *quark-gluon plasma*, within which the quarks are deconfined and move independently. ... The production and detection of a quark-gluon plasma in ultra-relativistic heavy ion collisions would not only be a remarkable achievement in itself, but by enabling one to study quantum chromodynamics (QCD) over large distance scales it would enable one to study fundamental aspects of QCD and confinement unattainable in few-hadron experiments. ... A second, chiral-symmetry restoring, transition is also expected at somewhat higher energy density, or perhaps coincident with the deconfinement transition; such a transition would be heralded by the quarks becoming effectively massless, and low mass pionic excitations no longer appearing in the excitation spectrum.”

The high priority of such a collider was confirmed in the 1984-6 National Academy of Sciences survey of Nuclear Physics [170], which stated:

“A major scientific imperative for such an accelerator derives from one of the most striking predictions of quantum chromodynamics: that under conditions of sufficiently high temperature and density in nuclear matter, a transition will occur from excited hadronic matter to a quark-gluon plasma, in which the quarks, antiquarks and gluons of which hadrons are composed become ‘deconfined’ and are able to move about freely. The quark-gluon

plasma is believed to have existed in the first few microseconds after the big bang, and it may exist today in the cores of neutron stars, but it has never been observed on Earth. Producing it in the laboratory will thus be a major scientific achievement, bringing together various elements of nuclear physics, particle physics, astrophysics, and cosmology.”

The glossary of the above document [170] defined Quark-Gluon Plasma in the following way:

“An extreme state of matter in which quarks and gluons are deconfined and are free to move about in a much larger volume than that of a single hadron bag. It has never been observed on earth.”

In the 1984 proposal for RHIC from Brookhaven National Laboratory [171], the QGP was described as follows:

“The specific motivation from QCD is the belief that we can assemble macroscopic volumes of nuclear matter at such extreme thermodynamic conditions as to overcome the forces that confine constituents in normal hadrons, creating a new form of matter in an *extended confined plasma of quarks and gluons*.”

The 1989 NSAC Long Range Plan [172], in reconfirming the high priority of RHIC, states:

“The most outstanding prediction based on the theory of the strong interaction, QCD, is that the properties of matter should undergo a profound and fundamental change at an energy density only about one order of magnitude higher than that found in the center of ordinary nuclei. This change is expected to involve a transition from the confined phase of QCD, in which the degrees of freedom are the familiar nucleons and mesons and in which a quark is able to move around only inside its parent nucleon, to a new deconfined phase, called the quark-gluon plasma, in which hadrons dissolve into a plasma of quarks and gluons, which are then free to move over a large volume.”

The 1994 NSAC Assessment of Nuclear Science [173] states:

“When nuclear matter is heated to extremely high temperatures or compressed to very large densities we expect it to respond with a drastic transformation, in which the quarks and gluons, that are normally confined within individual neutrons and protons, are able to move over large distances. A new phase of matter, called Quark-Gluon-Plasma (QGP), is formed. At the same time chiral symmetry is restored making particles massless at the scale of quark masses. Quantum Chromodynamics (QCD) of massless quarks is chirally (or left-right) symmetric, but in the normal world this

symmetry is spontaneously broken giving dynamical masses to quarks and the particles composed of quarks.”

The 1996 NSAC Long Range Plan [174] repeats the emphasis on chiral symmetry restoration in addition to deconfinement:

“At temperatures in excess of T_c nuclear matter is predicted to consist of unconfined, nearly massless quarks and gluons, a state called the *quark-gluon plasma*. The study of deconfinement and chiral symmetry restoration is the primary motivation for the construction of the Relativistic Heavy Ion Collider (RHIC) at Brookhaven National Laboratory.”

The most recent National Academy of Sciences survey of Nuclear Physics [175] puts it this way:

“At RHIC such high energy densities will be created that the quarks and gluons are expected to become deconfined across a volume that is large compared to that of a hadron. By determining the conditions for deconfinement, experiments at RHIC will play a crucial role in understanding the basic nature of confinement and shed light on how QCD describes the matter of the real world. ...Although the connection between chiral symmetry and quark deconfinement is not well understood at present, chiral symmetry is expected to hold in the quark-gluon plasma.”

Finally, the 2004 NuPECC (Nuclear Physics European Collaboration Committee) Long Range Plan for nuclear physics research in Europe [176] states:

“The focus of the research in the ultra-relativistic energy regime is to study and understand how collective phenomena and macroscopic properties, involving many degrees of freedom, emerge from the microscopic laws of elementary particle-physics. ... The most striking case of a collective bulk phenomenon predicted by QCD is the occurrence of a phase transition to a deconfined chirally symmetric state, the quark gluon plasma (QGP).”

In short, every statement concerning the QGP in planning documents since the conception of RHIC has pointed to deconfinement of quarks and gluons from hadrons as the primary characteristic of the new phase. More recent definitions have tended to include chiral symmetry restoration as well. Based on the above survey, we believe that the definition used in this paper would be very widely accepted within the worldwide physics community as a “minimal” requirement for demonstrating formation of a Quark-Gluon Plasma.

Acknowledgements: We thank the RHIC Operations Group and RCF at BNL, and the NERSC Center at LBNL for their support. This work was supported in part by the HENP Divisions of the Office of Science of the U.S. DOE; the U.S. NSF; the BMBF of Germany; IN2P3, RA, RPL, and EMN of France; EPSRC of the United Kingdom; FAPESP of Brazil; the Russian Ministry of Science and Technology; the Ministry of Education and the NNSFC of China; Grant Agency of the Czech Republic, FOM of the Netherlands, DAE, DST, and CSIR of the Government of India; Swiss NSF; the Polish State Committee for Scientific Research; and the STAA of Slovakia.

References

- [1] P. Jacobs and X.N. Wang, hep-ph/0405125.
- [2] D.H. Rischke, Prog. Part. Nucl. Phys. 52 (2004) 197.
- [3] P. F. Kolb and U. Heinz, in Quark Gluon Plasma 3, eds. R.C. Hwa and X.N. Wang (World Scientific, Singapore, 2003); nucl-th/0305084.
- [4] M. Gyulassy, I. Vitev, X.N. Wang and B.W. Zhang, in Quark Gluon Plasma 3, eds. R.C. Hwa and X.N. Wang (World Scientific, Singapore, 2003), nucl-th/0302077; R. Baier, D. Schiff, B.G. Zakharov, Ann. Rev. Nucl. Part. Sci. 50 (2000) 37.
- [5] B. Tomášik and U.A. Wiedemann, in Quark Gluon Plasma 3, eds. R.C. Hwa and X.N. Wang (World Scientific, Singapore, 2003); hep-ph/0210250.
- [6] M. Gyulassy, nucl-th/0403032.
- [7] M. Gyulassy and L. McLerran, Nucl. Phys. A750 (2005) 30.
- [8] RIKEN-Brookhaven Research Center Scientific Articles, Vol. 9: New Discoveries at RHIC: the current case for the Strongly Interactive QGP (May, 2004).
- [9] J. Glanz, Like Particles, 2 Houses of Physics Collide, New York Times, January 20, 2004 (Section F, page 1); K. Davidson, Universe-Shaking Discovery, or More Hot Air?, San Francisco Chronicle, January 19, 2004.
- [10] G. Brumfiel, What's In a Name?, Nature, July 26, 2004.
- [11] J.W. Harris and B. Müller, Ann. Rev. Nucl. Part. Sci. 46 (1996) 71.
- [12] U. Heinz and M. Jacob, nucl-th/0002042.
- [13] K.H. Ackermann et al., Nucl. Instrum. Methods A499 (2003) 624.
- [14] F. Karsch, Lecture Notes in Physics 583 (2002) 209.
- [15] O. Kaczmarek, F. Karsch, E. Laermann and M. Lütgemeier, Phys. Rev. D62 (2000) 034021.
- [16] T. Matsui and H. Satz, Phys. Lett. B178 (1986) 416; F. Karsch, M.T. Mehr and H. Satz, Z. Phys. C37 (1988) 617.
- [17] M. Asakawa and T. Hatsuda, Phys. Rev. Lett. 92 (2004) 012001; S. Datta et al., J. Phys. G 30 (2004) S1347.
- [18] E. Laermann and O. Philipsen, Ann. Rev. Nucl. Part. Sci. 53 (2003) 163.
- [19] Z. Fodor and S.D. Katz, JHEP 0404 (2004) 050.
- [20] Z. Fodor and S.D. Katz, Phys. Lett. B534 (2002) 87; Z. Fodor and S.D. Katz, JHEP 0203 (2002) 014.

- [21] L.D. Landau, *Izv. Akad. Nauk Ser, Fiz.* 17 (1953) 51; L.D. Landau and E.M. Lifshitz, *Fluid Mechanics*.
- [22] E. Shuryak, *Prog. Part. Nucl. Phys.* 53 (2004) 273.
- [23] R. Stock, *J. Phys. G* 30 (2004) S633.
- [24] T. Biro and B. Müller, *Phys. Lett. B* 578 (2004) 78, and references therein.
- [25] R. Hagedorn, *Nuovo Cim. Suppl.* 3 (1965) 147.
- [26] H. Sorge, *Phys. Lett.* B402 (1997) 251.
- [27] H. Sorge, *Phys. Rev. Lett.* 82 (1999) 2048.
- [28] S.A. Bass and A. Dumitru, *Phys. Rev.* C61 (2000) 064909.
- [29] D. Teaney, J. Lauret, and E. Shuryak, *Phys. Rev. Lett.* 86 (2001) 4783; nucl-th/0110037.
- [30] P.F. Kolb, J. Sollfrank and U. Heinz, *Phys. Rev.* C62 (2000) 054909.
- [31] H. Sorge, *Phys. Rev.* C52 (1995) 3291.
- [32] P. Huovinen, P.F. Kolb, U. Heinz, P.V. Ruuskanen and S.A. Voloshin, *Phys. Lett.* B503 (2001) 58.
- [33] H. van Hecke, H. Sorge and N. Xu, *Phys. Rev. Lett.* 81 (1998) 5764.
- [34] N. Xu and Z. Xu, *Nucl. Phys.* A715 (2003) 587c.
- [35] D. Teaney, *Phys. Rev.* C68 (2003) 034913.
- [36] K. Morita, S. Muroya, C. Nonaka and T. Hirano, *Phys. Rev.* C66 (2004) 054904, and references therein.
- [37] P. Braun-Munzinger, K. Redlich and J. Stachel, in *Quark Gluon Plasma 3*, eds. R.C. Hwa and X.N. Wang (World Scientific, Singapore, 2003); nucl-th/0304013.
- [38] K. Huang, *Statistical Mechanics* (John Wiley and Sons, 1988).
- [39] E. Fermi, *Prog. Theor. Phys.* 5 (1950) 570.
- [40] E.V. Shuryak, *Phys. Lett.* B42 (1972) 357; J. Rafelski and M. Danos, *Phys. Lett.* B97 (1980) 279; R. Hagedorn and K. Redlich *Z. Phys. C* 27 (1985) 541.
- [41] P. Braun-Munzinger, J. Stachel, J.P. Wessels and N. Xu, *Phys. Lett.* B365 (1996) 1.
- [42] V. Koch, *Nucl. Phys.* A715 (2003) 108c.
- [43] U. Heinz, *Nucl. Phys.* A661 (1999) 140c.
- [44] A.M. Poskanzer and S.A. Voloshin, *Phys. Rev.* C58 (1998) 1671.
- [45] G. Torrieri and J. Rafelski, *Phys. Lett.* B509 (2001) 239; Z. Xu, *J. Phys. G* 30 (2004) S325; M. Bleicher and H. Stocker, *J. Phys. G* 30 (2004) S111.

- [46] J.D. Bjorken, FERMILAB-PUB-82-59-THY and erratum (unpublished).
- [47] M. Gyulassy, P. Levai and I. Vitev, Nucl. Phys. A661 (1999) 637; M. Gyulassy, P. Levai and I. Vitev, Nucl. Phys. B571 (2000) 197; M. Gyulassy, P. Levai and I. Vitev, Phys. Rev. Lett. 85 (2000) 5535; M. Gyulassy, P. Levai and I. Vitev, Nucl. Phys. B594 (2001) 371.
- [48] E. Wang and X.N. Wang, Phys. Rev. Lett. 87 (2001) 142301.
- [49] R. Baier, Y.L. Dokshitzer, A.H. Mueller, S. Peigne and D. Schiff, Nucl. Phys. B483 (1997) 291; R. Baier, Y.L. Dokshitzer, A.H. Mueller and D. Schiff, Nucl. Phys. B531 (1998) 403; R. Baier, Y.L. Dokshitzer, A.H. Mueller and D. Schiff, Phys. Rev. C60 (1999) 064902; R. Baier, Y.L. Dokshitzer, A.H. Mueller and D. Schiff, JHEP 0109 (2001) 033.
- [50] U.A. Wiedemann, Nucl. Phys. B588 (2000) 303; U.A. Wiedemann, Nucl. Phys. A690 (2001) 731; C.A. Salgado and U.A. Wiedemann, Phys. Rev. Lett. 89 (2002) 092303; C.A. Salgado, U.A. Wiedemann, Phys. Rev. D68 (2003) 014008.
- [51] W. Cassing, K. Gallmeister and C. Greiner, Nucl. Phys. A735 (2004) 277.
- [52] G.R. Farrar, H. Liu, L.L. Frankfurt and M.I. Strikman, Phys. Rev. Lett. 61 (1998) 686; S.J. Brodsky and A.H. Mueller, Phys. Lett. B206 (1988) 685; B.K. Jennings and G.A. Miller, Phys. Lett. B236 (1990) 209; B.K. Jennings and G.A. Miller, Phys. Rev. D44 (1991) 692; B.K. Jennings and G.A. Miller, Phys. Rev. Lett. 69 (1992) 3619; B.K. Jennings and G.A. Miller, Phys. Lett. B274 (1992) 442.
- [53] X.N. Wang, Phys. Lett. B579 (2004) 299.
- [54] M. Djordjevic and M. Gyulassy, Phys. Lett. B560 (2003) 37.
- [55] A. Airapetian et al. [HERMES Collaboration], Eur. Phys. J. C 20 (2001) 479; V. Muccifora [HERMES Collaboration], Nucl. Phys. A715 (2003) 506.
- [56] J.M. Moss et al., hep-ex/0109014.
- [57] X.N. Wang and X.F. Guo, Nucl. Phys. A 696 (2001) 788; B.W. Zhang and X.N. Wang, Nucl. Phys. A720 (2003) 429.
- [58] R. Baier, Nucl. Phys. A715 (2003) 209c.
- [59] J. Breitweg et al., Eur. Phys. J. C 7 (1999) 609.
- [60] A.H. Mueller, Nucl. Phys. B335 (1990) 115; A.H. Mueller, Nucl. Phys. B572 (2002) 227.
- [61] L.D. McLerran and R. Venugopalan, Phys. Rev. D49 (1994) 2233.
- [62] L.D. McLerran, hep-ph/0311028.
- [63] E. Iancu and R. Venugopalan, in Quark Gluon Plasma 3, eds. R.C. Hwa and X.N. Wang (World Scientific, Singapore, 2003); hep-ph/0303204.

- [64] V.N. Gribov and L.N. Lipatov, *Sov. J. Nucl. Phys.* 15 (1972) 438 and 675; L.N. Lipatov, *Sov. J. Nucl. Phys.* 20 (1975) 94; G. Altarelli and G. Parisi, *Nucl. Phys. B126* (1977) 298; Yu. L. Dokshitzer, *Sov. Phys. JETP* 46 (1977) 641.
- [65] E.A. Kuraev, L.N. Lipatov and V.S. Fadin, *Phys. Lett. B60* (1975) 50; *Sov. Phys. JETP* 44 (1976) 443; *Sov. Phys. JETP* 45 (1977) 199; L.N. Lipatov, *Sov. J. Nucl. Phys.* 23 (1976), 338; Ya. Ya. Balitsky and L.N. Lipatov, *Sov. J. Nucl. Phys.* 28 (1978) 822; *Sov. Phys. JETP Lett.* 30 (1979) 355.
- [66] D. Kharzeev and M. Nardi, *Phys. Lett. B507* (2001) 121; D. Kharzeev and E. Levin, *Phys. Lett. B523* (2001) 79.
- [67] V.V. Anisovich and V.M. Shekhter, *Nucl. Phys. B55* (1973) 455; J.D. Bjorken and G.E. Farrar, *Phys. Rev. D9* (1974) 1449; K.P. Das and R.C. Hwa, *Phys. Lett. B68* (1977) 459; Erratum *ibid.* 73 (1978) 504; R.G. Roberts, R.C. Hwa and S. Matsuda, *J. Phys. G* 5 (1979) 1043.
- [68] C. Gupt, R.K. Shivpuri, N.S. Verma and A.P. Sharma, *Nuovo Cim. A75* (1983) 408; T. Ochiai, *Prog. Theor. Phys.* 75 (1986) 1184; T.S. Biro, P. Levai and J. Zimanyi, *Phys. Lett. B347* (1995) 6; T.S. Biro, P. Levai and J. Zimanyi, *J. Phys. G* 28 (2002) 1561.
- [69] S.A. Voloshin, *Nucl. Phys. A.* 715 (2003) 379c; D. Molnar and S.A. Voloshin, *Phys. Rev. Lett.* 91 (2003) 092301; R.J. Fries, B. Müller, C. Nonaka and S.A. Bass, *Phys. Rev. Lett.* 90 (2003) 202303; V. Greco, C.M. Ko and P. Levai, *Phys. Rev. Lett.* 90 (2003) 202302; Z.W. Lin and C.M. Ko, *Phys. Rev. Lett.* 89 (2002) 202302; Z.W. Lin and D. Molnar, *Phys. Rev. C68* (2003) 044901.
- [70] B. Müller, *nucl-th/0404015*.
- [71] C. Adler et al. [STAR Collaboration], *Phys. Rev. Lett.* 90 (2003) 082302.
- [72] R.C. Hwa and C.B. Yang, *Phys. Rev. C66* (2002) 025205; R.C. Hwa and C.B. Yang, *Phys. Rev. C67* (2003) 034902; R.C. Hwa and C.B. Yang, *Phys. Rev. C70* (2004) 024905.
- [73] W. Reisdorf and H.G. Ritter, *Ann. Rev. Nucl. Part. Sci.* 47 (1997) 663.
- [74] J.-Y. Ollitrault, *Phys. Rev. D46* (1992) 229.
- [75] X.N. Wang and M. Gyulassy, *Phys. Rev. Lett.* 86 (2001) 3496.
- [76] B.B. Back et al. [PHOBOS Collaboration], *Phys. Rev. C65* (2002) 061901R.
- [77] J. Adams et al. [STAR Collaboration], *nucl-ex/0311017*.
- [78] K.J. Eskola, K. Kajantie, P.V. Ruuskanen and K. Tuominen, *Nucl. Phys. B570* (2000) 379.
- [79] W. Czyz and L.C. Maximon, *Annals Phys.* 52 (1969) 59.
- [80] B.B. Back et al. [PHOBOS Collaboration], *nucl-ex/0301017*.
- [81] K. Adcox et al. [PHENIX Collaboration], *Phys. Rev. Lett.* 87 (2001) 052301.

- [82] M.M. Aggarwal et al. [WA98 Collaboration], *Eur. Phys. J. C* 18 (2001) 651.
- [83] C. Adler et al. [STAR Collaboration], *Phys. Rev. C* 70 (2004) 054907.
- [84] J.D. Bjorken, *Phys. Rev. D* 27 (1983) 140.
- [85] J. Adams et al. [STAR Collaboration], *Phys. Rev. Lett.* 92, (2004) 182301.
- [86] O. Barannikova et al. [STAR Collaboration], nucl-ex/0403014.
- [87] C. Adler et al. [STAR Collaboration], *Phys. Rev. Lett.* 89 (2002) 092301; J. Adams et al. [STAR Collaboration], *Phys. Lett. B* 595 (2004) 143; J. Adams et al. [STAR Collaboration], *Phys. Rev. C* 70 (2004) 041901; J. Adams et al. [STAR Collaboration], nucl-ex/0406003.
- [88] N. Xu and M. Kaneta, *Nucl. Phys. A* 698 (2002) 306c.
- [89] R. Hagedorn, CERN-TH-3918/84.
- [90] E. Schnedermann, J. Sollfrank, and U. Heinz, *Phys. Rev. C* 48 (1993) 2462.
- [91] P. Braun-Munzinger, J. Stachel, J. Wessels, and N. Xu, *Phys. Lett. B* 344 (1995) 43; P. Braun-Munzinger, I. Heppe, and J. Stachel, *Phys. Lett. B* 465 (1999) 15.
- [92] S.A. Bass et al., *Phys. Rev. C* 60 (1999) 021902.
- [93] A. Dumitru and S.A. Bass, *Phys. Lett. B* 460 (1999) 411.
- [94] S.S. Adler et al. [PHENIX Collaboration], *Phys. Rev. C* 69 (2004) 034909.
- [95] E. Yamamoto et al. [STAR Collaboration], *Nucl. Phys. A* 715 (2003) 466c.
- [96] K. Schweda et al. [STAR Collaboration], *J. Phys. G* 30 (2004) S693.
- [97] K. Adcox et al. [PHENIX Collaboration], *Phys. Rev. Lett.* 88 (2002) 242301.
- [98] A.M. Poskanzer and S.A. Voloshin, *Phys. Rev. C* 58 (1998) 1671.
- [99] N. Borghini, P.M. Dinh and J.Y. Ollitrault, *Phys. Rev. C* 64 (2001) 054901.
- [100] C. Alt et al. [NA49 Collaboration], *Phys. Rev. C* 68 (2003) 034903.
- [101] C. Adler et al. [STAR Collaboration], *Phys. Rev. C* 66 (2002) 034904.
- [102] A. Tang et al. [STAR Collaboration], *AIP Conf. Proc.* 698 (2004) 701; J. Adams et al. [STAR Collaboration], nucl-ex/0409033.
- [103] G. Agakichiev et al. [CERES/NA45 Collaboration], *Phys. Rev. Lett.* 92 (2004) 032301.
- [104] J. Adams et al. [STAR Collaboration], *Phys. Rev. Lett.* 92 (2004) 052302.
- [105] C. Adler et al. [STAR Collaboration], *Phys. Rev. Lett.* 87 (2001) 182301.
- [106] P. Huovinen, private communications (2003).
- [107] E. Shuryak, *Prog. Part. Nucl. Phys.* 53 (2004) 273.

- [108] B.B. Back, et al. [PHOBOS Collaboration], Phys. Rev. Lett. 89 (2002) 222301.
- [109] X. Dong, S. Esumi, P. Sorensen, N. Xu, and Z. Xu, Phys. Lett. B597 (2004) 328.
- [110] J. Castillo et al. [STAR Collaboration], J. Phys. G 30 (2004) S1207.
- [111] S.S. Adler et al. [PHENIX Collaboration], Phys. Rev. Lett. 91 (2003) 182301.
- [112] C. Nonaka, R.J. Fries and S.A. Bass, Phys. Lett. B583 (2004) 73; C. Nonaka et al., Phys. Rev. C69 (2004) 031902.
- [113] For general introduction of two-particle correlation studies, see U.A. Wiedemann and U. Heinz, Phys. Rept. 319 (1999) 145; B. Jacak and U. Heinz, Ann. Rev. Nucl. Part. Sci. 49 (1999) 529.
- [114] G. Bertsch, Nucl. Phys. A498 (1989) 173c.
- [115] D. Rischke and M. Gyulassy, Nucl. Phys. A597 (1996) 701; D. Rischke and M. Gyulassy, Nucl. Phys. A608 (1996) 479.
- [116] C. Adler et al. [STAR Collaboration], Phys. Rev. Lett. 87 (2001) 082301; K. Adcox et al. [PHENIX Collaboration], Phys. Rev. Lett. 88 (2002) 242301.
- [117] J. Adams et al. [STAR Collaboration], Phys. Rev. Lett. 92 (2003) 062301.
- [118] S. Soff, hep-ph/0202240; D. Zschesche, S. Schramm, H. Stocker, and W. Greiner, Phys. Rev. C65 (2001) 064902; S. Soff, S.A. Bass, and A. Dumitru, Phys. Rev. Lett. 86 (2001) 3981.
- [119] U. Heinz, hep-ph/0407360.
- [120] C.Y. Wong, J. Phys. G 30 (2004) S1053.
- [121] J. Adams et al. [STAR Collaboration], Phys. Rev. Lett. 91 (2003) 262302.
- [122] M. Stephanov, K. Rajagopal, and E. Shuryak, Phys. Rev. Lett. 81 (1998) 4816.
- [123] S. Voloshin, V. Koch, and H.G. Ritter, Phys. Rev. C60 (1999) 024901.
- [124] S. Jeon and V. Koch, Phys. Rev. Lett. 85 (2000) 2076.
- [125] M. Asakawa, U. Heinz, and B. Müller, Phys. Rev. Lett. 85 (2000) 2072.
- [126] S.A. Bass, P. Danielewicz, and S. Pratt, Phys. Rev. Lett. 85 (2000) 2689.
- [127] Q. Liu and T. Trainor, Phys. Lett. B567 (2003) 184.
- [128] M. Gazdźicki and St. Mrówczyński, Z. Phys. C54 (1999) 127.
- [129] D. Adamova et al. [CERES Collaboration], Nucl. Phys. A727 (2003) 97.
- [130] S.S. Adler et al. [PHENIX Collaboration], Phys. Rev. Lett. 93 (2004) 092301.
- [131] G. Westfall et al. [STAR Collaboration], J. Phys. G 30 (2004) S1389.

- [132] J. Adams et al. [STAR Collaboration], nucl-ex/0411003; T.A. Trainor et al. [STAR Collaboration], hep-ph/0406116.
- [133] I. Bearden et al. [NA44 Collaboration], Phys. Rev. C65 (2002) 044903.
- [134] J. Adams et al. [STAR Collaboration], Phys. Rev. C 71 (2005) 031901(R).
- [135] J. Adams et al. [STAR Collaboration], Phys. Rev. Lett. 90 (2003) 172301.
- [136] X.N. Wang and M. Gyulassy, Phys. Rev. D44 (1991) 3501; X.N. Wang and M. Gyulassy, Comput. Phys. Commun. 83 (1994) 307.
- [137] C. Adler et al. [STAR Collaboration], Phys. Rev. Lett. 89 (2002) 202301.
- [138] I. Arsene et al. [BRAHMS Collaboration], Phys. Rev. Lett. 91 (2003) 072305.
- [139] S.S. Adler et al. [PHENIX Collaboration], Phys. Rev. Lett. 91 (2003) 072303.
- [140] B.B. Back et al. [PHOBOS Collaboration], Phys. Rev. Lett. 91 (2003) 072302.
- [141] J. Adams et al. [STAR Collaboration], Phys. Rev. Lett. 91 (2003) 072304.
- [142] D. Antreasyan et al., Phys. Rev. D19 (1979) 764.
- [143] X.N. Wang, Phys. Rept. 280 (1997) 287; M. Lev and B. Petersson, Z. Phys. C21 (1987) 155; T. Ochiai et al., Prog. Theor. Phys. 75 (1986) 288.
- [144] J. Adams et al. [STAR Collaboration], Phys. Rev. Lett. 93 (2004) 252301.
- [145] D. Hardtke et al. [STAR Collaboration], Nucl. Phys. A715 (2003) 272.
- [146] F. Wang et al. [STAR Collaboration], J. Phys. G. 30 (2004) S1299; J. Adams et al. [STAR Collaboration], nucl-ex/0501016.
- [147] X.N. Wang, Phys. Lett. B 595 (2004) 165.
- [148] I. Vitev and M. Gyulassy, Phys. Rev. Lett. 89 (2002) 252301.
- [149] K.J. Eskola, H. Honkanen, C.A. Salgado, and U.A. Wiedemann, Nucl. Phys. A747 (2005) 511.
- [150] D. Kharzeev, E. Levin and L. McLerran, Phys. Lett. B561 (2003) 93.
- [151] J. Adams et al. [STAR Collaboration], Phys. Rev. Lett. 91 (2003) 172302.
- [152] T. Falter and U. Mosel, Phys. Rev. C66 (2002) 024608.
- [153] K. Gallmeister, C. Greiner and Z. Xu, Phys. Rev. C67 (2003) 044905.
- [154] B.B. Back et al. [PHOBOS Collaboration], Phys. Rev. Lett. 88 (2002) 022302.
- [155] I. Arsene et al. [BRAHMS Collaboration], Phys. Rev. Lett. 93 (2004) 242303.
- [156] V. Guzey, M. Strikman, and W. Vogelsang, Phys. Lett. B603 (2004) 173.
- [157] D. Kharzeev, Y.V. Kovchegov and K. Tuchin, Phys Lett. B599 (2004) 23.

- [158] A.D. Frawley et al. [PHENIX Collaboration], J. Phys. G30 (2004) S675.
- [159] J. Adams et al. [STAR Collaboration], Phys. Rev. C 70 (2004) 064907.
- [160] D. Kharzeev, Y.V. Kovchegov and K. Tuchin, Phys. Rev. D68 (2003) 094013.
- [161] D. Kharzeev, E. Levin and L. McLerran, hep-ph/0403271.
- [162] R. Vogt, hep-ph/0405060.
- [163] A. Ogawa et al. [STAR Collaboration], nucl-ex/0408004.
- [164] M.M. Aggarwal et al. [WA98 Collaboration], Phys. Rev. Lett. 81 (1998) 4087;
M.M. Aggarwal et al. [WA98 Collaboration], Phys. Rev. Lett. 84 (2000) 578;
M.M. Aggarwal et al. [WA98 Collaboration], Eur. Phys. J. C 23 (2002) 225.
- [165] D. d'Enterria, J. Phys. G 30 (2004), S767.
- [166] D.H. Rischke and M. Gyulassy, Nucl. Phys. A608 (1996) 479.
- [167] J. Adams et al. [STAR Collaboration], nucl-ex/0411036.
- [168] D. Kharzeev et al., Phys. Rev. Lett. 81 (1998) 512 (1998); D. Kharzeev, hep-ph/0406125.
- [169] A Long Range Plan for Nuclear Science (NSAC Report, 1983).
- [170] Physics Through the 1990s: Nuclear Physics, J. Cerny et al. (National Academy Press, Washington, D.C., 1986).
- [171] RHIC and Quark Matter: Proposal for a Relativistic Heavy Ion Collider at Brookhaven National Laboratory (BNL Report 51801, August 1984).
- [172] Nuclei, Nucleons, Quarks: Nuclear Science in the 1990's (NSAC Long Range Plan Report, December 1989).
- [173] Nuclear Science: Assessment and Promise (NSAC Report, May 1994).
- [174] Nuclear Science: A Long Range Plan (NSAC Report, February 1996).
- [175] Nuclear Physics: The Core of Matter, The Fuel of Stars, J.P. Schiffer, et al. (National Academy Press, Washington, D.C., 1999).
- [176] NuPECC Long Range Plan 2004: Perspectives for Nuclear Physics Research in Europe in the Coming Decade and Beyond, ed. M. Harakeh, et al. (April 2004).